Dissertation

Characterization of novel predictive biomarkers in colorectal cancer

submitted by
MSc, BSc
Verena STIEGELBAUER

for the Academic Degree of
Doctor of Medical Science (Dr. scient. med.)

at the

Medical University of Graz
Division of Oncology

under the Supervision of

Assoz.-Prof. Dr. Armin GERGER

Assoz.-Prof. Dr. Martin PICHLER

Assoz.-Prof. Dr. Georg HUTTERER

PD Dr.med.scient. Alexander DEUTSCH

Eidesstattliche Erklärung

Ich erkläre ehrenwörtlich, dass ich die vorliegende Arbeit selbstständig angefertigt und abgefasst, und jene Personen und Institutionen, die am Zustandekommen der Forschungsdaten beteiligt waren, namentlich genannt habe. Andere als die angegebenen Quellen habe ich nicht verwendet und die den benutzten Quellen wörtlich oder inhaltlich entnommenen Stellen habe ich als solche kenntlich gemacht. Die Arbeit an der Dissertation und daraus entstandener Publikationen wurde gemäß den Regeln der „Good Scientific Practice“ durchgeführt.

Ein Teil dieser Arbeit wurde bereits veröffentlicht: Pichler and Stiegelbauer *et al*.; Genome-wide microRNA analysis identifies miR-188-3p as novel prognostic marker and molecular factor involved in colorectal carcinogenesis; Clin. Cancer Res., 2016

_____ _____

Graz, am Unterschrift

Declaration

I hereby declare that this thesis is my own original work and that I have fully acknowledged by name all of those individuals and organizations that have contributed to the research for this thesis. Due acknowledgement has been made in the text to all other material used. Throughout this thesis and in all related publications I followed the guidelines of “Good Scientific Practice”.

Parts of this thesis have been already accepted for publication in the following: Pichler and Stiegelbauer *et al*.; Genome-wide microRNA analysis identifies miR-188-3p as novel prognostic marker and molecular factor involved in colorectal carcinogenesis; Clin. Cancer Res., 2016

_____ _____

Date: Signature

Acknowledgement

First of all I would like to thank my supervisor Armin Gerger for providing this research project and for giving me the opportunity to work on this interesting topic. I would like to thank my Co-supervisor Martin Pichler for being a great mentor. I am grateful for the valuable advice and help with planning of experiments, daily lab-work and with scientific writing. He supported me to publish my results, he helped me to become an independent researcher and he always had time to discuss results while having one busy day after another. I also express my gratitude to my thesis committee members Alexander Deutsch and Georg Hutterer for their guidance and feedback.

I thank my team colleagues from the oncology research group for helping me with practical issues, for good discussions, nice chats and for being friends.

I would also like to thank BMA Karin Wagner from the Center for Medical Research of the Medical University of Graz and Elke Winter from Institute of Pathology for their technical assistance and friendly help.

Many thanks also to the research group of George Calin from the MD Anderson Cancer Institute for valuable input and great collaborations.

Thanks to all of my friends who supported me during this time and beyond. Last but not least, I am deeply thankful for all the support I got from my family, especially from my parents.

Abbreviations

APC	Adenomatous polyposis coli
BER	base excision repair
BRAF	v-Raf murine sarcoma viral oncogene homolog B
B2M	Beta-2 Microglobulin
CRC	Colorectal Cancer
CPA4	Carboxypeptidase 4
cDNA	complementary DNA
cMYC	v-myc avian myelocytomatosis viral oncogene homolog
CTNNA2	Catenin Alpha 2
DKK1	Dickkopf-related protein
DMEM	Dulbecco's Modified Eagle Medium
DNA	Deoxyribonucleic Acid
ECM	Extracellular matrix
EGFR	Epidermal growth factor receptor
EMEM	Eagle's minimum essential medium
EMT	Epithelial to mesenchymal transition
FAP	Familial adenomatous polyposis
GALNT	N-Acetylgalactosaminyltransferase
GALNT5	N-Acetylgalactosaminyltransferase
GAPDH	Glyceraldehyd 3-phosphate dehydrogenase
GFP	Green fluorescence protein
HEK	Human embryonic kidney
HGF	hepatocyte growth factor
hMSH2	human mutS homolog 2
HNPPC	hereditary non-polyposis colorectal cancer
HOXB7	Homeobox 7
IgG	Immuoglobulin G
ISH	In situ hybridisation
KRAS	Kirsten rat sarcoma viral oncogene homolog
KRTAP1	Keratin associated protein 1
KRTAP2-3	Keratin associated protein 2-3
mCRC	metastatic colorectal cancer

MiRNA	Micro RNA
MLLT4	Mixed Lineage Leukemia; Translocated to, 4
mt	mutated
MUC13	Mucin 13
NLK	Nemo like kinase
PBS	Phosphate buffered saline
PCR	Polymerase chain reaction
PDGF	Platelet derived growth factor
PI3K	Phosphoinositide 3-kinase
PMSF	Phenylmethylsulfonyl fluoride
pre-miRNA	pre micro RNA
pri-miRNA	primary micro RNA
qRT-PCR	quantitative Real Time PCR
RIPA	Radio immunoprecipitation assay
RISC	RNA induced silencing complex
RNA	Ribonucleic Acid
RNU6B	RNA, U6B small nuclear
RPM	Rounds per minute
SiRNA	Small interfering RNA
SNP	Single nucleotide polymorphism
TBS	Tris buffered saline
TCGA	The Cancer Genome Atlas
TGF	Transforming growth factor
TYMS	Thymidylate synthase
TBS-T	Tris buffered saline with Tween 20
UTR	untranslated region
VEGF	Vascular endothelial growth factor
VEGFR	Vascular endothelial growth factor receptor
WST	water soluble tetrazolium
wt	wildtype
5-FU	5-Fluorouracil

List of figures

List of tables

Inhalt

Abstract

MicroRNAs (miRNAs) are small, non-coding, single-stranded RNAs that are known to be important regulators of carcinogenesis and might be useful potential prognostic factors and therapeutic targets in colorectal cancer (CRC). In the current study we focused on two specific miRNAs, namely miR-196b-5p and miR-188-3p, and analysed their role as potential prognostic biomarkers, their biological functions and their molecular mechanisms of action.

In the first part of this study miR-196b-5p expression was quantified by qRT-PCR in two independent cohorts comprising 292 CRC patients in total to investigate its potential as biomarker. In the second part of this thesis an analysis of genome-wide miRNA sequencing data of 228 CRC patients from the cancer genome atlas (TCGA) was performed and identified miR-188-3p as significantly associated with survival. This observation was further validated in a large independent validation cohort (n=332). Transient and stable gain and loss of function experiments were performed in a panel of CRC cell lines, to evaluate the impact of miR-196b-5p and miR-188-3p on proliferation, chemo-sensitivity, migration, invasion and metastases formation *in vitro* and *in vivo*. The molecular pathways influenced by these miRNAs were characterized using mRNA transcriptome profiling, *in silico* target prediction tools, luciferase-interaction assays and pheno-copy gene knock-down experiments.

Low miR-196b-5p expression was significantly associated with metastases and poor survival in both independent CRC patient cohorts ($p<0.05$). Inhibition of miR-196b-5p resulted in increased cancer cell migration/invasion and metastases formation in nude mice ($p<0.05$). We showed that *HOXB7* and *GalNT5* mRNAs are regulated by miR-196b-5p via targeting their 3´UTR, which in turn led to a decrease of CRC cell migration. We identified high miR-188-3p expression as an independent prognostic factor (screening cohort: hazard ratio = 4.137, 95%CI=1.568-10.917, p=0.004; validation cohort: hazard ratio HR=1.538, 95%CI=1.107-2.137, p=0.010, respectively). Enhanced miR-188-3p expression resulted in increased migratory behavior of CRC cells *in vitro* and metastases formation *in vivo* ($p<0.05$). The pro-migratory phenotype of miR-188-3p is regulated by direct interaction with MLLT4, a novel migration related gene in CRC.

In conclusion, the results of this thesis suggest that miR-196b-5p and miR-188-3p are novel independent prognostic factors in CRC patients which can be party explained by the direct interaction with genes involved in cancer cell migration.

Zusammenfassung

MicroRNAs (miRNAs) sind kurze, nicht-kodierende, einzelsträngige RNA Sequenzen und stellen wichtige Regulatoren in der Karzinogenese dar. Zudem haben sie großes Potential als prognostische Faktoren und sind mögliche Angriffspunkte der Kolorektalkarzinom-therapie. In der vorliegenden Arbeit wurde der Fokus auf zwei miRNAs (miR-196b-5p und miR-188-3p) gelegt und ihre Rolle als Biomarker in Bezug auf das Kolorektalkarzinom analysiert.

Im ersten Teil dieser Arbeit wurde die miR-196b-5p Expression mittels quantitativer RT-PCR in zwei unabhängigen Kohorten (292 Kolorektalkarzinom Patienten) vermessen um die mögliche Rolle dieser miRNA als Biomarker zu untersuchen. Im zweiten Teil dieser Arbeit wurden genomweite miRNA Sequenzierungsdaten von 288 Patienten (aus dem TCGA Datensatz) analysiert und hierbei konnte eine Assoziation zwischen miR188-3p und Patienten-Überleben gezeigt werden. Um dieses Ergebnis zu bestätigen wurde noch eine weitere Kohorte von 332 Patienten mittels qRT-PCR vermessen. Zudem wurden transiente und stabile miRNA Überexpressions- und Inhibitionsexperimente durchgeführt um den Einfluss beider miRNAs auf Zellproliferation, Chemosensitivität, Migration, Invasion und Metastasenbildung *in vitro* und *in vivo* zu untersuchen. Eine Charakterisierung der molekularen „pathways“, die durch diese miRNAs beeinflusst werden, erfolgte mittels Microarray-Analyse, *in silico* Analysen zur Identifikation von potentiellen Zielgenen und Luciferase Assays.

In der vorliegenden Arbeit wurde gezeigt, dass in beiden analysierten Patientenkohorten eine niedrige miR-196b-5p Expression mit Metastasenbildung und kürzerer Überlebenszeit assoziiert ist ($p<0.05$). Eine Inhibierung der miR-196b Expression führte zu einer verstärkten Migration bzw. Invasion in Kolorektalkarzinom-Zelllinien und zu erhöhter Metastasenbildung im Mausmodell. Es konnte nachgewiesen werden, dass die Gene *HOXB7* und *GalNT5* durch miR-196b-5p reguliert werden, wodurch wiederum die Zell-migration beeinflusst wird.

MiR-188-3p konnte ebenfalls als unabhängiger prognostischer Marker identifiziert werden (Screening-Kohorte: hazard ratio = 4.137, 95%CI=1.568-10.917, p=0.004; Validierungs-Kohorte: hazard ratio HR=1.538, 95%CI=1.107-2.137, p=0.010). Eine Überexpression von miR-188-3p führte zu einer verstärkten Migration von Kolorektalkarzinom-Zelllinien *in*

vitro und erhöhter Metastasenbildung *in vivo*. Dieser Phänotyp kann teilweise durch die Regulierung von MLLT4, ein Gen, welches eine potentielle Rolle im Migrationsprozess spielt, durch miR-188-3p erklärt werden.

Zusammengefasst weisen die Ergebnisse dieser Arbeit darauf hin, dass miR-196b-5p und miR-188-3p als neue unabhängige prognostische Faktoren bei Kolorektalkarzinom-Patienten zum Einsatz gebracht werden könnten.

1. Introduction

1.1 Colorectal Cancer

1.1.1 Epidemiology and risk factors

Colorectal cancer (CRC) is the third most common cancer diagnosed in males and second in females and represents the most common cancer of the digestive system. In 2015, about 69090 men and 63600 women were diagnosed with CRC (1). Age, family history and sex are independent risk factors for CRC. There is an increased incidence of CRC with age, with about 7 percent of CRC cases appearing in those younger than 50 years. The risk is slightly lower among women than men. Approximately 75 percent of new cases occur in those with unknown predisposing factors. Patients with a family history of CRC but without a genetic syndrome account for 15–20 percent of cases. HNPCC (hereditary non-polyposis colorectal cancer) accounts for about 5 percent of cases and familial adenomatous polyposis (FAP) accounts for about 1 percent (2). Those patients with a family history of CRC in a parent, sibling or child show a twofold increased risk of this disease (3, 4).CRC pathogenesis

The majority of CRC cases begins with an adenomatous polyp arising from the glandular epithelium of the intestine (5). The transformation process comprises essential events characterized by the activation of oncogenes such as *KRAS* (Kirsten rat sarcoma viral oncogene homolog), *c-MYC* (v-myc avian myelocytomatosis viral oncogene homolog) and *NRAS* (neuroblastoma RAS viral oncogene homolog) and by inactivation of tumor suppressor genes [*e.g.*, *p53* (tumor protein p53) and *APC* (adenomatous polyposis coli)] or DNA repair genes such as *hMSH2* (human mutS homolog 2) or *hMSLH1*. The accumulation of different somatic or inherited changes within the genome and epigenome in accordance with changes in chromosomal copy number and structure, shifts the normal intestinal lining to an adenomatous polyp, then high-grade adenoma and finally to a carcinoma (6, 7). CRC can also arise from nonpolypoid and depressed lesions. Although these lesions are less prevalent than that of the polypoid adenoma, they show a more aggressive behaviour and faster growth and they are more difficult to diagnose (8, 9).

1.1.3 Treatment regimes

Surgical resection for patients with localized disease has dramatically improved the 5-year survival rates, however, more than half of all patients diagnosed with CRC finally develop recurrence of their disease and metastasis (10, 11). Over the past decades, there have been several changes in the treatment options for patients with metastatic CRC, including the incorporation of new chemotherapeutic drugs and the introduction of novel targeting agents, including inhibitors of angiogenesis and epidermal growth factor receptor signaling, which improved survival time of metastatic CRC (mCRC) patient (12).

Chemotherapeutic drugs

5-Fluorouracil (5-FU) is a key anticancer drug used for CRC treatment (13, 14). It exhibits its cytotoxic effects by incorporating fluoronucleotides into RNA and DNA molecules, but its main toxicity is mediated by inhibiting the nucleotide synthetic enzyme thymidylate synthase (TYMS) (15). However, one of the major problems in managing metastatic colorectal cancer is both the inherent and acquired resistance to 5-FU-based therapy. During the last two decades more effective cytotoxic agents such as Irinotecan, a topoisomerase I inhibitor, and Oxaliplatin, a platinum derivative, have been introduced as treatment regimens for mCRC patients. The activity of Irinotecan and Oxaliplatin was first demonstrated in patients that failed on fluoropyrimidine (16-18). Irinotecan is one of the main chemotherapeutic drugs for metastatic colorectal cancer. After its introduction for the treatment of advanced colorectal cancer survival has improved dramatically. Irinotecan is now given in combination with 5-Fluorouracil, Oxaliplatin and several molecularly-targeted anticancer drugs, resulting in the extension of overall survival to longer than 30 months (18, 19).

EGFR targeted therapy

The epidermal growth factor receptor (EGFR) is a member of the ErbB family of receptors that promote tumor cell proliferation in several epithelial malignancies (20). Therefore, anti-EGFR drugs are potential candidates used in oncology. Monoclonal antibodies against EGF receptor are used as a standard therapeutic approach for some types of solid tumors. The chimeric IgG1 mouse/human antibody cetuximab and the human IgG2 antibody panitumumab are considered to be equally successful in mCRC treatment. These antibodies bind to the EGFR on the cell surface and inhibit its activation by preventing

ligand binding and dimerization (18, 21). However, it has been extensively reported that primary resistance to these targeting agents is mediated by mutations in downstream signalling molecules (22). A study by Misale *et al.* (23) revealed that the development of resistance to anti-EGFR therapy in CRC is associated with molecular alterations of *KRAS*. Although *KRAS* mutations confer strong resistance to anti-EGFR antibodies, not all CRC patients with *KRAS* wildtype (*KRASwt*) have a benefit from these therapeutic antibodies. Therefore, novel biomarkers are necessary to better identify which *KRASwt* patients would benefit from this therapy (24). A few studies have demonstrated that a high gene copy number of EGFR could be a potential marker for EGFR targeted therapy in CRC, as patients with low gene copy number are unlikely to respond to anti-EGFR agents (25, 26). Recently, rare mutations in exons 3 and 4 in both the *NRAS* gene and *KRAS* gene have shown predictive potential in regard to treatment with panitumumab (18, 27).

VEGF inhibitors

Angiogenesis is a hallmark of cancer and is widely regarded as an important therapeutic target in many different types of cancer, including CRC (28). It has been suggested that antiangiogenic treatment blocks the formation of new blood vessels and probably lead to normalization of the existing tumor vasculature. The vascular endothelial growth factor (VEGF) is a pro-angiogenic factor that plays a key role in the process of tumor angiogenesis, and the VEGF pathway has therefore been an important target for anti-cancer drug development (18, 29-31). VEGF-neutralizing antibodies can inhibit the activation of VEGFR1 (vascular endothelial growth factor receptor 1), VEGFR2 (vascular endothelial growth factor receptor 2) and the co-receptors NP1 (Neuropilin 1) and NP2 (Neuropilin 2) by binding to these receptors. Bevacizumab, a humanized monoclonal antibody against all isoforms of VEGF, is the first anti-angiogenic agent approved for the treatment of CRC (32, 33). It has also been used as combined therapy with common chemotherapeutic drugs such as 5-FU and capecitabine as well as Irinotecan and Oxaliplatin. Developing resistance to these therapies may be due to resistance to the anti-VEGF antibody, resistance to the chemotherapeutic agent with which bevacizumab was applied or a resistance to both. It has been shown that several pathways in addition to the VEGF pathway play a role in tumor angiogenesis. Therefore, resistance mechanisms to anti-angiogenic therapy may also include VEGF-independent anti-angiogenesis pathways (18, 34).

1.2 MicroRNAs

MiRNAs are small, non-coding, endogenous, single-stranded RNAs that play a crucial role as post-transcriptional regulators by inducing the mRNA degradation or suppressing the translation to a protein of their target genes (35). These small RNA molecules are known to be important regulators of carcinogenesis and one particular miRNA can act as a tumor suppressor or a tumor promoter ("oncomiR") depending on the cellular and molecular context (36, 37). About one third of all human genes are regulated by miRNAs and a single miRNA can target around 200 or more transcripts that are key regulators of multiple signalling pathways in the cell (38, 39). Different miRNA expression signatures occur in all cancerous tissues and profiling them on a global scale can give novel diagnostic and prognostic knowledge (36, 40, 41). More than 50% of known human miRNA genes are found in fragile chromosomal regions that are susceptible to amplification, translocation or deletion during cancer development (42). Given their chemical stability in formalin-fixed tissue (43), miNAs have potential as diagnostic and prognostic biomarkers and therefore might overcome at least some of the analytical problems linked to previously established protein-coding gene expression tools (44).

1.2.1 MicroRNA biogenesis

MiRNAs are transcribed as long primary transcripts called pri-miRNAs. In the nucleus, these sequences are cleaved into precursor miRNAs (pre-miRNAs) by a nuclease called Drosha, an enzyme that belongs to the RNAse III family. Short hairpin RNAs of approximately 70 nucleotides are generated and transported to the cytoplasm by Exportin-5 (XPO5). Finally, these RNA sequences are cleaved by an enzyme called Dicer, an RNAse III enzyme, resulting in the final products of ~22 nucleotides duplexes (45). A helicase then unwinds the miRNA and one strand is defined to be the mature strand, the other one is quickly degraded. The mature miRNA is incorporated into a ribonucleotide silencing complex, also called RISC, and this complex regulates silencing of genes (46). The key molecules of the RISC complex are Argonaute proteins, which directly interact with the miRNA. Most eukaryotes investigated have multiple Argonaute family members with several Argonautes responsible for diverse functions, for instance Ago2 is the only Argonaute protein competent of endonuclease cleavage (47).

MiRNAs are targeting the matching mRNA by binding to its complementary bases (46). Regulation of post-transcriptional gene expression by miRNAs is carried out by

endonuclease cleavage of the target mRNA. This process is regulated by the Argonaute protein Ago 2 within the RISC complex (47). Degradation of mRNA released by deadenylation seems to be an important mechanism by which miRNAs down-regulate gene expression. Furthermore, miRNAs can down-regulate the concentration of mRNAs that containe sequences to which they are not perfectly matching (48). Target sites showing fully complementary nucleotides result in mRNA degradation, whereas mismatched interactions between the target mRNA and miRNA lead to repression of protein translation (49, 50). MiRNAs regulate protein translation by either direct or indirect mechanisms. Direct effects are processed at different phases of protein translation, including the repression of the initiation, prevention of ribosome assembly, which is necessary for initiation of translation, and inhibition of elongation or termination of translation process. Translational repression via indirect effects is triggered by destabilisation and subsequent degradation of the target mRNA (46).

1.2.2 The role of miRNAs in CRC

MiRNAs are key regulators of oncogenesis, invasion, progression, angiogenesis and metastasis in colorectal cancer. Both upregulation and downregulation of miRNA have been shown to play a role in CRC carcinogenesis (51). Several proteins that are involved in key signalling pathways of CRC, such as members of the Wnt/beta-catenin and phosphatidylinositol-3-kinase (PI-3-K) pathways, KRAS, p53, extracellular matrix regulators as well as epithelial-mesenchymal transition (EMT) proteins and transcription factors seem to be regulated by miRNAs (38, 52, 53). New findings also suggest that miRNAs might have an influence on chemosensitivity in tumor cells. Therefore, researchers are highly interested in the potential role of miRNAs in pharmacogenomics (54). A recent study by Pardini *et al.* (55) revealed that changes of base excision repair (BER) genes expression levels, such as a post-transcriptional modulation caused by microRNAs, could have an impact on the efficiency of this repair system. Single-nucleotide polymorphisms (SNP) within the 3′-untranslated region (3'UTR) of the target mRNA could lead to an alteration in binding of specific miRNAs that regulate gene expression. Such changes could affect patient prognosis and therapy outcomes. Hence, characterization of polymorphisms in miRNA-related genes or target sites might offer a foundation for miRNA-based therapy approaches.

1.2.3 MiRNAs and colorectal tumor migration, invasion, and metastasis

The major cause of cancer related death comes from complications arising from cancer cell migration and invasion and metastasis (56). Tumor migration and invasion are processes comprising several events including MMP activation, EMT (epithelial to mesenchymal transition), the breakdown of extracellular matrix (ECM), microcirculation establishment, cell motility increase and invasion, and distant metastasis (dissemination via blood and lymph). Metastases are related to silencing of epigenetic miRNAs with tumor suppressor capacities by CpG island hyper-methylation, a process that is not explored well yet (57).

MiRNAs and EMT

The epithelial-mesenchymal transition is a mechanism of epithelial cancer cell transformation to motile mesenchymal cancer cells. Essential features of EMT include the loss of epithelial characteristics such as cell adhesion, down-regulation of epithelial marker (E-cadherin) and up-regulation of mesenchymal markers (vimentin, N-cadherin, fibronectin) and increased cell motility and invasiveness. A few signalling pathways, such as Wnt, Notch, TGF-β, hepatocyte growth factor (HGF) and platelet derived growth factor (PDGF) play a role in initiating EMT (58).

MiRNAs are regulators of EMT in CRC by either modulating the expression of oncogenes and tumor suppressors or partly by acting as tumor promotor or tumor suppressor themselves. These important regulatory features of miRNA-activated upstream factors are inducing the EMT process (59). For instance, the miR-200 family (including miR-200a, miR-200b, miR-200c, miR-141, and miR-429) plays an important role in the regulation of EMT in cancer, including CRC (60). The miR-200 family members were shown to increase E-cadherin expression by binding complementary sites in the 3'UTR of Zeb1 and Zeb2 gene. It has been demonstrated that Zeb 1 is a key transcriptional repressor of the basement membrane components in CRC. Loss of this basement membrane was considered as a key step in inducing cancer progression and metastases (61, 62). Additionally, a study by Pichler *et al*. showed that high miR-200a expression is linked with membranous E-cadherin expression in CRC and a decrease of miR-200a expression is associated with poor survival of CRC patients. Their study revealed that miR-200a is a regulator of EMT-related gene expression and seems to be differentially expressed in CRC stem cells, suggesting that miR-200a might be a potential drug target in CRC (63).

Invasion and metastasis

The process of cancer progression and metastasis involves several events including local cancer cell invasion, cancer cell migration into blood vessels, survival in the circulatory system, extravasation and colonization of distant organs (64). Notably, each of these events has been shown to be associated with dysregulated miRNA expression (58). For example, miR-21 overexpression is commonly observed in human CRC, which is associated with metastasis development in CRC. It has been shown that CRC cell lines expressing high levels of miR-21 positively regulating invasion and migration ability (65, 66). A study by Harris *et al*. demonstrated that miR-126 directly targets the vascular cell adhesion molecule 1 (VCAM-1) gene that regulates adhesion of lymphocytes to vascular endothelium, which may be helpful to circulating cancer cells (67). MiR-155 and the miR-17-92 cluster have been suggested to play a key role in B cell differentiation as well as inducing the regulation of T cell lineage pathways, which may support immune evasion of cancer cells in blood circulation (68).

Several miRNAs might be key regulators in metastasized cancer cell survival in distant organs. An increasing number of studies have reported the existence of CRC stem cells, and miRNAs are known to play a role in the regulation of the 'stemness' of cancer cells. For instance, miR-34a might acts as a cell-fate determinant to choose between self-renewal and differentiation in early-stage CRC stem cells, as demonstrated by a study by Bu et al. (69).

2. Aim of the study

Since miRNAs might serve as predictive and prognostic factors and even as therapeutic targets we aimed to identify miRNAs as novel biomarkers in CRC. Several miRNAs are already known to be dysregulated in CRCs and have been linked to biological processes involved in tumor progression and response to anti-cancer therapies. In the present thesis we wanted to examine the clinical and biological relevance of miR-196b-5p and miR188-3p and study the molecular pathways regulated by these miRNAs in CRC.

The following steps were taken to achieve these goals:

- Quantification of miRNA expression levels in CRC patient samples by qRT-PCR and analysis of genome-wide miRNA sequencing data of CRC patients from the cancer genome atlas (TCGA)
  - Comparison of miRNA expression levels between CRC tumors and corresponding normal mucosa
  - Analysis of miRNA expression in clinically relevant CRC cancer subsets (i.e. regarding tumor grading, age at diagnosis, histology as well as KRAS, NRAS, BRAF mutational status
  - Overall survival analysis

- Characterization of the biological role of these two miRNAs
  - Performing *in vitro* proliferation (WST-1) and migration/invasion assays (Scratch assay, Transwell assay, Real Time migration and invasion assay)
  - Testing the influence of these two miRNAs on sensitivity to chemotherapeutic drugs
  - *In vivo* confirmation of *in vitro* observations in nude mice

- Identification of molecular mechanisms regulated by miR-188-3p and miR-196b-5p
  - Microarray analysis to identify potential interacting partners
  - In silico analysis to search putative target genes
  - Luciferase assay to confirm a direct interaction of miRNA and mRNA target
  - "Pheno-copy" experiments

3. Materials and Methods

3.1 Cell culture

3.1.1 Cultivation of cell lines

The human CRC cell lines HRT18, RKO and HCT116 and the embryonal kidney cell line HEK were purchased from American Type Culture Collection (Manassas, CA, USA) and their origin was proven by DNA identity STR-analysis by the Core facility at the Center for Medical Research (Medical University of Graz). For HCT116 McCoy's 5A modified Medium (w/o L-Glutamine, 2.2g/L sodium bicarbonate) was used. HRT18 cells were maintained in RPMI 1640 (GIBCO Lifetech, Vienna, Austria) containing 2mmol of L-glutamine. For RKO cells EMEM (w/o L-Glutamine) was used. HEK cells were grown in DMEM (4.5 g/L glucose). All growth media contained 10% foetal bovine serum gold (Biochrome, Austria) and antibiotics (50 units per ml of penicillin, 50µg/ml of streptomycin). Cells were incubated in a 5% CO_2 humidified atmosphere at 37°C.

3.1.2 Trypsinization of cells

Adherent cells need to be detached from culture flasks before counting and seeding them again in the desired culture well or flask (Corning, Corning, NY). Detachment of cells was performed using trypsin/EDTA (Invitrogen, Carlsbad, CA). First, culture medium was removed and cells were washed with pre-warmed (37°C) Phosphate Buffered Saline (PBS; 4ml for 75cm^2 flasks, 2ml for 25cm^2 flasks or 1ml for 6 well plates, respectively). Afterwards, pre-warmed 1X trypsin/EDTA (2ml for 75cm^2 flasks, 1ml for 25cm^2 flasks or 0.5ml for 6 well plates, respectively) was added and incubated for 3-5 minutes until single cells are present (control under microscope). To stop the reaction, 3-fold volume of culture medium containing FBS was added. Detached cells were resuspended in culture medium, collected in a 15ml falcon tube (Falcon ® Corning, Corning, NY) and centrifuged for 5 minutes at 800 rpm (rounds per minute). The supernatant was removed and the cell pellet was resuspended in 10 ml of fresh medium. Cell counting and determination of viability was done using a Biorad TC20 Cell Counter (Biorad, Hercules, CA). Therefore, 10 µl of cell suspension were mixed with 10 µl of trypan blue (Sigma) and were applied to a chamber of a Biorad Cell Counting slide. The appropriate amount of cell suspension was then transferred to a new tissue culture flask or well plate.

3.1.3 SiRNA transfection

CRC cells were cultured in complete growth medium containing 10% FBS and 1% penicillin/streptomycin (50 units per ml of penicillin, 50 µg/ml of streptomycin) at 37°C. Cells were trypsinized and transiently transfected with siRNA for *HOXB7* (20 nM, Hs_HOXB7_1, Qiagen, Hilden Germany), *GalNT5* (20 nM, Hs_GalNT5_1, Qiagen) or *MLLT4* (20nM, Hs_MLLT4_5, Qiagen) mRNA using the fast forward transfection procedure according to the HiPerFect Transfection Reagent (Qiagen) protocol. As a negative control, the AllStars Negative Control (20 nM, Qiagen) was used. In detail, 2.3 ml growth medium containing $2{,}5x10^5$ cells were seeded in each well of a 6 well plate (Corning, Corning, NY) and a transfection mix containing 20 nM of respective siRNA, 10 µl of HiPerfect Transfection Reagent and serum-free medium (total volume 100 µl) was prepared. The transfection mix was incubated for 10 minutes at room temperature and was then added to the cells. Transfected cells were incubated under their normal growth conditions (37°C, 5% CO_2). RNA and protein isolation was performed after 48 and 72 hours, respectively.

3.1.4 MiRNA transfection

For a transient transfection approach with the aim to reduce or overexpress the miR196b-5p or miR-188-3p expression, CRC cells were transfected using the fast forward transfection protocol as suggested by the HiPerFect Transfection Reagent (Qiagen) protocol according to the manufacturer's instructions. In detail, 2,3 ml of growth medium containing $2{,}5x10^5$ cells per well in a 6 well plate (Corning, Corning, NY) were seeded and a transfection mix containing 50 nM of respective miRNA mimic (50 nM, Syn-Hsa-mir196b-5p or 50 nM of Syn-Hsa-mir188-3p Qiagen), inhibitor (50 nM, Anti-Hsa-mir196b-5p or 50 nM of Anti-Hsa-mir188-3p , Qiagen) or respective control (50 nM, AllStars Negative Control, Qiagen), 10 µl of HiPerfect Transfection Reagent and serum-free growth medium (total volume 100 µl) was prepared. The transfection mix was incubated for 10 minutes at room temperature and was then added to the cells. Transfected cells were incubated under their normal growth conditions (37°C, 5% CO_2). MiRNA isolation was performed 48 hours post transfection. Protein isolation was done after 48 and 72 hours.

3.1.5 Lentiviral particles transduction

CRC cells were seeded in 12-well plates (Corning) at a density of $1x10^5$ cells per well 24 hours prior to viral infection and incubated overnight in 2 ml of complete growth medium containing 10% FBS and 1% antibiotics (50 units per ml of penicillin, 50 µg/ml of streptomycin). On the day of transfection the medium was removed and 2 ml of complete growth medium containing 8 µg/ml polybrene (Santa Cruz Biotechnology, Santa Cruz, CA) and 5 µl of ViralPlus Transduction Enhancer (ABM, Richmond, BC, Canada) were added. Cells were infected by adding 20 µl ($\geq$ $1x10^7$ TU/mL) of miR196b-5p overexpression lentiviral particles (shMIMIC Human Lentiviral microRNA hsa-miR-196-5p, Dharmacon, Vienna, Austria) miR196b-5p silencing lentiviral particles (ABM) or blank control lentiviral particles (ABM) respectively. For miR-188-3p overexpression in HCT116 cells we used 20 µl ($\geq$ $1x10^7$ Transduction units/mL) of shMIMIC Human Lentiviral microRNA hsa-miR-188-3p (Dharmacon, Vienna, Austria). Stably transfected HCT116 and RKO cells were incubated under their normal growth conditions (37°C, 5% CO_2) and selected for three weeks using 0.5 µg/ml puromycin dihydrochloride (Gibco, Carlsbad, CA) and HRT-18 cells were selected by adding 2.5 µg/ml puromycin dihydrochloride, respectively (70). Optimal puromycin concentrations were determined for each cell line testing a range of different concentrations (0.25 – 2.5 µg/ml).

3.2 Cellular Assays

3.2.1 WST-1 proliferation assay and chemotherapeutic resistance assay

To test whether altered miRNA expression influences cellular growth rates of CRC cells, we applied the WST-1 proliferation assay (Roche Applied Science, Mannheim, Germany). In more detail, 50 nM of respective miRNA mimic (50 nM, Syn-Hsa-mir196b-5p or 50 nM of Syn-Hsa-mir188-3p Qiagen), inhibitor (50 nM, Anti-Hsa-mir196b-5p or 50 nM of Anti-Hsa-mir188-3p , Qiagen) or respective control (50 nM, AllStars Negative Control, Qiagen) were mixed with RNAse free water (up to a volume of 25 µl) and added per well of a 96 well plate (Corning). Afterwards, 24.25 µl of serum free medium and 0.75 µl of HiPerfect Transfection Reagent (Qiagen) were added to each well and incubated for 10 minutes. After standard trypsinization, 150 µl of growth medium containing $3x10^3$ CRC cells per well of a 96 well plate were added to the transfection mix. Cells were incubated under their normal growth conditions (37°C, 5% CO_2) and WST-1 proliferation reagent (diluted 1:10 in gowth medium; Roche Applied Science, Mannheim, Germany) was applied after 24, 48,

72 and 96 hours according to the manufacturer's recommendations. After three hours the colorimetric changes were measured using a SpectraMax Plus (Molecular Devices, CA, US) at a wavelength of 450 nm with a reference wavelength at 620 nm. Three independent experiments in six technical replicates were performed.

The same assay was used for testing the chemotherapeutic resistance of cells to 5-Fluorouracil, Irinotecan and Oxaliplatin. In detail, 24 hours after transient transfection of CRC cells in wells of a 96-well plate growth medium was aspirated and 100 µl of growth medium with seven different two-fold diluted concentrations of 5-Fluorouracil (0-40 µM), Oxaliplatin (0-30µM) or Irinotecan (0-30 µM) were added to the cells. After 96 hours, the WST-1 assay (diluted 1:10 in growth medium) was applied and incubated for three hours and the relative optical density compared to untreated cells was calculated.

3.2.2 xCELLigence system

Cell migration of transiently transfected CRC cell lines was assayed using the xCELLigence Real-Time Cell Analyzer (RTCA; Roche Diagnostics Mannheim, Germany). In detail, transfected cells were washed with 2ml of PBS, trypsinized and centrifuged at 800 rpm for four minutes. The supernatant was removed and cells were resuspended in 500µl of serum-free medium. Cells were plated in each well of a CIM-plate-16(Roche) in 70 µl of serum-free medium at a density of $6x10^4$ cells. For the invasion assay CIM-plate-16 wells were pre-coated with 20 µl of matrigel diluted 1:40 in growth medium for 0.5 h at 37°C. The lower medium chamber contained 160 µl of growth medium with 10% FBS (the serum should attract the cells to move through the membrane of the CIM-plates). Cells were allowed to settle for 30 minutes at room temperature before being placed in the RTCA in a humidified incubator at 37°C with 5% CO_2. As cells move from the upper chamber towards attractant in the lower chamber they pass through a membrane containing 8 µm pores and then adhere to gold impedance microelectrodes. The resultant change in impedance signal correlates with the number of cells attached to these electrodes. Measurements of the cell index (CI) were performed every 15 minutes for 48 hours. Data acquisition and analyses were performed using the RTCA software (version 1.2, Roche Diagnostics). Three replicates of each cell line were performed.

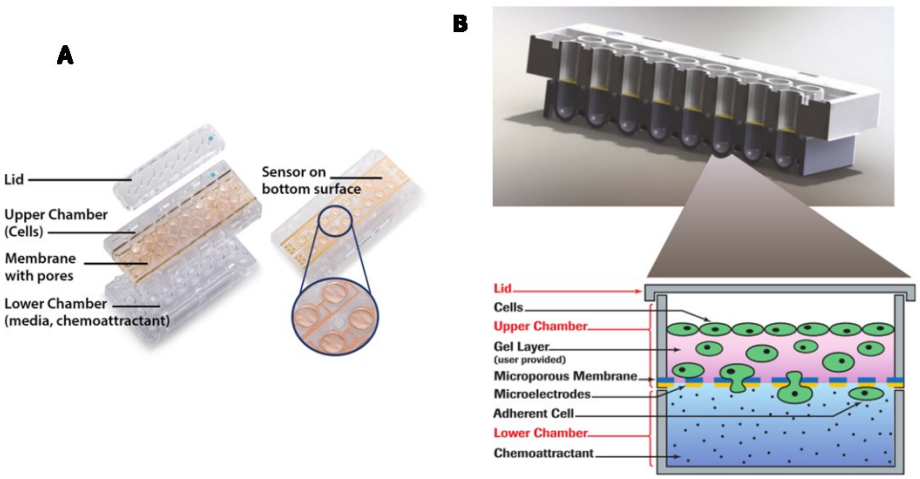

Figure 1: CIM-Plate Overview. (A) CIM-Plate components. (B) CIM-Plate detail. The expanded view shows the upper and lower chambers for a single well. The bottom surface of the upper chamber consists of a microporous membrane that cells can migrate through. Gold electrodes on the underside of the membrane detect the presence of adherent cells. Figure taken from: ACEA Biosciences; http://aceabio.com/applications/cell-invasion-and-migration.

3.2.3 Transwell migration assay

Transwell migration assay was conducted on CRC cells following stable or transient transfection with the specific miRNA mimic, inhibitor or the respective control. First, the coating of transwell inserts was performed. Therefore, transwell plates (Multiwell 24-well plate, polystyrene, Becton Dickinson) were assembled with Inserts (8 µm pore size, 3097 Cell Culture Inserts, 24-well format, Becton Dickinson). 100µl of 0.1% gelatine in 0.02M acetic acid (Sigma, Seelze, Germany) for migration or a defined matrix for invasion (Type IV collagen (0,8 µg/ml, Sigma), Human Laminin (0,05µg/ml, Sigma), Gelantin (2 mg/ml, Sigma) and PBS) were added per insert for coating the membrane under sterile conditions. The solutions were incubated at room temperature for one hour on a rotating platform. Afterwards, the liquid was taken out from the top using a pipette tip and incubated in the hood for one hour until the membrane was dried. Cells were starved in serum-free medium overnight before the experiment was performed. 500µl of serum-free growth medium was added per insert (also in the companion well below) and incubated at 37°C for one hour. Before seeding the cells, the medium in the insert and well was removed. 750 µl of serum-containing growth medium were added to the lower wells (the serum should attract the cells to migrate through the pores in the insert).

After 24 hours of incubation (37°C, 5% CO_2) for migration and 48 hours for invasion, cells were fixed and stained with 0.05% crystal violet in 25% ethanol/PBS. In detail, the cells in

the upper well were removed using a pipette tip and 500 µl of cold methanol were added and incubated at 4°C for 15 minutes to fix the cells. The inserts were rinsed with 2% ethanol briefly and 750 µl of 0.05% crystal violet in 25% ethanol/PBS were added and incubated for 15 minutes at room temperature. A cotton swab was used to remove cells that might be in the upper well side. Inserts were then rinsed with distilled water until the excess colour washed off. The membrane was dried for one hour and the number of migrated cells was counted (average of three representative areas of the membrane) using a light microscope at 10x magnification. The picture below shows a schematic set-up of the transwell system.

3.2.4 Wound healing assay

To further monitor cellular migration with a third independent method an *in vitro* wound-healing assay was performed. After transient or stable transfection, cells were washed with PBS, trypsinized and centrifuged at 800 rpm for four minutes. Supernatant was removed and cells were resuspended in 500 µl of serum-free medium. 70 µL of serum-free medium containing 5×10^4 cells were seeded in each chamber of an ibidi culture insert (ibidi GmbH, Martinsried, Germany.) in a 6-well plate. After 24 hours of incubation, the culture inserts were removed from the surface to form a defined gap in the cell monolayer. Cells were washed with PBS and medium containing 10% FBS was added and cancer cell migration toward the gap area was documented using a microscope at 10x magnification for a time period of 48 hours. The size of the gap at a selected position was measured using the cellSense Imaging software (Olympus, Hamburg, Germany) at the starting point of the experiment (0h= 0 hours), after 24 hours (24h) and up to 48 hours (48h). The ratio of the gap size at certain time points to the gap size at 0 hours (starting point) was calculated and replicates were averaged.

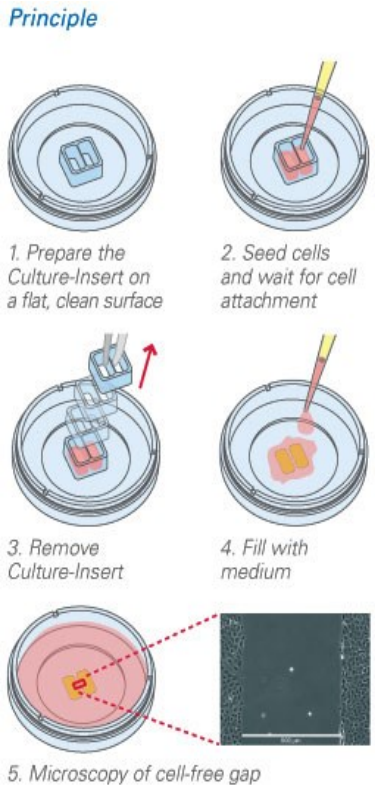

Figure 2: Schematic illustration of ibidi scratch assay. Cells are seeded in culture inserts. After cell attachment the insert is removed and cells are washed once with PBS. Afterwards medium is added and the scratch wound closure is observed over a certain time period. Figure taken from: Ibidi; http://ibidi.com/applications/wound-healing-and-migration/handling-of-culture-inserts

3.3 Xenograft model

3.3.1 Labelling of stably transduced cells

For labelling, CRC cells were seeded in 12-well plates (Corning) 24 hours prior to viral infection and incubated overnight in 2 ml of complete growth medium containing 10% FBS and 1% antibiotics. On the day of transfection the medium was removed and 2 ml of complete growth medium containing 8 µg/ml polybrene (Santa Cruz Biotechnology, Santa Cruz, CA) and 5 µl of ViralPlus Transduction Enhancer (ABM, Richmond, BC, Canada) were added. Afterwards, cells were infected by adding 10 µl of Lentiviral Dual Reporter Imaging Construct ($\geq 1x10^7$ Infection Units/ml; CMV-RFP-T2A-Luciferase, Biocat. Heidelberg, Germany) and incubated under their normal growth conditions (37°C, 5% CO_2).

3.3.2 In vivo metastases formation and bioluminescence imaging

This experiment was performed by a commercially external facility (EPO Berlin-Buch GmbH, Berlin, Germany) which was completely blinded to the other results of our studies. $2x10^6$ HCT116 cells were injected at a volume of 20µl into the spleen if NMRI:nu/nu mice (Janvier Labs, Paris, France). Per group 7-8 mice were inoculated with cells (HCT116 cells with either a miRNA (miR-196b-5p or miR188-3p) stable overexpression, inhibitor (for miR-196b-5p) or control construct, respectively, and afterwards received Tramadol for six days for pain suppression. All animal experiments were performed according the guidelines of the German Animal Protection Law and with approval by the local responsible authorities. Mice were observed daily for their health status. Body weight was measured twice per week as a parameter of health condition. Mice were sacrificed 33 days after cell injection and the size and number of liver metastases and intra-abdominal metastases as well as the presence of ascites were assessed. Bioluminescence measurement was performed to monitor the engraftment of metastases. Bioluminescence imaging of all mice were performed from dorsal up to five times. 5 mg/kg Luciferin (30mg/ml in distilled water, AAT Bioquest) was injected i.p. (intraperitoneal) and inoculated for 5 minutes before mice were anesthetised by inhalation of isoflurane. The measurement was done in a VisiLuxx Immager (Visitron System GmbH). The VisiView Software made enabled to take a bright field picture first. Afterwards 10 pictures with an exposition time of 30 sec were done to measure the luminescence signal. Signals were analyzed with the MetaMorphOffice Software. Single luminescence signals were collected and an overlay emerged from the luminescence signal and the bright field picture (70).

3.4 Gene expression analysis

3.4.1 RNA Isolation

Cells were cultured in well plates or tissues culture flask and after reaching 70-80% confluency cells were ready for RNA Isolation. Therefore, cells were washed with 1x PBS and afterwards 1 ml of TRIZOL reagent (Invitrogen, Carlsbad, CA) was directly added to the cells. Cells were transferred to a 2 ml Eppendorf tube (Eppendorf, Harmburg, Germany) and homogenized by passing through syringe and needle. Homogenized samples were incubated for 5 minutes at room temperature to permit the complete dissociation of nucleoprotein complexes.

For phase separation 100µl of BCP (Sigma) per 1 ml of TRIZOL reagent were added. Samples were vigorously vortexed for 15 seconds and incubated at room temperature for 2 to 3 minutes. Samples were centrifuged at 13000 rpm for 15 minutes at 4°C. Following centrifugation, the mixture separates into lower red, phenol-chloroform phase, an interphase, and a colourless upper aqueous phase. RNA remains exclusively in the aqueous phase. The upper aqueous phase was transferred carefully into a fresh tube without disturbing the interphase.

The RNA was precipitated by mixing the aqueous phase with 500 µl of isopropanol (Sigma). The mixture was incubated for 10 minutes at room temperature and centrifuged at 13000 rpm for 30 minutes at 4°C. The supernatant was removed completely and the RNA pellet was washed once with 75% ethanol, adding at least 1 ml of 75% ethanol per 1 ml of TRIZOL Reagent used for the initial homogenization. The samples were mixed by vortexing and centrifuged at 8000 rpm for 5 minutes at 4°C. The washing procedure was repeated twice and afterwards, ethanol was completely removed. The pellet was then air-dried and dissolved in RNAse free water.

3.4.2 cDNA synthesis

<u>mRNA</u>

For mRNA quantification, 1000 ng of total cellular RNA were reverse transcribed using the QuantiTect Reverse Transcription Kit (Qiagen, Hilden, Germany) according to the manufactor's instructions. First, a genomic DNA elimination step was performed at 42°C. The pipetting scheme for this step is listed in Table 1. The reactions were performed in a Biorad Thermo Cycler (Biorad, Hamburg, Germany). Afterwards, the reverse transcription

was done using the reaction mix listed in Table 2. The thermal cycling conditions are listed in Table 3.

Table 1: Genomic DNA elimination reaction

Reagents	Volume (µl)
gDNA Wipeout Buffer (7x)	**2**
RNase free water (up to 12 µl)	**x**
RNA (1000 ng)	**y**
Total	**14**

Table 2: Mastermix for cDNA synthesis

Reagents	Volume (µl)
QuantiScript Reverese Transcriptase	**1**
QuantiScript RT Buffer (5x)	**4**
RT Primer Mix	**1**
Template RNA (1000 ng)	**14**
Total	**20**

Table 3: Cycling program for cDNA synthesis

Temperature (°C)	**Time (min)**
42	**15**
95	**3**

miRNA

For quantification of miRNAs, 1000 ng of total cellular RNA were reverse transcribed using the miScript II RT kit (Qiagen) according to the manufactor's instructions. The pipetting scheme of the cDNA mastermix is listed in Table 4. The reactions were performed in a Biorad Thermal Cycler (Biorad). The thermal cycling conditions are listed in Table 5.

Table 4: Reverse Transcription reaction components (miRNA)

Reagents	Volume (µl)
MiScript Reverese Transcriptase Mix	**2**
MiScript High Spec Buffer (5x)	**4**
MiScript Nucleics Mix	**2**
RNase free water (up to 20 µl)	**x**
Template RNA (1000 ng)	**x**
Total	**20**

Table 5: Cycling program for cDNA synthesis (miRNA)

Temperature (°C)	**Time (min)**
37	**60**
95	**5**

3.4.3 Quantitative Real Time PCR (qRT-PCR)

Relative mRNA quantification

MRNA expression levels were measured using the Quantitect SYBR Green PCR kit (Qiagen) according to the manufactures instructions on a Light Cycler480 (Roche Diagnostics, Mannheim, Germany). QRT-PCR was done in triplicates for each sample

with specific primers (see Table 8). For relative gene quantification GAPDH and B2M were used as housekeeping genes. 1 µl of diluted cDNA (10 ng) and 24 µl of mastermix (see Table 6) were added to each well of a 96 well plate (Roche Diagnostics). The thermal cycling conditions are shown in Table 7.

Table 6: Mastermix for mRNA quantification by qRT-PCR

Reagents	**Volume (µl)**
Quantitect SYBR Green Master Mix (2x)	**12,5**
Forward primer (0,4 µM)	**1**
Reversed primer (0,4 µM)	**1**
RNasefree water	**9,5**
Template (10 ng)	**1**
Total	**25**

Table 7: Cycling conditions for qRT-PCR

Cycles	**Step**	**Target (°C)**	**Time (hh:mm:ss)**
1	Initial Activation	95	00:15:00
40	Denaturation	94	00:00:15
	Annealing	55	00:00:30
	Extension	72	00:00:30

Table 8: Primer sequences for qRT-PCR

GAPDH_fw AAGGTCGGAGTCAACGGATTT
GAPDH_rev ACCAGAGTTAAA AGCAGCCCTG
B2M_fw TGCTGTCTCCATGTTTGATGTATCT
B2M_rev TCTCTGCTCCCCACCTCTAAGT
GALNT5_fw TTGGAACATACGACCCTGGC
GALNT5_rev CACCACACATCCACACCTTG
HOXB7_fw TTCCTTCAACATGCACTGCG
HOXB7_rev TCAGTTCCTGAGCTTCGCAT
CPA4_fw AGGACCTGCAGATTTACCACG
CPA_rev GGGAGATCCACTCTCGGGAA
MUC13_fw GCTGTAACCAGACTGCGGAT
MUC13_rev TTGAGACTGGAAGCAACGCA
DKK1_fw TGACAACTACCAGCCGTACC
DKK1_rev CAGGCGAGACAGATTTGCAC
KRTAP2-3_fw AGCTGATCCTCAAGCACGAA
KRTAP2-3_rev GGGTGATGAGTCAGTGGGAC
KRTAP3-1_fw CTGCTGCAAGCCTGATACCT
KRTAP3-1_revGGTTGATCCCACTCAGTCCG
MLLT4_fw AAGCTGGCCGACATCATCC
MLLT4_rev AACTCCAAATCCTCGGTCGG
NLK_fw GGGGTCCTCATAAACAGCCAT
NLK_rev ACCAACATCCTGCAAAGGAGA
CTNNA2_fw CTGATCAGCTGGACAGTGCC
CTNNA2_rev AGGATGCTTTCACCGTGAGG

Relative miRNA quantification

Relative miRNA expression was determined using the miScript SYBR Green PCR kit (Qiagen) according to the manufactures instructions on a Light Cycler480 (Roche Diagnostics, Mannheim, Germany). QRT PCR was done in triplicates for each sample using specific miScript Primer Assays (Hs_miR-196b_1 or Hs_miR-188-3p_1). For relative miRNA quantification Rnu6b (Hs_RNU6-2_11) was used as housekeeping gene. 1

µl of diluted cDNA (1 ng) and 24 µl of mastermix (see table 9) were added to each well of a 96 well plate (Roche Diagnostics). The thermal cycling conditions are shown in table 10.

Table 9: Mastermix for miRNA quantification by qRT-PCR

Reagents	Volume (µl)
miScript SYBR Green Master Mix (2x)	**12,5**
miScript Primer Assay (10x)	**2,5**
miScript Universal Primer (10x)	**2,5**
RNase free water	**6,5**
Template (1 ng)	**1**

Table 10: Cycling conditions for miRNA qRT-PCR

Cycles	Step	Target (°C)	Time (hh:mm:ss)
1	Initial Activation	95	00:15:00
40	Denaturation	94	00:00:15
	Annealing	55	00:00:30
	Extension	70	00:00:30

3.4.4 Calculation of relative gene expression

Changes in mRNA or miRNA expression levels of the gene of interest in treated samples relative to their controls were determined using the ΔΔCt-method. ΔCt was calculated by subtracting the Ct-value of the housekeeping gene from the Ct-value of the gene of interest. ΔCt-value of control samples were subtracted from the ΔCt-value of the analysed samples to obtain the ΔΔCt-value. $2^{-\Delta\Delta Ct}$ was calculated to illustrate the results in a graph (71).

ΔCt = Ct gene of interest – Ct housekeeping gene

ΔΔCt = ΔCt sample – ΔCt control

3.4.5 Analysis of miRNA expression levels in patient samples

MiR-196b-5p

In order to investigate the prognostic value of miR-196-5p we measured this miRNA in two independent cohorts of middle European patients. In the cancerous tissue of 332 histologically confirmed CRC patients that were diagnosed between 2005 and 2012. In this bicenter study cohort, patient's tissues were provided from the Institute of Pathology, Medical University of Graz, Austria and the Department of Comprehensive Cancer Care, Masaryk Memorial Cancer Institute, Czech Republic (this cohort was analysed by Petra Vychytilova-Faltejskova, Marek Svoboda and Ondrej Slaby). The patients' clinico-pathological data were retrieved from medical records at the same institutions. All cases were reviewed based on pathology reports and histological slides for pTNM categories. Patients were treated by standard surgical procedures and received adjuvant treatment when appropriate (stage II with risk factors or stage III). Patients with advanced disease at the date of diagnosis received medical treatment according to the last version of European ESMO guidelines. Post-treatment surveillance of patients comprised routine clinical and laboratory examination. Regarding imaging methods, computed tomography was mainly used. Dates of death were obtained from the medical history, central registry of the Austrian or Czechia Bureau of Statistics or by telephone calls to their relatives. Relative quantification of miRNA expression by quantitative RT-PCR (qRT-PCR) was performed as followed: Two to eight 10 µm-thick tissue sections were used for microdissection to obtain areas with at least 70% tumour cell content. MiRNAs were isolated by Elke Winter (Institute of Pathology, Medical University of Graz) using the miRNeasy FFPE Kit 50 (Qiagen, Hilden, Germany) according to the manufacturer's instructions. cDNA was synthesized from 500 ng of total RNA using a miScript Reverse Transcription Kit (Qiagen). Quantification of miRNAs was performed using the miScript SYBR Green PCR kit (Qiagen) and the specific miScript Primer Assays for miR-196b-5p (hsa-miR-196b-5p, MIMAT0001080, assay name: Hs_miR-196b_1) and RNU6b (assay name: Hs_RNU6-2_11) (all miScript Primer Assays from Qiagen) according to the manufacturer's protocol on a Light Cycler 480 real-time PCR system (Roche, Mannheim, Germany).

MiR-188-3p

Screening set (cohort 1)

In order to perform a whole miRNA transcriptome analysis in CRC tissue, data of 228 publicly available patients were analyzed by Christina Ivan (MD Anderson Cancer Center; Department of Experimental Therapeutics, Houston, TX) (with complete follow-up information from the Cancer Genome Atlas Project (TCGA; http://tcga-data.nci.nih.gov/) for CRC patients (Download date: December 2014). In more detail, we used level 3 Illumina miRNASeq (Illumina Sequencing technology: Genome Analyzer) for miRNA expression analysis. We derived the "reads_per_million_miRNA_mapped" values for mature miRNAs from the "isoform_quantification" files. To narrow the identified potentially prognostic miRNAs, we used the following strategy: (1) MiRNAs that could not be detected (read count=0) in more than one third of the patient samples were excluded from further analyses, (2) subsequently, hazard ratios (HR) and corresponding 95% confidence intervals (CI) for the clinical endpoint overall survival were calculated by univariate Cox proportional models for each of the miRNAs, and (3) only miRNAs with a hazard ratio 95% confidence intervals <0.9 or >1.1 (and a p-value <0.05) were included for confirmation in the following validation cohort (70).

Validation set (cohort 2)

In order to validate the prognostic value of the miRNAs obtained from the screening set, we analyzed the expression of all the six potentially prognostic miRNAs in the cancerous tissue of 332 histologically confirmed CRC patients that were diagnosed between 2005 and 2012. In this bicenter study cohort, patient's tissue was derived from the Institute of Pathology, Medical University of Graz, Austria and the Department of Comprehensive Cancer Care, Masaryk Memorial Cancer Institute, Czech Republic (this cohort was analysed by Petra Vychytilova-Faltejskova, Marek Svoboda and Ondrej Slaby. The patients' clinico-pathological data were retrieved from medical records at the same institutions. All cases were reviewed based on pathology reports and histological slides for pTNM categories. Patients underwent standard surgical procedures and received adjuvant treatment when reasonable (stage II with risk factors or stage III). Patients with advanced disease at the date of diagnosis received medical treatment according to the last version of European ESMO guidelines (72). Post-treatment surveillance included routine clinical and laboratory examination. Regarding imaging methods, computed tomography was

predominantly used. Dates of death were obtained from the medical history, central registry of the Austrian or Czechia Bureau of Statistics or by telephone calls to their relatives as previously reported. MiRNA measurement by quantitative RT-PCR (RT-qPCR) was performed as followed: Two to eight 10 µm-thick tissue sections were used for microdissection to get areas with at least 70% tumor cell content. MiRNA isolation was performed by Elke Winter (Institute of Pathology, Medical University of Graz) using the miRNeasy FFPE Kit 50 (Qiagen, Hilden, Germany) according to the manufacturer's recommendations. cDNA was reverse transcribed from 500 ng of total RNA using a miScript Reverse Transcription Kit (Qiagen). Relative miRNA quantification was performed using the miScript SYBR Green PCR kit (Qiagen) and the specific miScript Primer Assay Hs_miR-92b_2 (MIMAT0003218: 5'UAUUGCACUCGUCCCGGCCUCC), Hs_miR-221*_1(MIMAT0004568: 5'ACCUGGCAUACAAUGUAGAUUU), Hs_miR-331_1(MIMAT0000760: 5'GCCCCUGGGCCUAUCCUAGAA), Hs_miR-425-3p_1(MIMAT0001343: 5'AUCGGGAAUGUCGUGUCCGCCC), Hs_miR-188-3p_1(MIMAT0004613: 5'CUCCCACAUGCAGGGUUUGCA), Hs_miR-497_1(MIMAT0002820: 5'CAGCAGCACACUGUGGUUUGU) and Hs_RNU6-2_11 (all miScript Primer Assays from Qiagen) according to the manufacturer's protocol on a Light Cycler 480 real-time PCR device (Roche, Mannheim, Germany). Relative miRNA expression levels were calculated using normalization to RNU6B (after the formula 2^-(target gene – RNU6B)) as described above (70).

3.4.6 Microarray analysis

In order to identify the most differentially expressed genes after miR-196b-5p overexpression of HCT116 cells, total RNA from three biological replicates of stably transfected HCT116 cells was isolated using the miRNeasy Mini Kit (Qiagen; Hilden, Germany; Cat No. 217004) according to the manual. The quality of total RNA was checked onma Bioanalyzer BA2100 (Agilent; Foster City, CA) for quality. All samples showed a RIN value (RNA integrity number) of 9,8-10, representing excellent quality.
The whole transcriptome analysis was performed by Karin Wagner (Center for medical research, Medical University of Graz) using Affymetrix Human Gene 2.0 ST mRNA Arrays (Affymetrix; Santa Clara, CA; Cat No. 902112). In detail, 250ng of the total RNA was amplified with Affymetrix WT PLUS Reagent Kit (Affymetrix; Santa Clara, CA; Cat No. 703147) as suggested by the manufacturers protocol. In addition, the cDNA was checked for quality on the BioAnalyzer BA2100 (Agilent, Foster City, CA) using the RNA

6000 Nano LabChip (Agilent; Foster City, CA; Cat.No. 5065-4476). An examination of ~250ng generated cRNA showed a fragment size > 2000nt which was satisfying for further analysis. The hybridization cocktail was prepared as suggested by the manual and hybridized on the arrays for 18 hours at 45°C while rotating in the hybridization oven. Washing and staining (GeneChip® HT hybridization, Wash and Stain Kit; Affymetrix, Santa clara, CA; Cat No. 900720) was performed with the Affymetrix Genechip® fluidics station 450 according to the manual (protocol on fluidics station: FS450_0002). Arrays were scanned with the Affymetrix GeneChip scanner GCS3000.

Hybridization controls and pre-analysis were evaluated using the Affymetrix Expression Console EC 1.3.1. Hybridizations were done at the Division Core Facility Molecular Biology at the Centre of Medical Research at the Medical University of Graz. Data pre-processing and filtering was performed using Partek Genomics Suite, v.6.6 (RMA (background correction, quantile normalization across all chips in the experiment, log2 transformation, median polish summarization)). Raw data are available at the Gene Expression Omnibus (GEO; accession number GSE86575).

3.5 Western Blot analysis

3.5.1 Protein isolation

Total proteins from stably or transiently transfected CRC cells were extracted with radioimmunoprecipitation assay (RIPA) buffer (150 mM NaCl, 50 mM Tris-HCl, pH 7.5, 1% Triton, 0.1% SDS, 0.1% sodium deoxycholate and 1% Nonidet P40). First, cells were washed with PBS and trypsinized. Detached cells were resuspended in culture medium, collected in a 15ml falcon and centrifuged for 5 min at 800 rpm. The cells were again washed twice with cold PBS and 100-300 µl of RIPA buffer supplemented with 0,1 M DTT (Sigma) 1 M PMSF (Sigma) and Protease inhibitor cocktail (Thermo Scientific, Rockford, IL) were added to the cell pellet. Cells were incubated with RIPA buffer for 30 minutes and vortexed every five minutes for complete cell lysis. Afterwards, the cell lysate was centrifuged for 15 minutes at 13.000 rpm and the supernatant containing the cellular proteins was transferred to a fresh Eppendorf tube. Total protein concentration was measured using the Pierce 660 nm protein assay (Thermo Scientific) according to the manufacturer recommendations.

3.5.2 SDS PAGE and wet transfer

20 µg of total cellular proteins were supplemented with 2x sample loading buffer and heated for 10 minutes at 65°C. Afterwards, protein extracts were subjected to electrophoresis on a 4–15% Mini-PROTEAN® TGX™Precast Gel (Biorad, Hercules, CA). In addition 10µl of Precision Plus Protein Prestained Standards (Bio-Rad) were loaded onto the gel to identify protein molecular weights. Proteins were separated at 150 V for one hour using 1x running buffer (25 mM Tris, 192 mM glycine, 0.1% SDS, Biorad). Afterwards proteins were transferred onto a nitrocellulose membrane (Biorad) at 90 V for 1.5 hours using 1x transfer buffer (25 mM Tris, 192 mM glycine, 20% ethanol, Biorad). To evaluate the quality of the transfer, the membrane was stained with ponceauS (Sigma).

3.5.3 Detection of protein expression

The membrane was blocked with 5% (v/v) blocking solution (5% non-fat milkpowder in TBS-T, Biorad) for one hour at room temperature. Immunoblotting was performed and antibodies specific for GalNT5 (ab103324, Abcam, diluted 1:1000 in 1% non-fat dry milk in Tris buffered Saline/0.1% Tween-20), HOXB7 (clone DML05, Millipore, Vienna, Austria, diluted 1:1000 in 1% non-fat dry milk in Tris buffered Saline/0.1% Tween-20))

and MLLT4 (Cell signalling, Denvers, MA; diluted 1:1000 in 1% non-fat dry milk in Tris buffered Saline/0.1% Tween-20) were incubated overnight at 4°C. The membrane was washed three times with TBS-T (Biorad) for 15 minutes. HRP-conjugated anti-mouse or anti-rabbit antibodies (diluted 1:1000 in 1% non-fat dry milk in Tris buffered Saline/0.1% Tween-20), respectively (Dako, Glostrup, Denmark), were applied and incubated for two hours and afterwards the membrane was washed again three times with TBS-T for 15 minutes. Visualization was performed using an enhanced chemoluminescence detection system (Super Signal West Pico, Thermo Scientific, Rockford, IL) on a ChemiDoc Touch System (Biorad).

3.5.4 Detection of β-actin protein expression

To normalize protein expression levels, β-actin expression was detected on the membrane. Therefore, the membrane was stripped using Restore Western Blot Stripping Buffer (Thermo Scientific, Rockford, IL) and reprobed with a monoclonal anti-β-actin antibody (Sigma, diluted 1:5000 in 1% (v/v) blocking solution) overnight at 4°C followed by incubation with HRP-conjugated rabbit-anti-mouse antibody (Dako, Glostrup, Denmark) for two hours at room temperature. Washing steps and immunodetection were performed as described above (see section 3.5.3).

3.5.5 Relative quantification of protein expression

Relative quantification of protein expression was performed using the ImageJ (NIH, Bethesda, Maryland) software. Therefore, the band density of the protein of interest was measured and divided by the density of the loading control beta actin.

3.6 Luciferase Reporter Assay

Studying the transcriptional regulation using reporter gene expression is very common in cell biology research and pharmaceutical discovery. Luciferase is the most widely used genetic reporter for such gene expression studies. Firefly and Renilla luciferases have been widely used as co-reporters for normalization studies. Firefly luciferase is a cytoplasmic enzyme with a molecular weight of about 61 kDa. The intensity of light emission is proportional to the amount of luciferase and is measured using a luminometer and luminescence plate reader. Renilla luciferase is a 36 kDa monomeric protein, which does not require post-translational processing. Therefore, it can function as a real-time transcription reporter.

3.6.1 *In silico* target prediction

MiR-196b-5p

First, gene expression data obtained from the microarray analysis were filtered for transcripts that were at least 2-fold down-regulated by miR-196b-5p. These genes were merged with an array of miRNA-target prediction tools (comprising 12 distinct algorithms) obtained from the miRWalk 2.0 database (73). Second, 3' untranslated region (3'UTR) sequences of the subset of transcripts were obtained from the European Bioinformatics Institute and the Wellcome Trust Sanger Institute (ENSEMBL). These sequences were screened for the presence of miR-196b-5p seed match types (8mer, 7mer-A1, 7mer-m8, 6mer, and offset 6mer sites (74). This analysis revealed *GalNT5* as a potential target of miR-196b-5p. Based on the identified region we generated Luciferase reporter constructs containing a wild-type (WT, 5'TTCCATATAGCCTAGGTGTGTAGTAGG**CTACCT**ACACCATCTAGGTTTGTG AAGTACAC3'; CS-HmiT011246-MT06-01; GeneCopoeia) and a sequence-modified (MT, 5'TTCCATATAGCCTAGGTGTGTAGTAGG**ATAAAT**ACACCATCTAGGTTT TGTAAGTACAC3'CS-HmiT011246-MT06-02; GeneCopoeia) *GalNT5 (*polypeptide N-acetylgalactosaminyl transferase-5) 3'UTR region. (The *in silico* target prediction analysis was performed by Michael Karbiener; Medical University of Graz)

MiR-188-3p

To identify possible molecular interactors of miR-188-3p that are related to cellular migration we retrieved putative miRNA-mRNA interactions by nine prediction algorithms

from miRWalk 2.0 data base (http://zmf.umm.uni-heidelberg.de/apps/zmf/mirwalk2). We also accessed experimentally validated miRNA-mRNA interactions from miRWalk and miRTarBase (http://mirtarbase.mbc.nctu.edu.tw). We identified several putative miRNA target sites for miR-188-3p for further analyses following these criteria: at least five (more than a half of the total number of programs checked) algorithms predicted miRNA-mRNA interaction, or there was strong experimental evidence of miRNA-mRNA interaction. We identified MLLT4 as a potential target of miR-188-3p and generated Luciferase reporter constructs containing the wild-type (WT, 5'TGGTTCAGTGATTGCTTAAATGGCATGTGGACCGTGGGAAGCAGTAGGAGCG TAGTAAGA3'; CS-HmiT011246-MT06-01; GeneCopoeia) and a sequence-modified (MT, 5'TGGTTCAGTGATTGCTTAAATGGCATGTGGACC**A**T**AAAC**GCAGTAGGAGCGT AGTAAGA3'; CS-HmiT011246-MT06-02; GeneCopoeia) MLLT4 3`UTR region (70).

3.6.2 Transient transfection

We ordered the pEZX-MT06 target reporter vectors containing the putative miRNA binding site (from GeneCopoeia) and transiently transfected them into HEK cells by using the Lipofectamin 2000 reagents according to the manufacturer recommendations (Invitrogen, Carlsbad, CA). In detail, HEK cells were cultured in DMEM (high glucose) medium (Gibco, Vienna, Austria) containing 10% FBS and 1% penicillin/streptomycin at 37°C. The cells were seeded in 500 µl of growth medium in 24 well plates (Corning) and grown up to 70% confluency. Before transfection, the cells were washed with PBS and 400 µl of Opti-MEM® I reduced-serum medium were added to each well. A transfection mix containing miRNA mimic (50 nM, Qiagen), 200ng of pEZX-MT06-01 (WT) plasmid or pEZX-MT06-02 (MT) construct, respectively, was prepared. The solution was mixed with 2 µl of Lipofectamine 2000 (Invitrogen), filled up to a final volume of 100 µl with Opti-MEM® I reduced-serum medium (Invitrogen) and incubated for 30 minutes at room temperature. Afterwards, the transfection mix was added to the cells. As a 100% reference value we co-transfected the negative control (50 nM, AllStars Negative Control, Qiagen) and the plasmids. An empty control plasmid pEZX-MT06 (CmiT000001-MT06, GeneCopoeia, Rockville, MD) was co-transfected with the miRNA mimic or the respective negative control, respectively, to normalize the luciferase activity (70).

3.6.3 Luciferase assay

24 hours after transfection, cells were washed with PBS and lysed in 100 µl of 1x passive lysis buffer according to the Luc-Pair Luciferase Assay Kit 2.0 (GeneCopoeia, Rockville, MD). 20 µl of each lysate were transferred to wells of a white 96 well plate and 50 µl of the Firefly Luciferase Working Solution (FLuc Working Solution; Luc Sub I diluted 1:100 in Luc Buffer I) were applied. The solution was incubated for five minutes at room temperature for the Firefly Luciferase activity measurements following the instructions of the Luc-Pair Luciferase Assay Kit 2.0. Afterwards, 50 µl of Renilla Luciferase Working Solution (RLuc Working Solution; Luc Sub II diluted 1:100 in Luc Buffer II) were added to each sample, incubated for five minutes at room temperature and Renilla Luciferase activity was measured. The Luciferase assays were run on a LUMIstar Luminometer (BMG Labtech,Ortenberg, Germany) in three independent biological replicates.

3.7 In situ hybridisation

Fresh frozen tissue sections of three CRC tumors and adjacent normal colon mucosa were first digested using 5 µg/mL proteinase K at room temperature for five minutes and were then loaded onto Ventana Discovery Ultra for in situ hybridization analysis. The tissue samples were incubated with double-DIG labeled mercury LNA miR-188-3p probe (Cat # 38532-15, Exiqon, Woburn, MA) or control U6 snRNA probe (Exiqon) for 2 hours at 45 °C. The digoxigenin-label was then detected with a polyclonal anti-DIG antibody conjugated with Alkaline Phosphatase using NBT-BCIP as the substrate. The signal intensities of miR-188-3p and U6 expression were quantified by using the intensity measurement tools of the Image-Pro Plus software package (Media Cybernetics) as previously reported (40, 70). In situ hybridisation and analyis were performed at the Center for RNA Interference and Non-coding RNAs (Houston, TX) by Xinna Zhang.

3.8 Statistical analyses

All statistical analyses were performed using SPSS version 20 software (SPSS Inc., Chicago, IL, USA) or MedCalc software (version 13.1.2.0). Unpaired or paired student t-test, Fisher's exact test, Chi-squared test, Mann-Whitney and Kruskal-Wallis test were applied where appropriate to analyze the association between miRNA expression and clinico-pathological parameters. Data of gene expression was log2-transformed. Overall survival was defined as the time from date of diagnosis to the date of death by any cause,

and it was assessed using the Kaplan-Meier method. The log-rank test was performed to compare the survival curves of individual groups. Univariate and multivariate Cox proportional hazards models including age, gender, tumor location, tumor stage (according to the AJCC/UICC 2010 TNM classification) and miRNA expression levels (These analyses were performed by Christina Ivan and Martin Pichler (MD Anderson Cancer Center; The Center for RNA Interference and Non-coding RNAs, Houston, TX). To test the proportional Hazard assumption in cox models Schoenfeld residuals test was used. The reported results include hazard ratios (HR) and 95% confidence intervals (CI). The predictive accuracy of the multivariate models was quantified using the Harrel's concordance index (c-index). The interpretation of the c-index is similar to the interpretation of the area under a ROC curve. A value of 1.0 indicates that the features of the model perfectly separate patients with different outcomes while a value of 0.5 indicates the features contain prognostic information equal to that obtained by chance alone (70, 75). A two-sided $p<0.05$ was considered as statistically significant.

4. Results

4.1 The role of miR-196b-5p in CRC

4.1.1 MiR-196b as a prognostic factor

Fist, to investigate the clinical significance of miR-196b-5p expression in CRC patients, we measured miR-196b-5p levels by qRT-PCR in two independent cohorts and further evaluate its role as a potential prognostic factor in CRC treatment. Table 11 summarizes the characteristics of both cohorts.

Table 11: Comparison of clinico-pathological characteristics of CRC patients in 2 CRC cohorts (cohort 1 (n = 110); cohort 2 (n = 182))

		Cohort Nr. 1 (n=110)	**Cohort Nr. 2 (n=182)**	**p-value**
		No (%)	No (%)	
Age	median	62	64	p<0.05*
	minimum	31	30	
	maximum	80	92	
Sex	female	40 (36.4)	83 (45.6)	p<0.05**
	male	70 (63.4)	99 (54.6)	
Tumor stage	stage II	11 (10)	71 (39)	p<0.05**
	stage III	40 (36.4)	51 (28)	
	stage IV	59 (53.6)	60 (31)	
			GX 4 (2.2)	
Tumor grading	G1	2 (1.8)	45 (24.7)	p<0.05**
	G2	81 (73.6)	98 (53.8)	
	G3+G4	27 (36.4)	35 (19.2)	

To analyze whether miR-196b-5p expression is associated with clinico-pathological parameters and survival of CRC patients, the cohorts were dichotomized into two groups (low and high miR-196b-5p levels) in accordance with the criteria mentioned in the

Methods section. In cohort 1, low miR-196b-5p expression is significantly associated with stage IV CRC (i.e. metastatic disease, $p<0.05$, chi-square test), whereas no association was observed for gender, age or tumor grading (data not shown). In cohort 2, low miR-196-5p expression is associated with high (G3+G4) tumor grade and stage IV CRC ($p<0.05$, chi-square test). As shown in the Kaplan-Meier curves for 5-year overall survival of patients (Figure 3), low miR-196b-5p expression is significantly associated with poor prognosis in both independent cohorts ($p<0.05$, log-rank test).

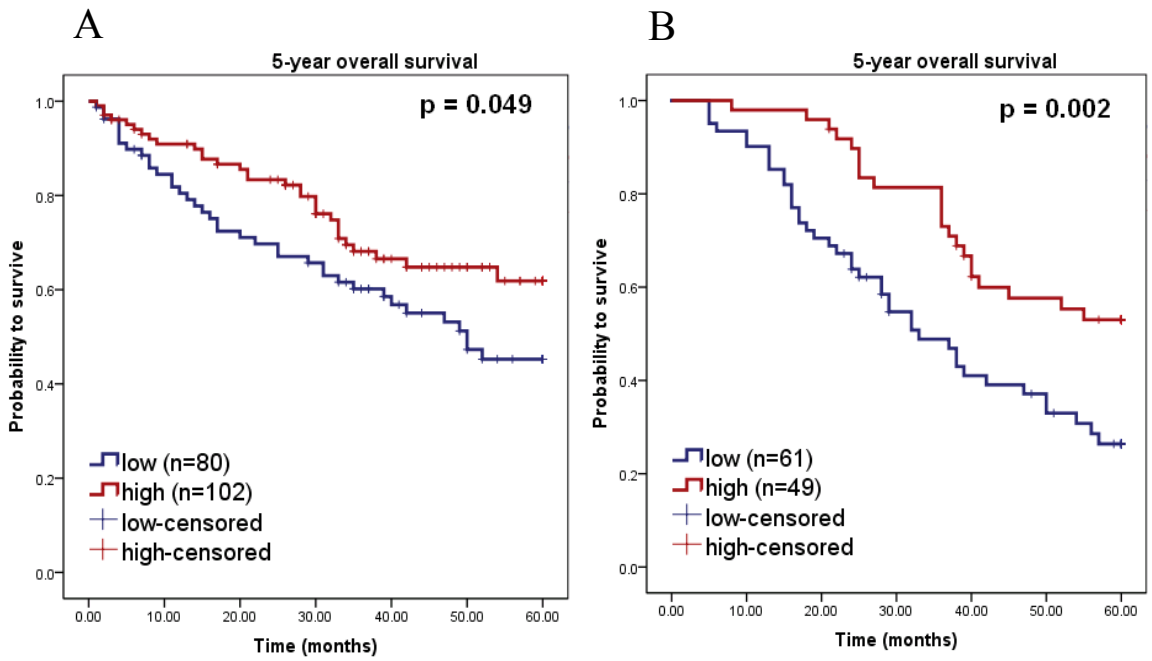

Figure 3: Kaplan Meier curves for overall survival. Kaplan-Meier curves for overall survival in cohort 1 **(A)** of 110 colorectal cancer patients. Patients were divided into two groups according to miR-196b-5p expression. A low of miR-196b- is a significant factor for poor prognosis ($p = 0.002$, log-rank test). In the cohort 2 **(B)** of 182 colorectal cancer patients low expression of miR-196b is a significant factor for poor prognosis ($p=0.049$, log-rank test).

4.1.2 MiR-196b-5p expression in CRC cell lines

Based on the findings that low miR-196b-5p expresison is significantly associated with metastases and poor patient outcome in both CRC cohorts analyzed, we further characterized the biological role of miR-196b-5p in CRC. Therefore, we measured the miR-196b-5p expression in eight different CRC cell lines using qRT-PCR and confirmed

the expression of this miRNA in CRC cells with some varying degree of expression levels. The calculated expression levels of miR-196b-5p are shown in Figure 4.

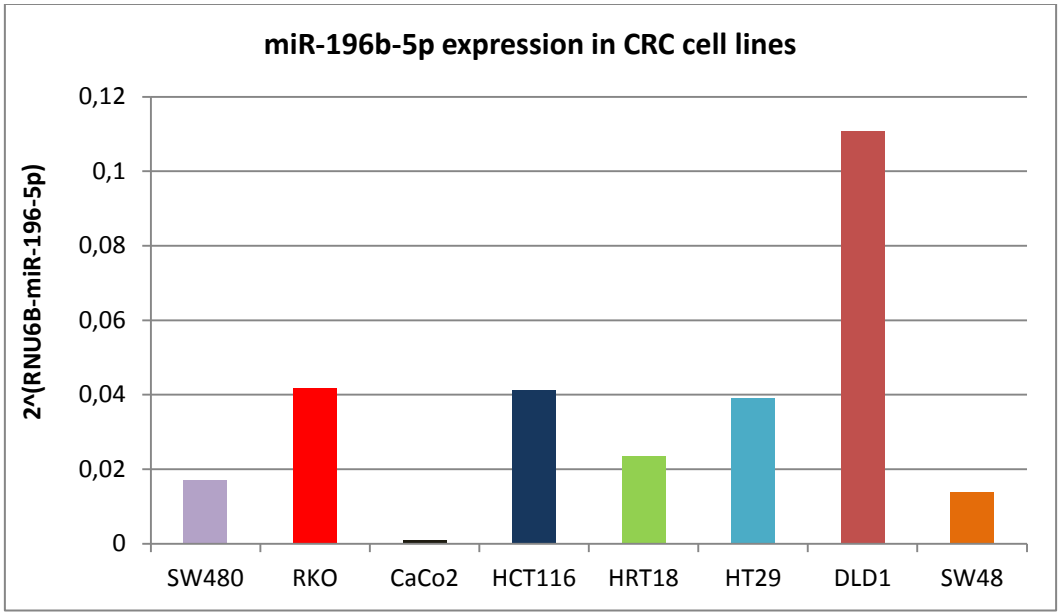

Figure 4: MiR-196b-5p expression in CRC cell lines. MiR-196b-5p expression was detected in all tested colorectal cancer cell lines at varying levels (n=8). Bar charts graph shows the expression levels of miR-196b-5p in eight different CRC cell lines as measured by qRT PCR.

4.1.3 The biological role of miR-196b-5p in CRC

To study the biological role of miR-196b-5p, we performed gain (miR-196b-5p mimic) and loss (miR-196b-5p inhibitor) of function experiments by transiently transfecting three independent CRC cell lines (HCT116, RKO and HRT18). To prove whether the transfection of these cell lines was successful we isolated the total cellular RNA after transient transfection and measured the miR-196b-5p expression by qRT-PCR. As shown in Figure 5 we could successfully overexpress and silence miR-196b-5p in all three cell lines.

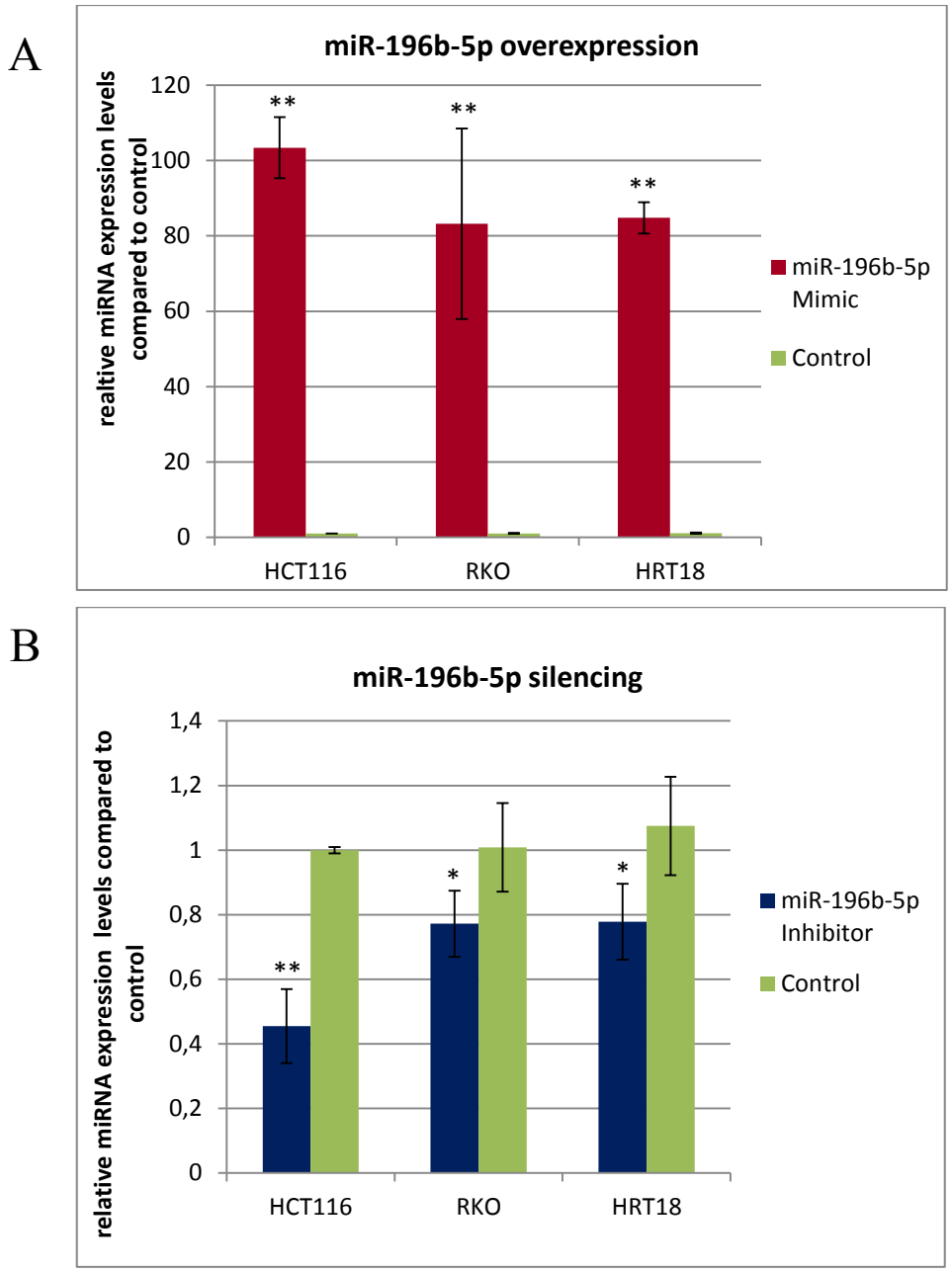

Figure 5: A statistically significant overexpression (A) or inhibition (B) of miR-196b-5p expression was confirmed by qRT-PCR after 48 hours of transient transfection in all three CRC cell lines. Transfection of inhibitor resulted in a 55% decrease of miR-196b expression levels compared to control in HCT116 cells. In RKO and HRT18 transfection of miR-196b-5p inhibitor led to 23% reduction of miR-196-5p expression compared to the control. (* = significant, $p < 0.05$; **, $p < 0.01$; ***, $p < 0.001$).

MiR-196b-5p expression does not influnce cellular growth of CRC cells

After confirming a successful transient overexpression or silencing of miR-196b-5p we checked wheter miR-196b-5p levels have an impact on cellular growth. By performing a

WST-1 cellular proliferation assay we could not detect any significant difference in cellular growth in HCT116 and HRT18 cells, whereas the RKO cells showed a slight but significant (p=0.0028) growth inhibition after 96 hours of transient overexpression (see Figure 6).

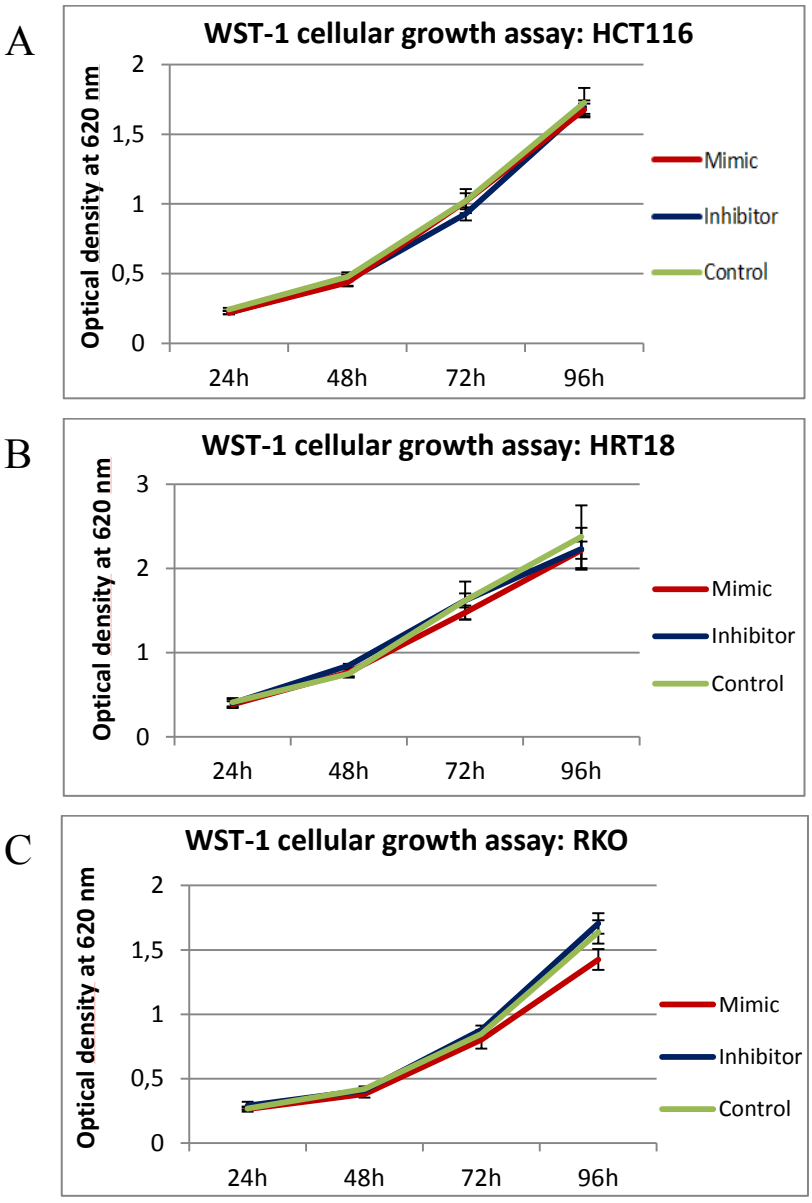

Figure 6: WST-1 Assay. Cellular growth of HCT116 **(A)** and HT18 **(B)** cells was not influenced after miR-196b-5p overexpression or inhibition, as measured by WST-1 assay. **(C)** RKO showed a significant (p=0.0028) decrease of cellular growth in miR-196b-5p overexpressing cells after 96 hours. (p-value <0.05 considered as significant).

Chemosensitivity of CRC cells is not influenced by miR-196b-5p expression levels

In regard to previously published studies about a possible link of miR-196b-5p expression and response to chemotherapeutic drugs (12, 13), we next analyzed the influence of miR-

196b-5p expression levels on drug sensitivity for the three most commonly used drugs in CRC treatment (5-Fluorouracil (0-40 µM), Oxaliplatin (0-30µM) and Irinotecan (0-30 µM). As shown in Figure 7-9, testing several concentrations of these drugs, we could not detect any significant differences regarding sensitivity to chemotherapeutic agents in CRC cells that were transiently transfected with miR-196b-5p mimic or inhibitor compared to control cells as measured by the WST-1 proliferation assay.

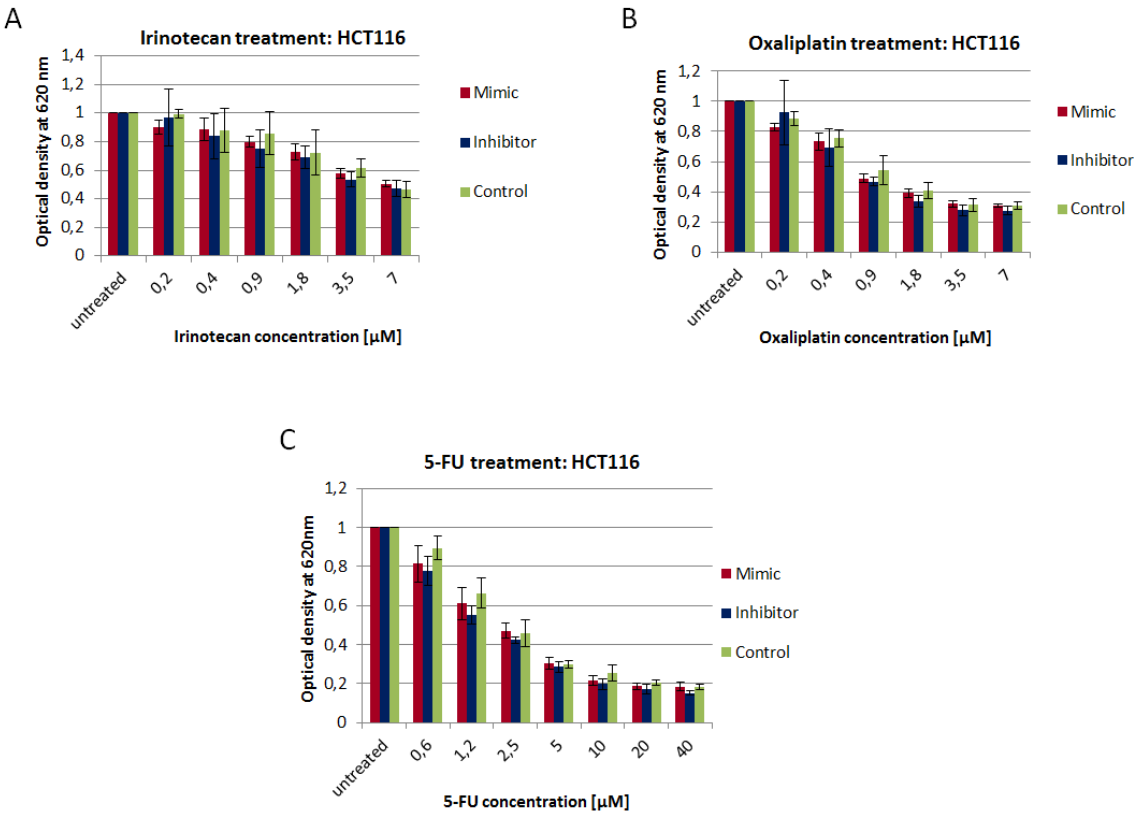

Figure 7: Chemosensitivity assays HCT116. **(A-C)** MiR-196b-5p expression levels did not show any significant effect on drug sensitivity against commonly used colorectal cancer drugs in HCT116 cells after transient overexpression or inhibition of miR-196b-5p expression as measured by WST-1 assay.

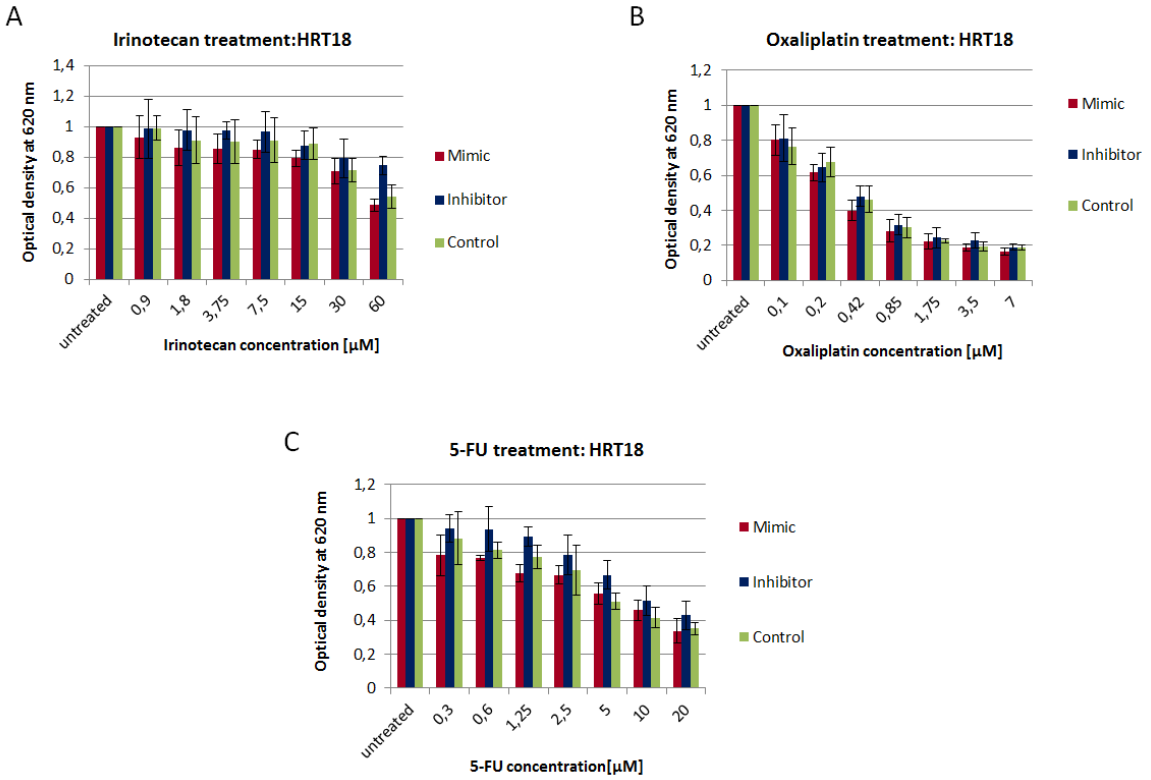

Figure 8: Chemosensitivity assays HRT18. (A-C) MiR-196b-5p expression levels did not show any significant effect on drug sensitivity against commonly used colorectal cancer drugs in HRT18 cells after transient overexpression or inhibition of miR-196b-5p expression as measured by WST-1 assay.

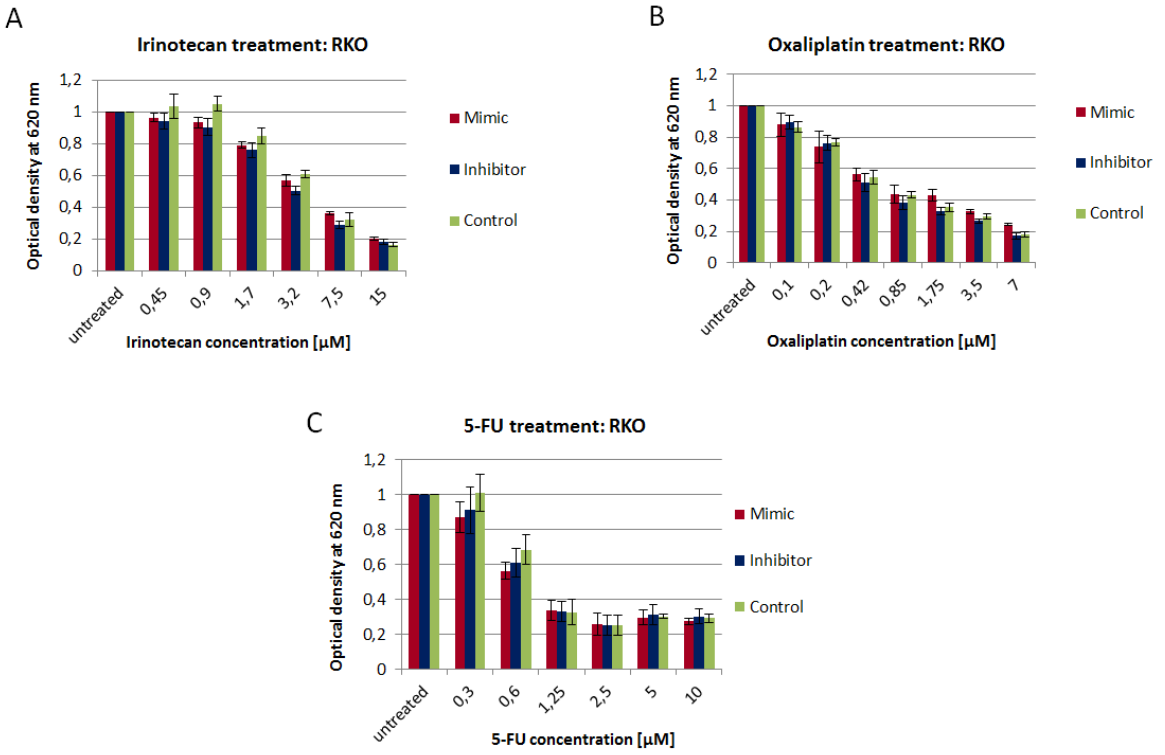

Figure 9: Chemosensitivity assays RKO. (A-C) MiR-196b-5p expression levels did not show any significant effect on drug sensitivity against commonly used colorectal cancer drugs in RKO cells after transient overexpression or inhibition of miR-196b-5p expression as measured by WST-1 assay.

MiR-196b-5p modulates cellular migration

After showing that miR-196b-5p does not influence celluar growth of CRC cells, we were further interested wheter miR-196b-5p expression has an effect on cellular migration. For this approach we analyzed the migration behavior after ectopic miR-196b-5p expression. Therefore, we used the real-time xCELLigence system, which enabled us to measure the migratory process at multiple time points over 48 hours. Transfection of CRC cells with the miR-196b-5p inhibitor (i.e. low miR-196b-5p levels) led to an increased migration rate in this model system, whereas overexpression of miR-196b-5p (i.e. mimic) resulted in low migration rates in HCT116 and RKO cells (Figure 10A-C).

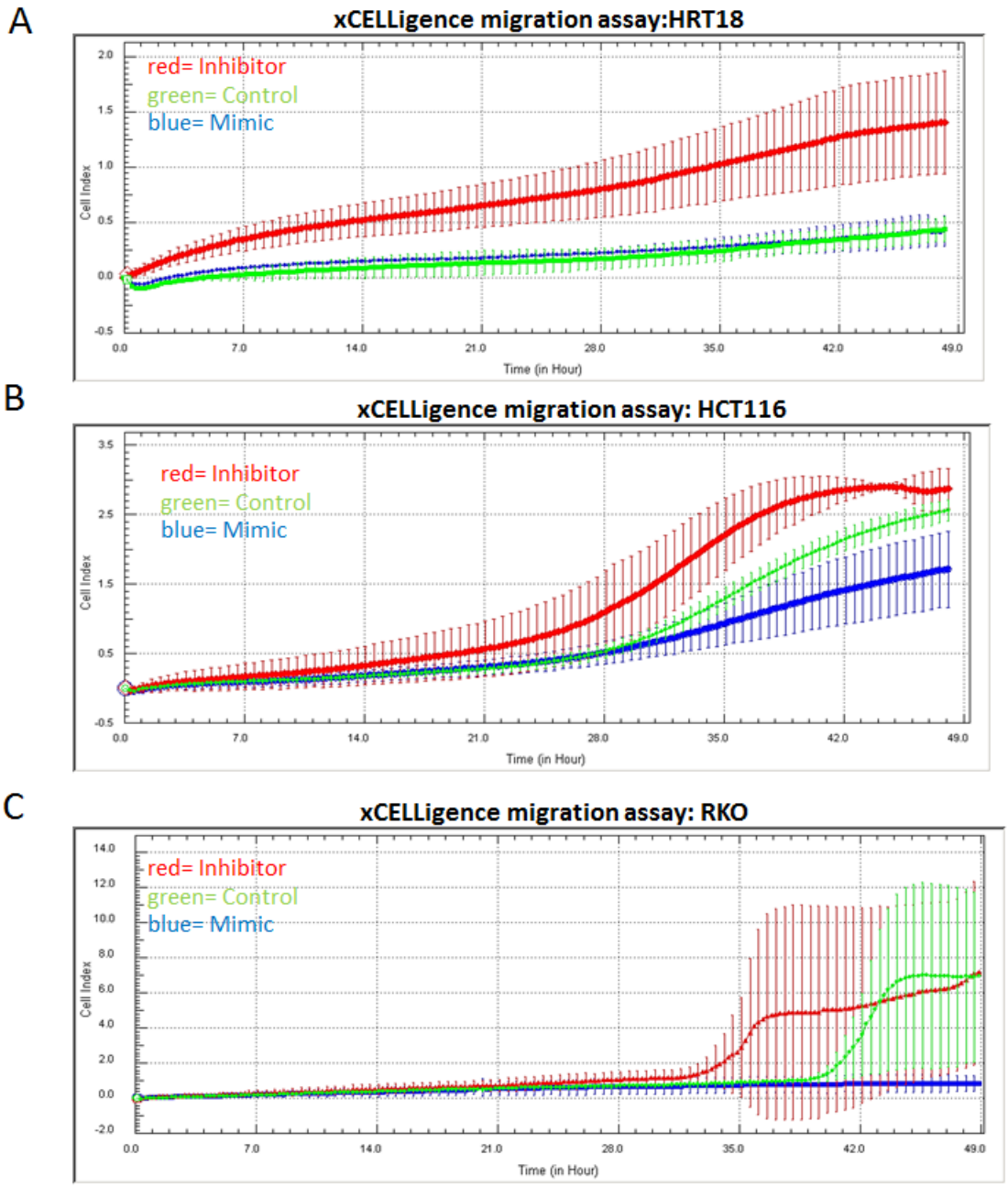

Figure 10: xCELLigence migration assay. Inhibition of miR-196b-5p resulted in higher migration rates in HRT18 cells **(A)** and HCT116 cells **(B)** as measured by the xCELLigence Real Time system ($p<0.05$= significant; n=3). Overexpression of miR-196b-5p led to decreased migration rates in RKO cells **(C)**.

To confirm these resuts with an independent method, we performed a transwell migration assay and a scratch assay using all three cell lines. The scratch wound healing assay substantiated our findings that low levels (i.e. inhibitor) of miR-196b-5p are associated with enhanced migration, whereas overexpression of miR-196b-5p resulted in a decrease of cellular migration of CRC cells (Figure 11A-C).

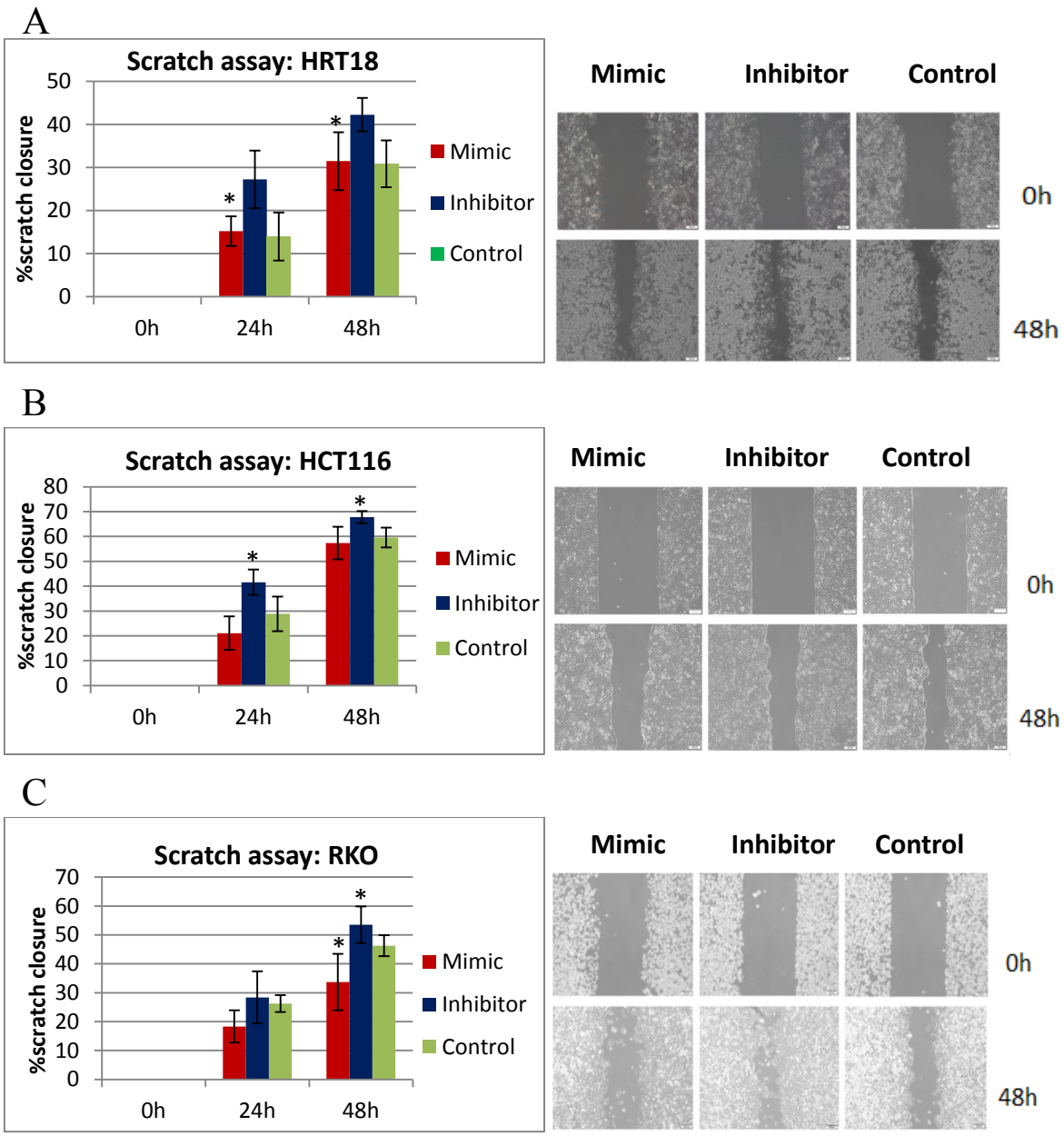

Figure 11: Scratch assays in three different CRC cell lines after transient miR-196b-5p overexpression or inhibition. **(A-C)** Pictures demonstrating scratch wound healing assays in HCT116, HRT18 and RKO cells after transfection of miR-196b-5p mimic, inhibitor or respective control. 0h = scratch at beginning, 24h = scratch after 24 hours, 48h = scratch after 48 hours. Bar charts graphs showing the results of measurement of scratch closure after 24 and 48 hours for the miR-196-5p stably overexpressing or silencing CRC cells. The miR-196b-5p silenced cells closed the scratch significantly earlier than the control (* = significant, $p < 0.05$; **, $p < 0.01$; ***, $p < 0.001$; student´s t-test).

By performing a transwell migration assay we could confirm that forced miR-196b-5p expression results in decreased migration, whereas inhibition of miR-196b-5p expression cells leads to enhanced migration in HCT116 and RKO cells (see Figure 12). Since HRT18

did not migrate through the transwell membrane under the selected conditions we could not analyse the migration rate for this cell line.

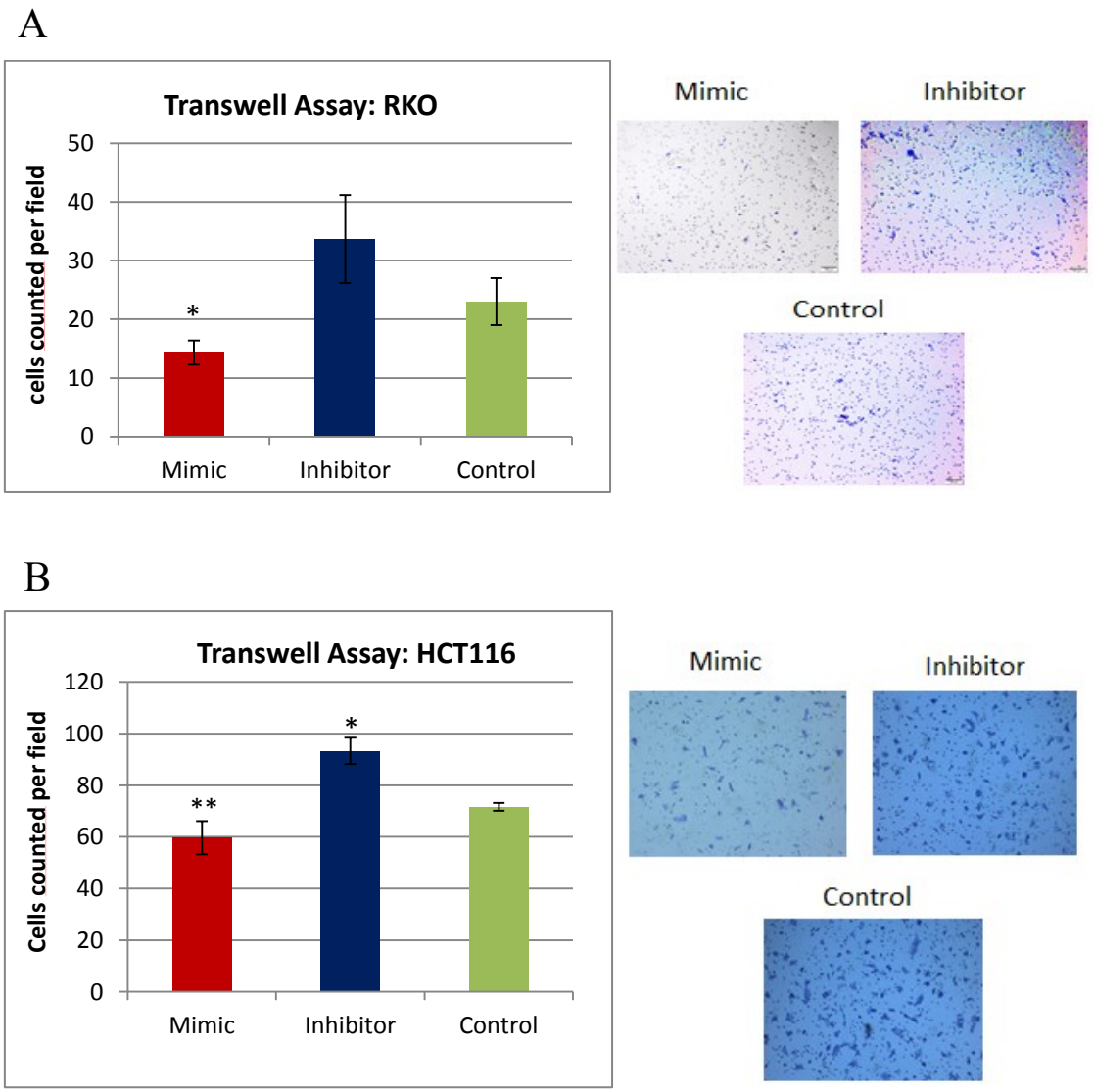

Figure 12: Transwell assays. (A-B) Bar charts graphs showing the results of transwell assays in RKO and HCT116 cells. As demonstrated in the representative pictures of transwell assays, miR-196b-5p silencing results in a higher number of migrated cells through the transwell membrane in both CRC cell lines (* = significant, $p < 0.05$; **, $p < 0.01$; ***, $p < 0.001$; student´s t-test).

In addition, we performed an invasion assay of HCT116 cells using the real time xCELLigence system and a transwell assay. Our analyses showed that low levels of miR-196b-5p lead to increased HCT116 cancer cell invasion in both invasion assays (Figure 13 and 14). In conlusion, these results indicate that there is a correlation with the results of our patient survival data and metastatic stage IV patient.

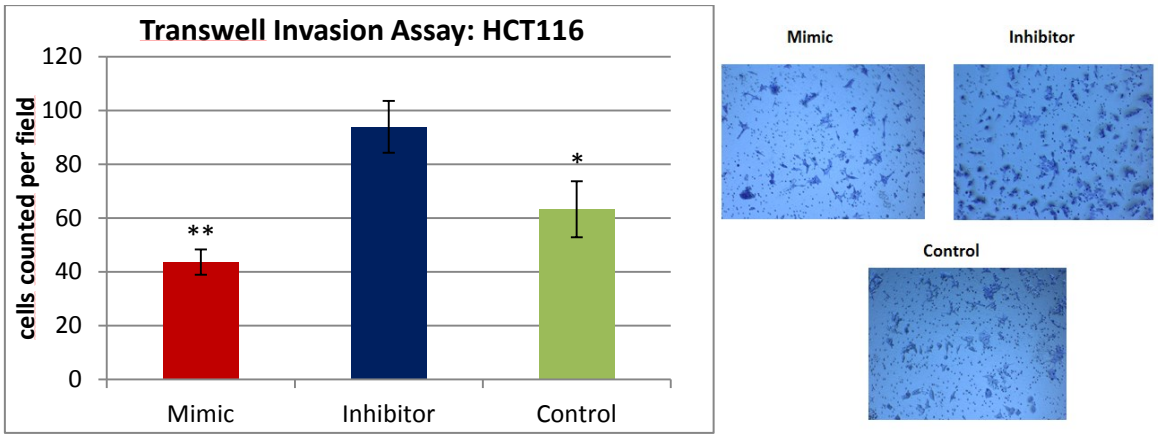

Figure 13: Transwell invasion assay. Inhibition of miR-196b-5p expression led to increased invasion in HCT116 cells as measured by transwell invasion assay. Bar charts graph showing the result of the transwell invasion assay in HCT116 cells after ectopic miR-196b-5p expression (* = significant, $p < 0.05$; **, $p < 0.01$; ***, $p < 0.001$; student´s t-test).

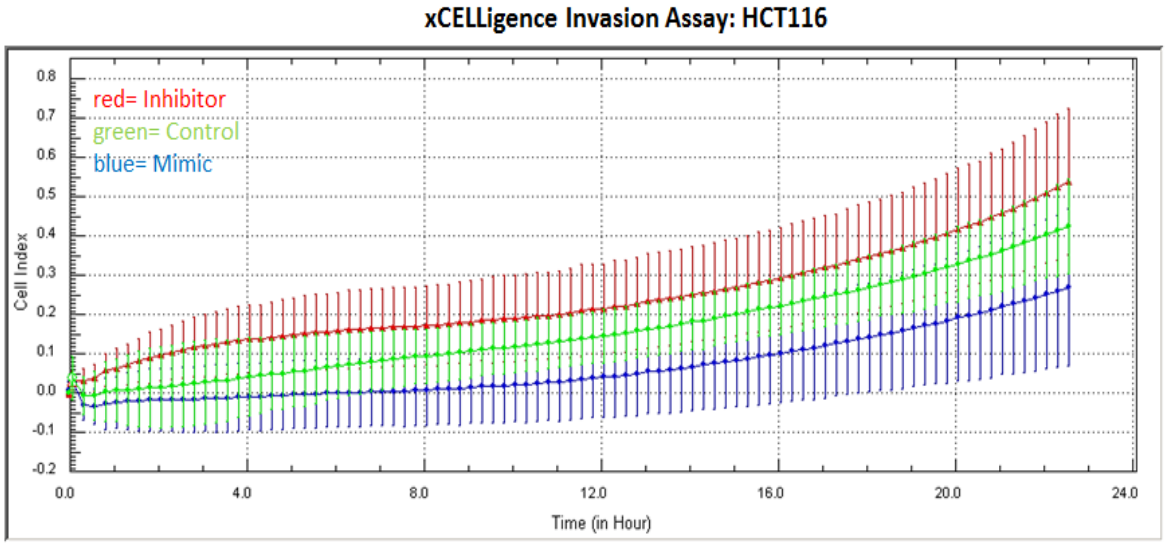

Figure 14: xCELLigence invasion assay. Low expression of miR-196b-5p resulted in higher invasion rates of HCT116 cells compared to control cells as measured by the xCELLigence Real Time Invasion Assay (n=3; p value <0.05 considered as significant).

To confirm our results from transient transfection experiment, we generated cell lines stably overexpressing or inhibiting miR-196b-5p expression. Therefore, we performed a stable transfection for all three independent CRC cell lines using lentiviral particles and performed a qRT- PCR to confirm the stable miR-196b-5p overexpression or silencing, respectively (Figure 15A-C). A decrease of miR-196b-5p expression levels could not be achieved in all three cell lines by tansfecting the inhibitor construct (Figure 15D-F) but we

successfully obtained a GFP (green fluorescent protein) signal in all the transfected cells which indicates a successful stable transfection.

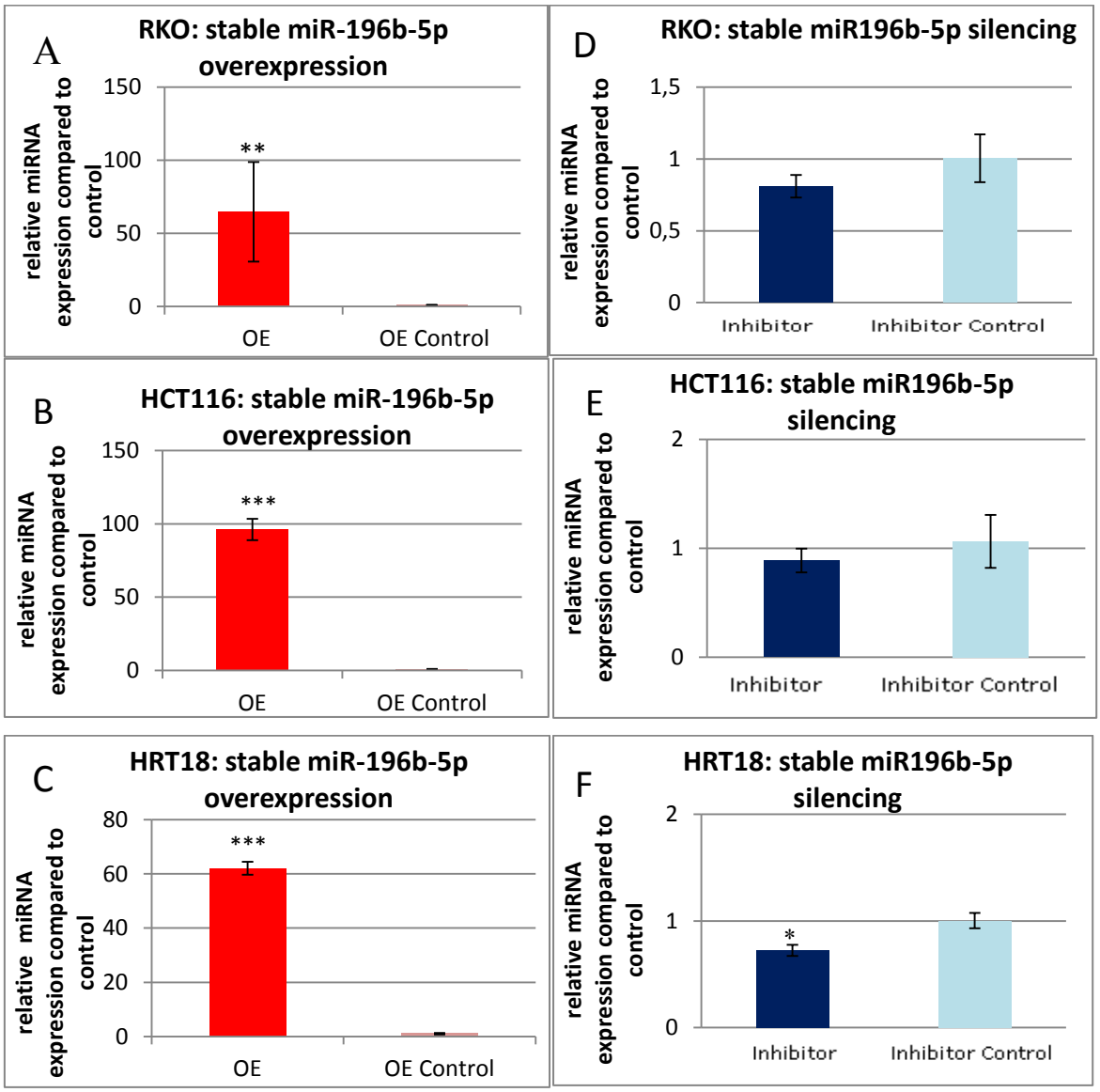

Figure 15: Quantitative RT PCR of stably transfected CRC cells. (A-C) We confirmed a statistically significant overexpression (OE) of miR-196-5p in the stably transfected CRC cells as shown in the bar charts graphs. **(D-E)** Inhibition of miR-196b-5p was detected by qRT-PCR (* = significant, $p < 0.05$; **, $p < 0.01$; ***, $p < 0.001$; student´s t-test).

Consequently, we confirmed the previously obtained results of transient gain and loss of function experiments by performing a scratch wound assay and transwell migration assay in the stably transfected cell lines. We observed changes of cancer cell migration in all three cell lines using the scratch wound assay (see Figure 16). Using the transwell assay system we confirmed that stable miR-196b-5p inhibition results in enhanced migration of HCT116 and RKO cells as shown in Figure 17.

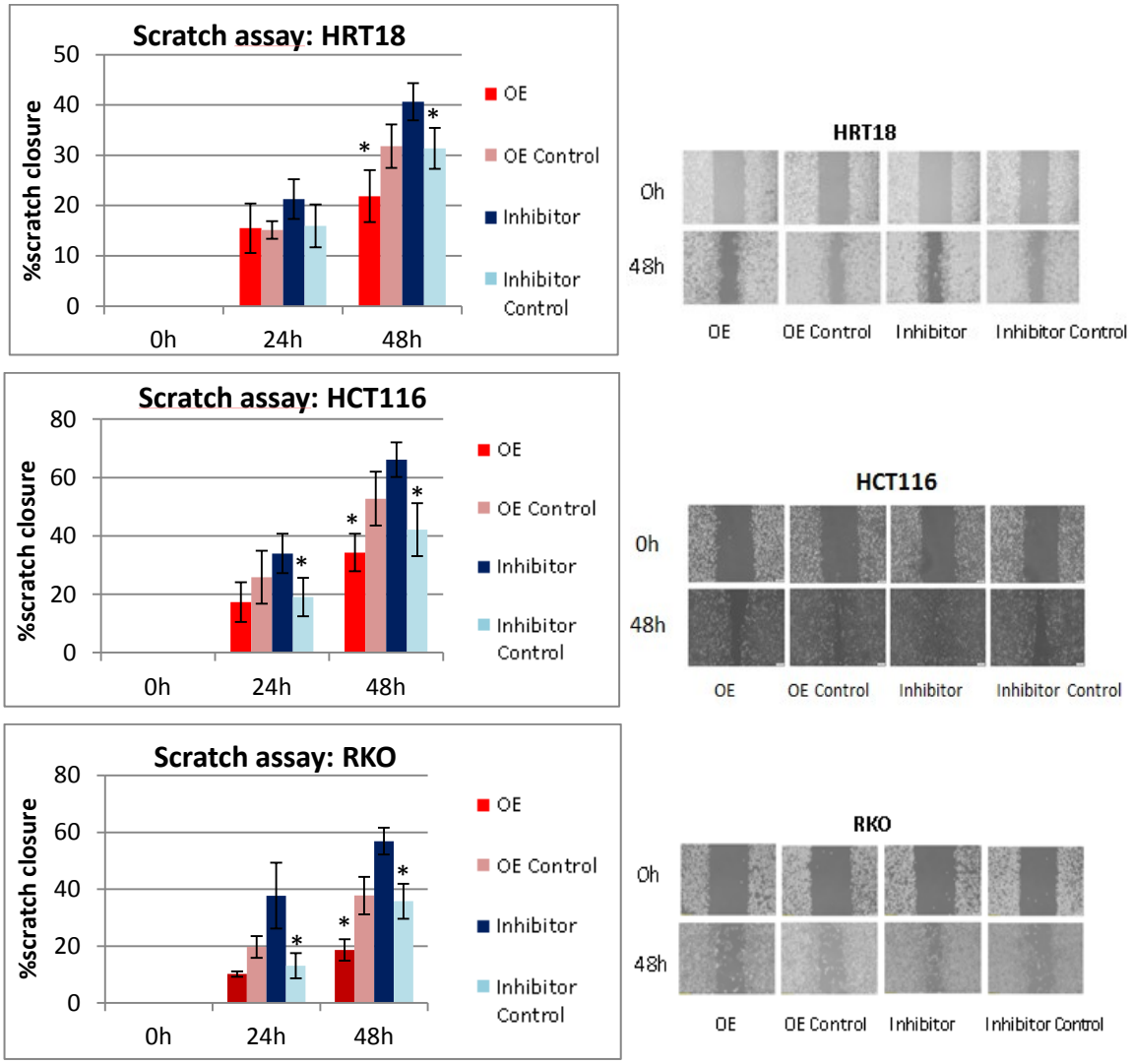

Figure 16: Scratch wound assays in three different stably miR-196b overexpressing or silencing of colorectal cancer cells. Representative pictures of scratch assays in HCT116, HRT18 and RKO cells after stable transfection of control (OE Control or Inhibitor Control), miR-196b-5p mimic (OE) or inhibitor. 0h = scratch at beginning, 24h = scratch after 24 hours, 48h = scratch after 48 hours. Bar charts graphs demonstrating the results of measurement of scratch closure after 24 and 48 hours for the three tested cell lines. Low miR-196b-5 expression resulted in a significantly earlier scratch wound closure compared to control cells (p value <0.05 considered as significant).

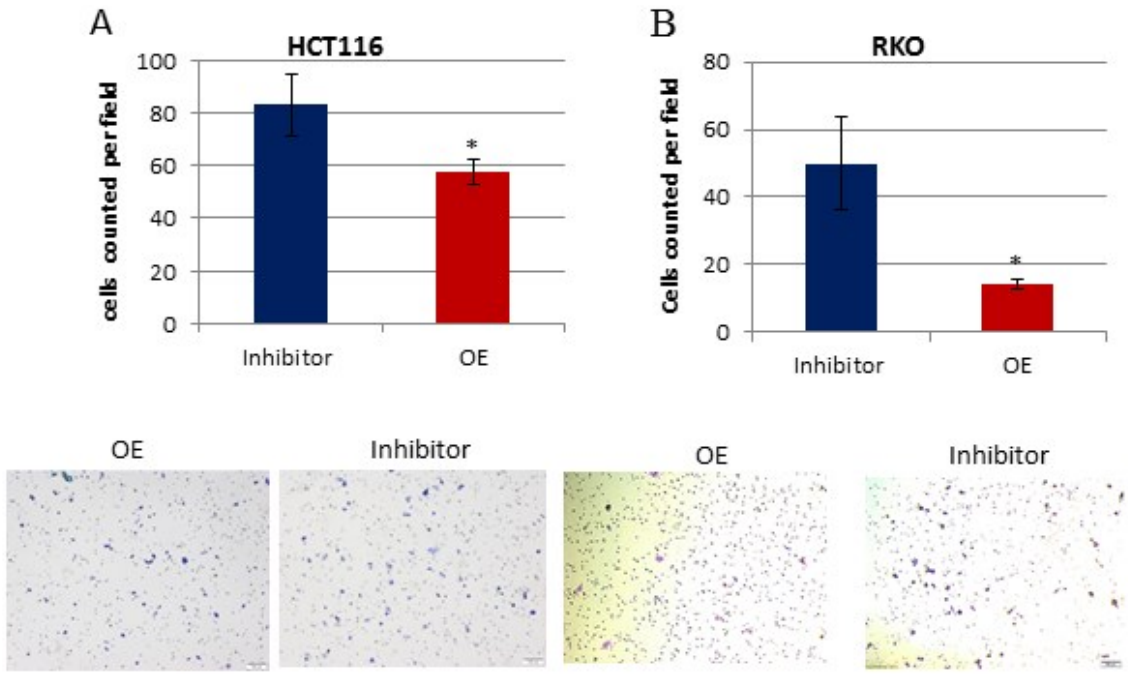

Figure 17: Transwell assay of stably transduced cell lines. Bar charts graphs showing the results of transwell assays in HCT116 **(A)** and RKO **(B)** cells. Inhibition of miR196b-5p resulted in increased number of migrated cells through the transwell membrane in both CRC cell lines (see representative pictures of crystal violet stained membranes). Since HRT18 did not migrate through the transwell membrane under the selected conditions we could not analyze the migration rate for this cell line (* = significant, $p < 0.05$; **, $p < 0.01$; ***, $p < 0.001$; student´s t-test).

4.1.4 Xenograft mouse model

To confirm the potentially pro-metastatic phenotype of low miR-196b-5p levels we performed an *in vivo* xenograft model. Therefore, we used stable miR-196b-5p overexpressing or silencing HCT116 cells, labelled them with a luciferase reporter for an *in vivo* imaging purpose and injected them into the spleen of nude mice. As shown in Figure 23, mice intra-splenic injection with miR-196b-5p inhibitor expressing cells revealed more frequently and more intense metastatic lesions ($p<0.05$). Seven out of eight mice (87.5%) in the group of miR-196b-5p inhibitor showed massive intra-abdominal metastases. On the contrary, only 3 out of 7 (42.8%) mice in the group of miR-196-5p overexpressing cells were positive for this feature (Figure 18). In conclusion, the *in vivo* data support our *in vitro* findings, showing that CRC cells with low expression of miR-196b-5p have significantly more and larger metastases than CRC cells with high miR-196-5p expression levels.

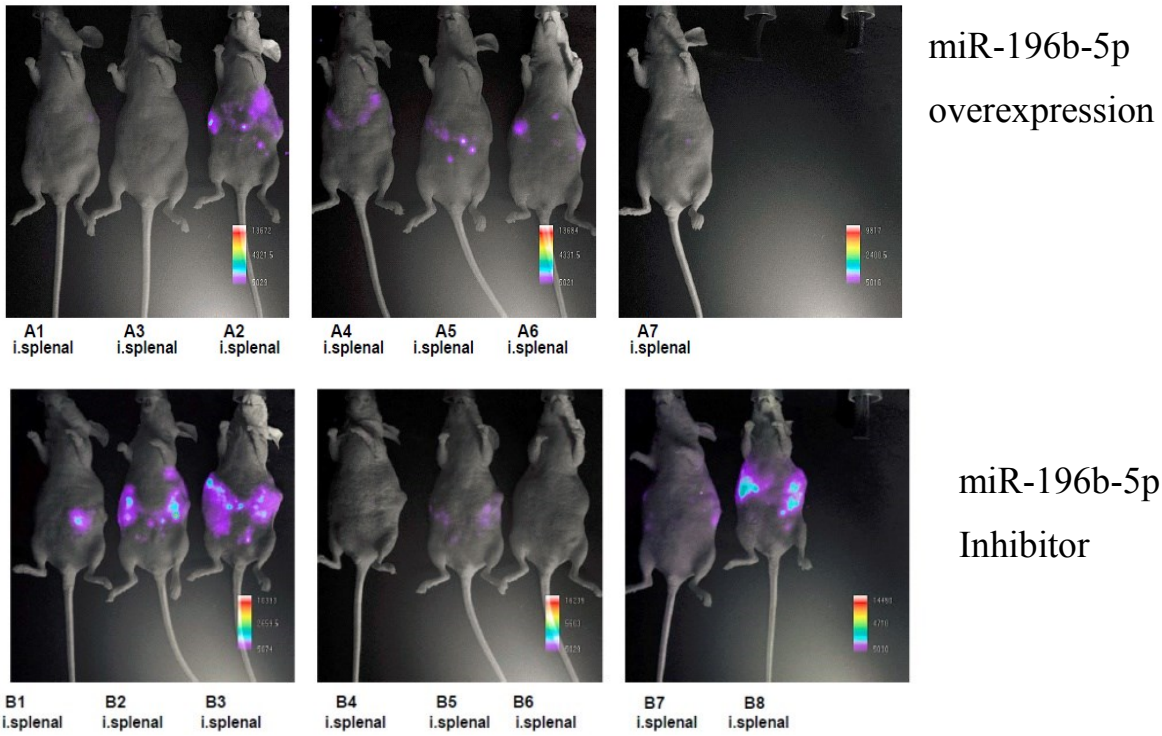

Figure 18: Xenograft mouse model. Representative pictures of in vivo imaging monitoring reveals more positive mice and a higher metastatic spread in mice with intra-spleen injection of stably miR-196b-5p inhibitor HCT116 cells ($p<0.05$).

4.1.5 Molecular mechanism of miR-196b-5p

To identify a possible molecular mechanisms that might explain this metastatic behavior, we next analyzed the expression levels of classical epithelial-mesenchymal transition (EMT) markers in miR-196b-5p overexpressing cells, but did not detect any significant differences Figure as shown in Figure 19.

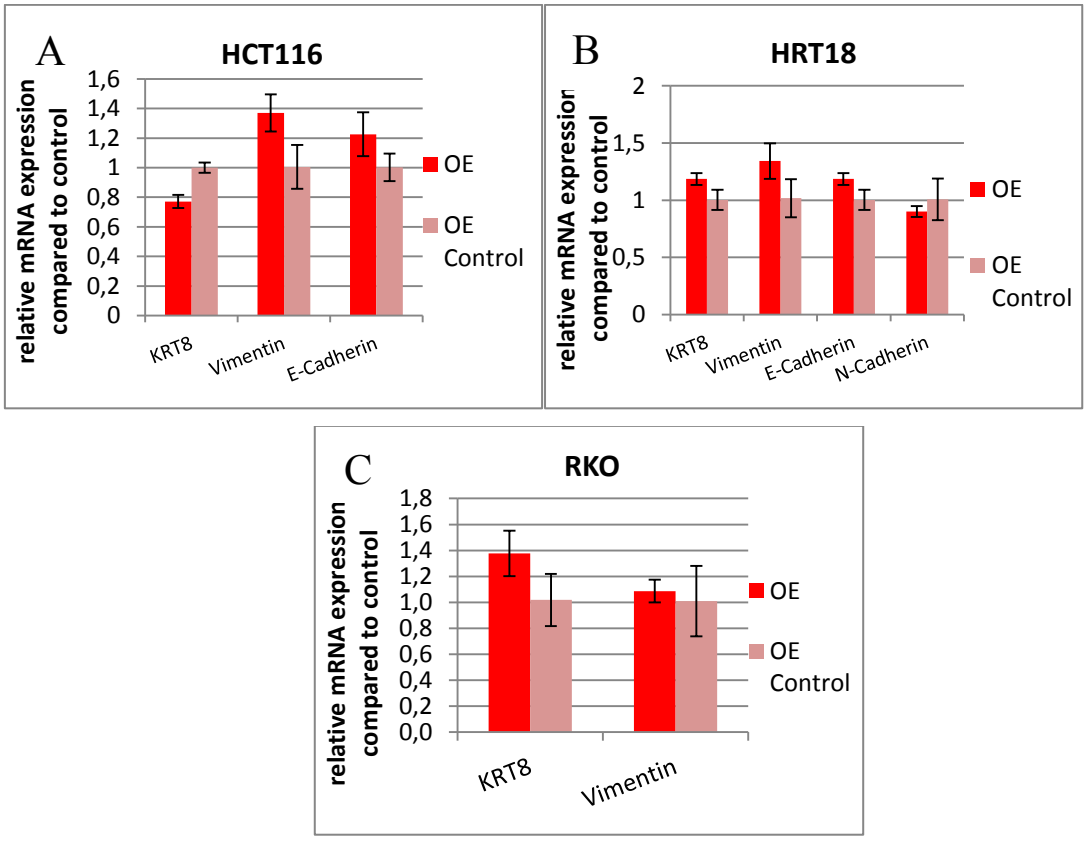

Figure 19: EMT marker. (A-C) Relative mRNA quantification of EMT marker expression levels was performed after stable miR196b-5p overexpression of HCT116, HRT18 and RKO cells. No significant differences were detected in miR-196b-5p overexpressing cells compared to control cells. E-Cadherin and N-Cadherin could not be detected in RKO cells. HCT116 cells did not show an N-Cadherin expression. (* = significant, $p < 0.05$; **, $p < 0.01$; ***, $p < 0.001$; student´s t-test)

Next, to find potential molecular miR-196b-5p interactors, we performed a microarray whole transcriptome profiling analysis in three independent biological replicates of HCT116 miR-196b-5p stably overexpressing cells and compared them to control cells (heat map see Figure 20 and Supplementary Table).

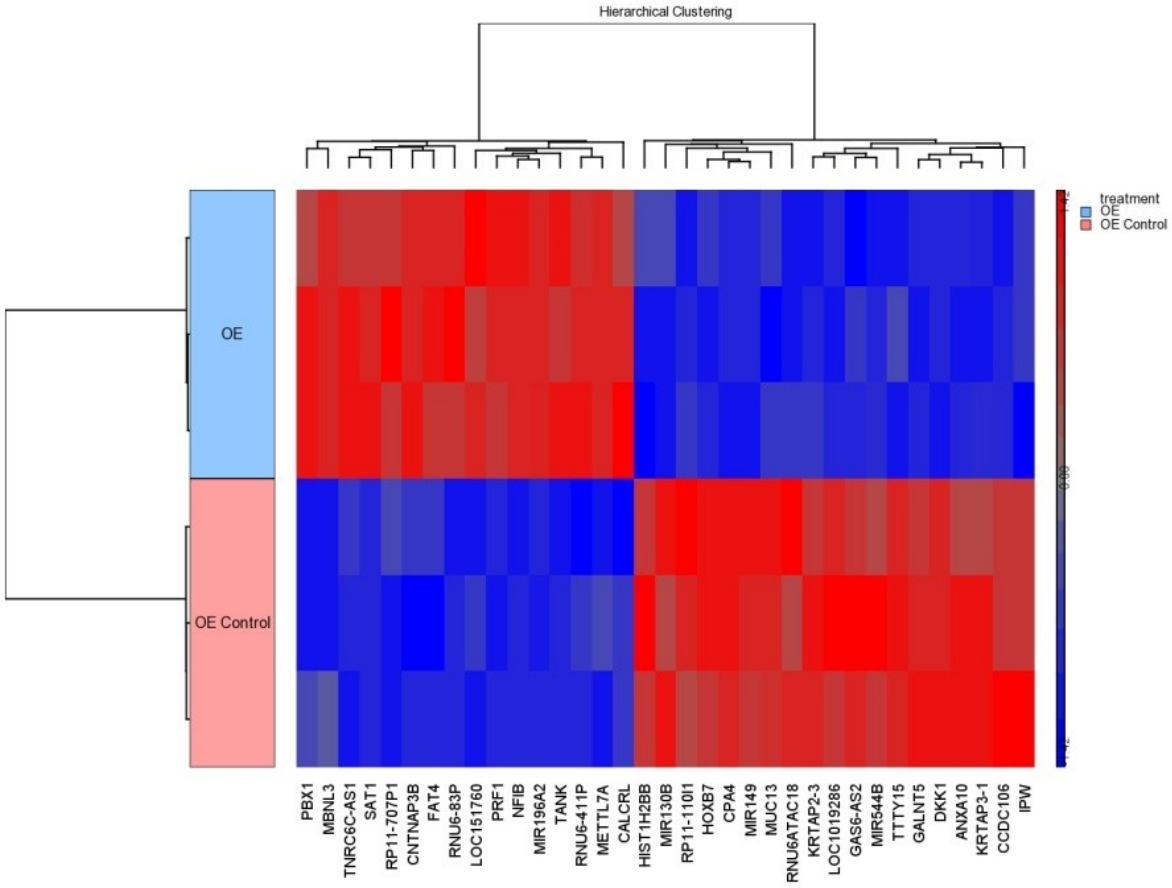

Figure 20: Microarray analysis. HeatMap of top 16 up-regulated and 18 down-regulated genes of stably miR-196b-5p overexpressing HCT116 cells (OE) compared to control (OE Control) cells. This picture shows genes clustered using hierarchical clustering (Pearson's dissimilarity, Ward' method) on expression values (p value <0.05 considered as significant).

Based on the microarray results, showing 38 significantly up-regulated and 41 downregulated genes after miR-196b-5p overexpression compared to control, an *in silico* target prediction analysis was performed to select potential molecular mRNA targets (results are listed in Table 12). We further performed a comprehensive literature search and selected only potential interactors which have been previously involved in cancer cell migration and invasion (i.e. *GalNT5*, *HOXB7*, *MUC13, DKK1, CPA4, KRTAP2-3, KRTAP1*).

Table 12: In silico target prediction. Results obtained from in silico target prediction analysis of dysregulated genes detected in whole transcriptome microarray analysis

Gene name	log2 Fold Change	Number of prediction tools that identified a putative target	Seed match count in 3'UTR (based on ENSEMBL database)
DDX3Y	-2.67	**2**	0
CPA4	-2.6	**4**	2
KRTAP3-1	-2.45	**2**	0
KRTAP2-3	-2.4	**1**	0
GALNT5	-2.13	**NA**	2
LOC101928102	-2.1	**1**	0
ANXA10	-1.9	**3**	0
MUC13	-1.8	**2**	0
DKK1	-1.77	**3**	0
ARL14EPL	-1.71	**1**	0
HOXB7	-1.55	**9**	2
ZNF804A	-1.54	**1**	0
HDGFRP3	-1.52	**2**	0
ZBED2	-1.52	**2**	0
CGN	-1.51	**4**	1

Consequently, we validated these down-regulated genes in HCT116 cells from the microarray analysis by quantitative RT-PCR (Figure 21A). We confirmed a downregulation of all selected genes in the stably miR-196b-5p overexpressing HCT116 cells compared to control. To confirm these candidates in a secound independent cell line we analyzed the expression levels of all seven genes in stable miR-196b-5p overexpression HRT18 cells. In this cell line, we could validate a significant down-regulation of *HOXB7* and *GalNT5* after miR-196b-5p overexpression (Figure 21B).

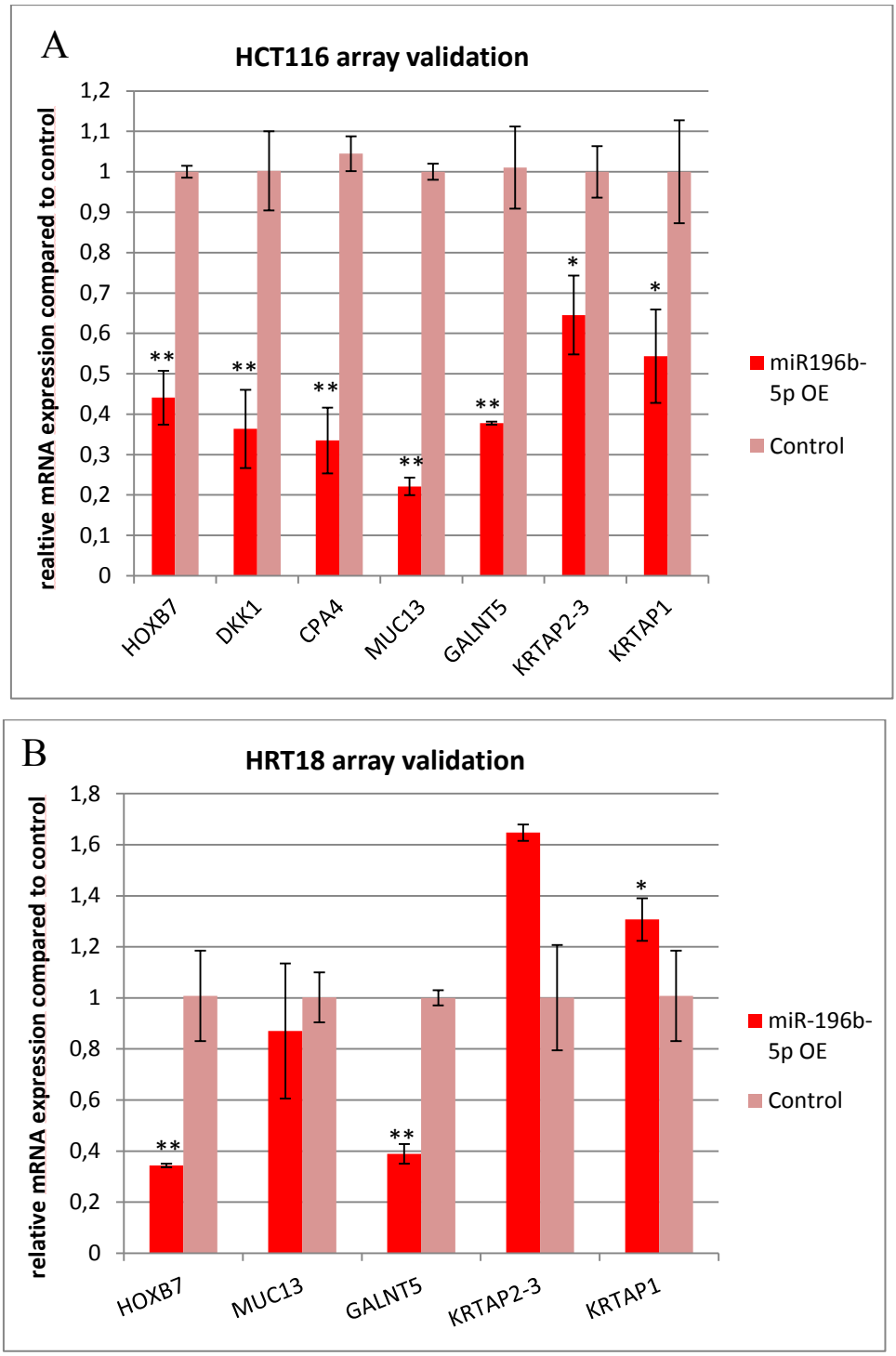

Figure 21: Validation of array data. (A) Confirmation of Array data in HCT116. A down-regulation of selected migration related genes after miR-196b-5p overexpression (OE) in HCT116 was confirmed by qRT-PCR. **(B)** Validation of array data in HRT18 cells. In this second independent cell line we confirmed a downregulation of HOXB7 and GalNT5. CPA4 and DKK1 could not be detected in HRT18 cells (* = significant, $p < 0.05$; **, $p < 0.01$; ***, $p < 0.001$; student´s t-test).

To further investigate whether these two potential target genes are influenced by miR-196b-5p expression in a different experimental setting, we performed transient loss and

gain of function experiments. First, we transiently transfected HCT116 and HRT18 cells and measured *GalNT5* and *HOXB7* after miR-196b-5p overexpression and silencing. Both were significantly down-regulated on mRNA and protein levels upon ectopically miR-196b-5p overexpression in HCT116 and HRT18 cells (Figure 22A-C).

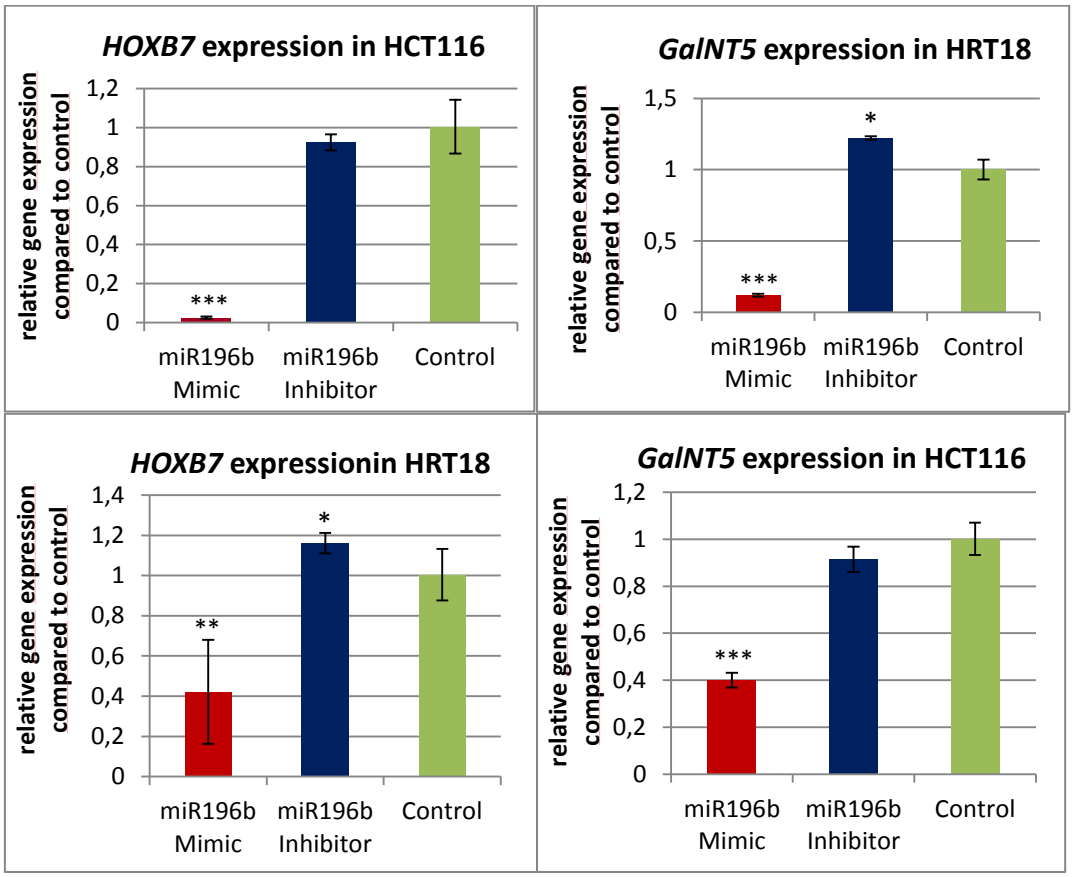

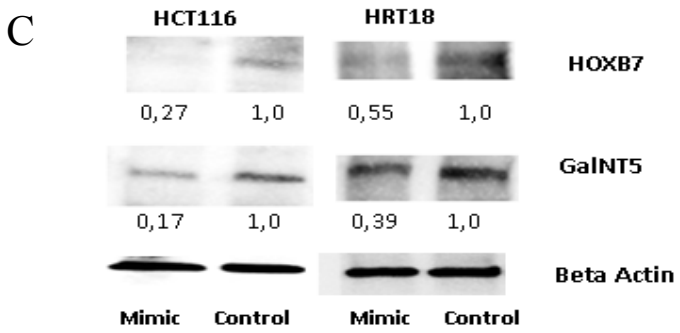

Figure 22: HOXB7 and GalNT5 are regulated by miR-196b-5p. A statistically significant downregulation of HOXB7 **(A)** and GalNT5 **(B)** mRNA expression after transient miR196b-5p overexpression in HCT116 and HRT18 cells was confirmed by qRT-PCR (* = significant, $p < 0.05$; **, $p < 0.01$; ***, $p < 0.001$; student´s t-test). **(C)** GalNT5 and HOXB7 protein expression were significantly down-regulated after 48 hours of miR-196b-5p Mimic transfection compared to the control as detected by Western blot analysis.

A direct interaction of miR-196b-5p and *GalNT5* mRNA was further confimed by cloning the predicted 3'UTR binding site in a luciferase-containing plasmid (binding site is shown in Figure 23A). A reduction of luciferase activity was detected in the wild-type sequence indicating that there is an interaction of miR-196b-5p with the *GalNT5* mRNA. The mutated binding site led to a restoration of normal luciferase activity (Figure 23B).

A

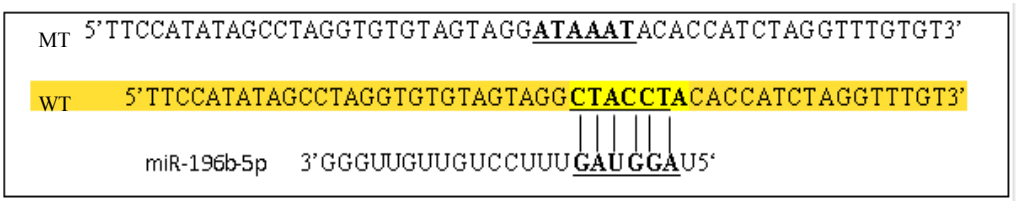

B

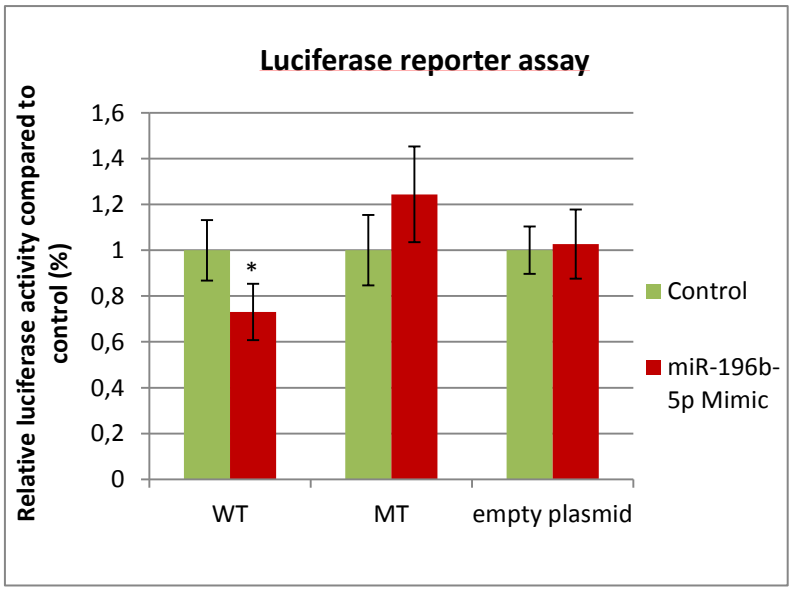

Figure 23: Luciferase Assay. (A) Predicted miR-196b-5p binding site within the 3´UTR (untranslated region) of *GalNT5* mRNA. Two *GalNT5* constructs were generated as indicated (miR-196b-5p wild-type (WT) binding site (marked in yellow) and mutated (MT) binding site). (B) Luciferase activity after co-transfection of the *GalNT5* wild-type (WT) or mutated (MT) constructs and control/miR-196b-5p mimetic in HEK cells. Three independent biological experiments were performed and the means and standard deviations are shown (*p<0.05, student´s t-test).

Finally, to prove our hypothesis whether miR-196b-5p exerts its effect on cellular migration by regulating *HOXB7* and *GalNT5* expression, we performed siRNA-mediated knock-down experiments for both genes to confirm the pheno-copy of the effects of miR-196b-5p overexpression. As demonstrated in Figure 24 we could confirm a significant down-regulation of both genes in HCT116 and HRT18 cells after siRNA treatment.

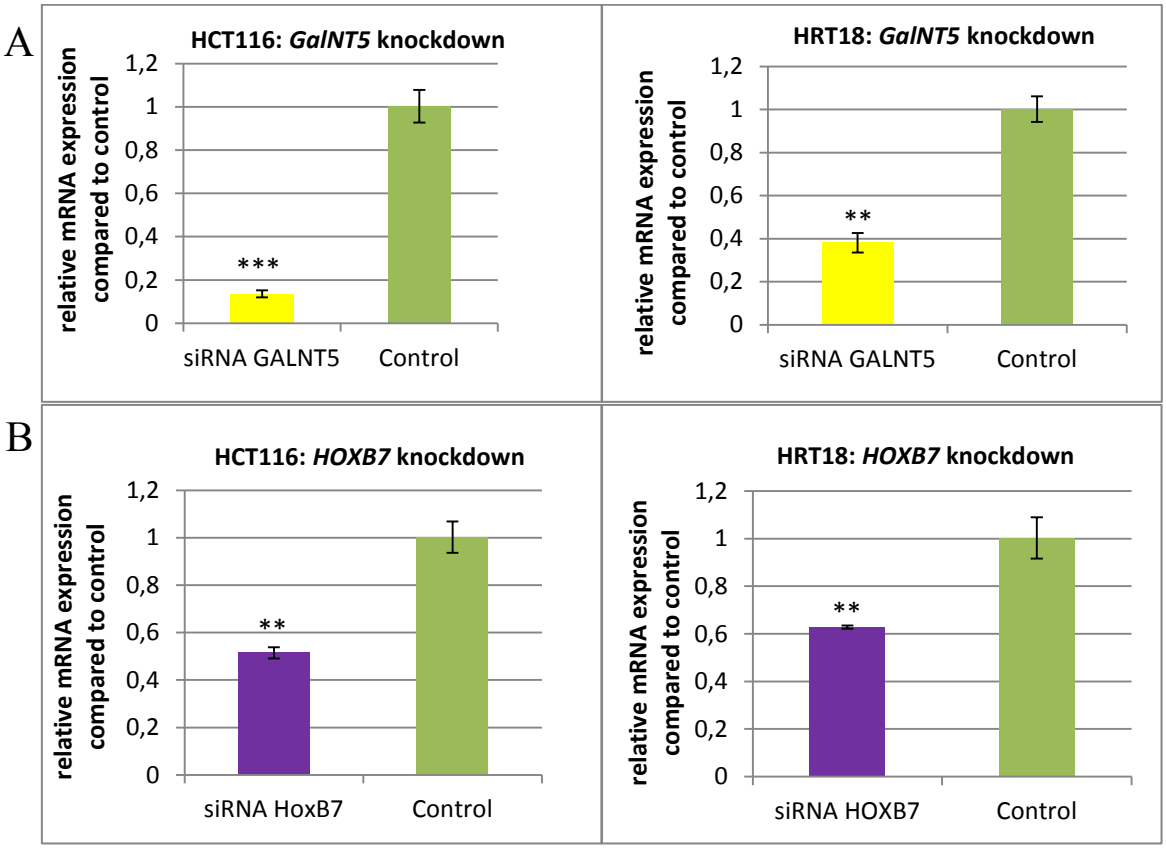

Figure 24: Knockdown of *GalNT5* and *HOXB7*. *GalNT5* **(A)** and *HOXB7* **(B)** mRNA expression after 48 hours of siRNA transfection as detected by qRT-PCR in HCT116 und HRT18 cells. We confirmed a statistically significant knockdown of *HOXB7* and *GalNT5* compared to control cells (* = significant, $p < 0.05$; **, $p < 0.01$; ***, $p < 0.001$).

A decrease of each mRNA expression resulted in a reduced migration of HCT116 and HRT18 cells in the scratch assay (see Figure 25) and this phenotype was even more pronounced when performing a knock-down of both genes (Figure 26).

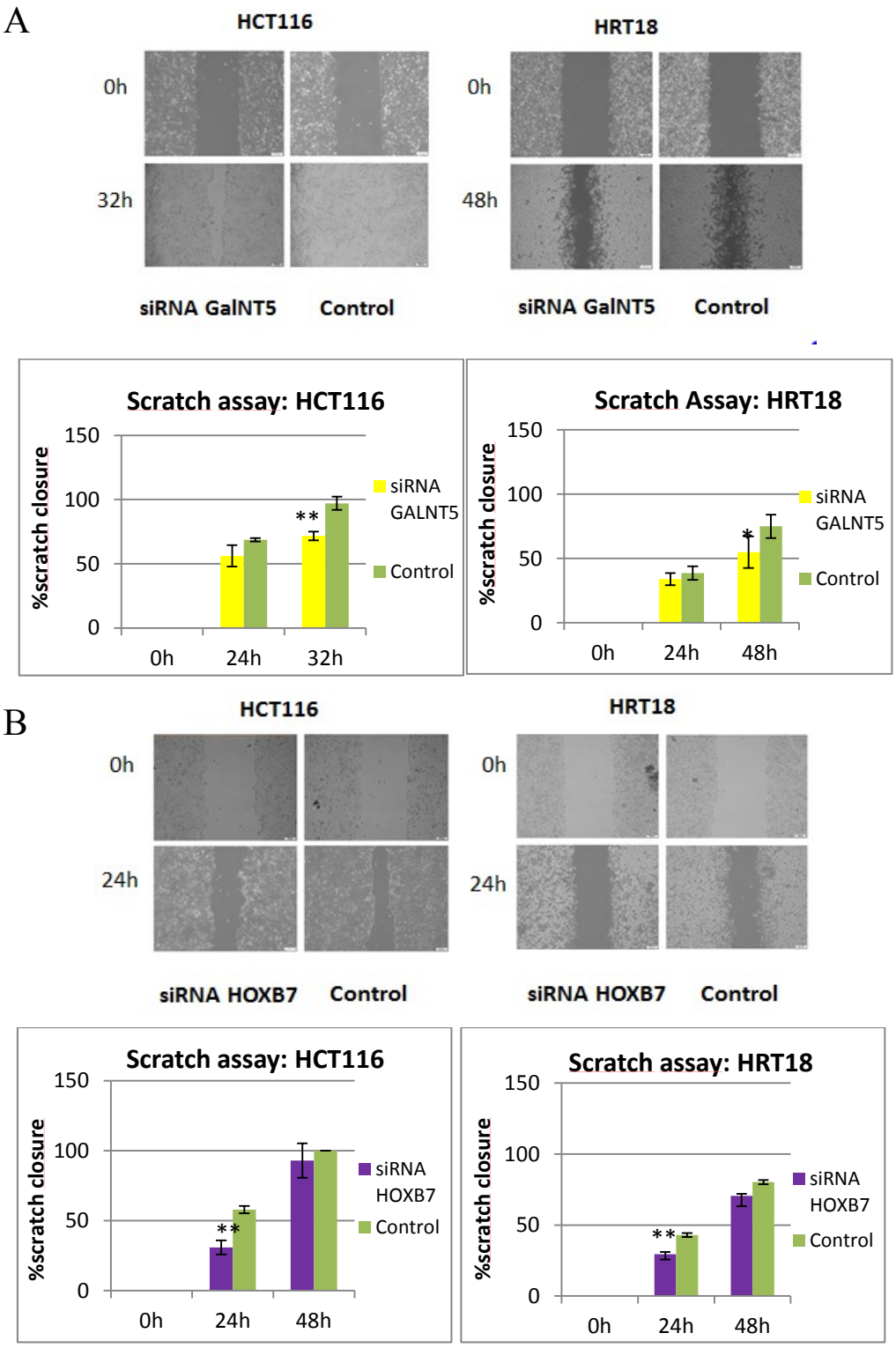

Figure 25: Scratch assays in two CRC cell lines after *GalNT5* or *HOXB7* silencing. Representative pictures of scratch assays in HCT116 and HRT18 after transfection *GalNT5* **(A)** or *HOXB7* **(B)** siRNA and respective control. 0h = scratch at beginning, 24h = scratch after 24 hours, 32h=scratch after 32h, 48h = scratch after 48 hours. Bar charts graphs demonstrating the results of scratch closure over 48 hours for the two tested cell lines. The scratch of control cells closed significantly earlier than the *GalNT5* and *HOXB7* silenced cells (* = significant, $p < 0.05$; **, $p < 0.01$; ***, $p < 0.001$; student´s t-test).

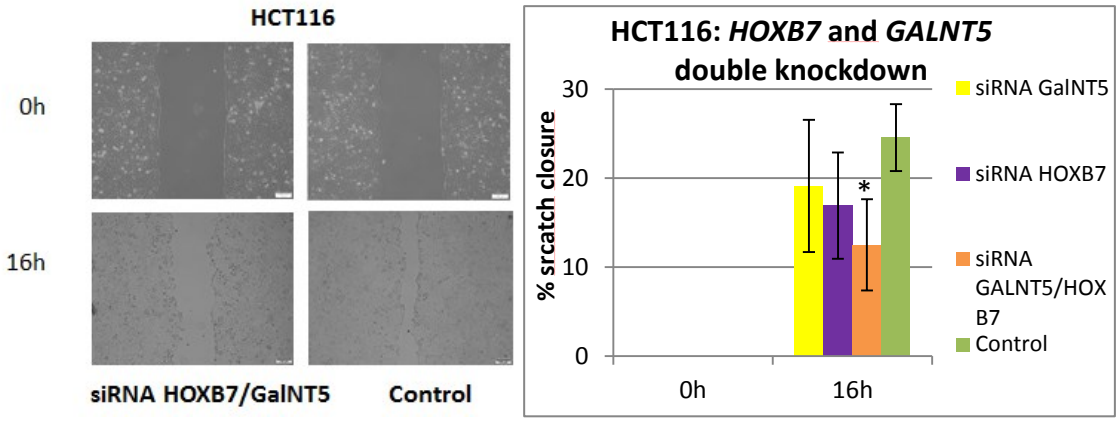

Figure 26: Scratch assay after double knockdown of HOXB7 and GalNT5. Double knockdown of HOXB7 and GalNT5 resulted in a significant reduction of cellular migration compared to control cells as shown in a representative example of the scratch assay in HCT116. Bar charts graph demonstrating the results of the measurement of scratch closure at the beginning (0h) and scratch wound closure after 16 hours (16h) (* = significant, $p < 0.05$; **, $p < 0.01$; ***, $p < 0.001$; student´s t-test).

4.2 MiR-188-3p as novel prognostic marker and molecular factor involved in CRC

4.2.1Mir-188-3p as prognostic factor

In this study genome-wide miRNA expression data that are publicly available from a large cohort of CRC patients were used to perform an unbiased approach to identify potential prognostic markers. We got expression data of 971 miRNAs in at least one tumor sample of the 228 CRC patients derived from the TCGA dataset. Table 13 shows the clinico-pathological characteristics of the screening (n = 228) and the validation (n = 332) cohort (70).

Table 13: Summary and comparison of clinico-pathological characteristics of CRC patients. (screening cohort (n = 228) and validation cohort (n = 332))

		Screening cohort	Validation cohort	p-value
		No (%)	No (%)	
Age	median	70	64	p=4.7e-08*
	minimum	34	18	
	maximum	90	92	
Sex	female	112 (49)	138 (42)	p=0.0928**
	male	116 (51)	194 (58)	
Stage	stage I	51 (22)	39 (12)	p=1.6e-06**
	stage II	80 (35)	83 (25)	
	stage III	56 (25)	91 (27)	
	stage IV	41 (18)	119 (36)	
Location	colon	186 (82)	296 (89)	p=0.0155**
	rectum	42 (18)	36 (11)	

Following the criteria mentioned in the Methods section, we found thirteen miRNAs whose expression levels were significantly ($p<0.05$, univariate Cox model) associated with prognosis in CRC patients (Table 14). Additionally, when performing the same analyses on 186 samples of colon cancer, excluding the rectum cancer cases, we identified two miRNAs significantly ($p<0.05$, univariate Cox model) associated with lower risk and thirteen miRNAs significantly associated with higher risk of death (Table 15) (70).

Table 14: List of all microRNAs that are significantly (p<0.05) associated with survival in the colorectal cancer screening cohort (cohort 1; n = 228)

miRNA	HR	lower95%CI	upper95%CI	p value
hsa.mir.425_MIMAT0001343	2.364164	1.345653129	4.153573985	0.002767
hsa.mir.195_MIMAT0004615	1.945962	1.07978293	3.506973078	0.026733
hsa.mir.3610_MIMAT0017987	1.914306	1.052975757	3.480199608	0.033236
hsa.mir.188_MIMAT0004613	1.874051	1.21968087	2.879497837	0.004155
hsa.mir.221_MIMAT0004568	1.782102	1.050126835	3.0242905	0.032256
hsa.mir.129.1_MIMAT0000242	1.712541	1.073807128	2.731214614	0.023885
hsa.mir.331_MIMAT0000760	1.695194	1.036829648	2.771604116	0.035365
hsa.mir.195_MIMAT0000461	1.66737	1.017733301	2.731681947	0.042382
hsa.mir.497_MIMAT0002820	1.646315	1.001009748	2.707619103	0.049537
hsa.mir.147b_MIMAT0004928	1.573449	1.016532898	2.435476519	0.041999
hsa.let.7e_MIMAT0004485	1.551875	1.016760374	2.368616937	0.041649
hsa.mir.92b_MIMAT0003218	0.496884	0.284619065	0.86745369	0.013889
hsa.mir.1976_MIMAT0009451	0.528338	0.292163225	0.955428652	0.034789

Table 15: List of all microRNAs that are significantly (p<0.05) associated with survival in the colon cancer only screening cohort (cohort 1; n = 186)

miRNA	HR	lower.95%CI	upper.95%CI	p value
hsa-mir331_MIMAT0000760	2.297344	1.271467516	4.150945004	0.005857
hsa-mir-425_MIMAT0001343	2.164009	1.242505403	3.768944613	0.006392
hsa-mir-188_MIMAT0004613	2.007447	1.266909656	3.180844187	0.003004
hsa-mir3607_MIMAT0017985	2.004293	1.040685249	3.860138956	0.037597
hsa-mir-221_MIMAT0004568	1.980054	1.151587704	3.404527778	0.013497
hsa-mir-497_MIMAT0002820	1.895216	1.13666149	3.159994029	0.014244
hsa-mir-195_MIMAT0000461	1.845756	1.07835644	3.15926722	0.025413
hsa-mir-455_MIMAT0003150	1.779172	1.091786031	2.899333923	0.020755
hsa-mir-455_MIMAT0004784	1.778764	1.076350881	2.93956392	0.024638
hsa-mir-326_MIMAT0000756	1.665797	1.084566556	2.558514766	0.019767
hsa-mir-1291_MIMAT0000242	1.662969	1.027604971	2.691175687	0.038374
hsa-mir-147b_MIMAT0004928	1.64919	1.028162273	2.645329416	0.037971
hsa-mir-29c_MIMAT0000681	1.62336	1.029026488	2.560961225	0.037253
hsa-mir374a_MIMAT0004688	0.484745	0.235754184	0.99670507	0.04896

We choosed six miRNAs of these miRNAs from the whole CRC cohort and colon only cases in accordance with the pre-specified criteria and further validated the potentially prognostic miRNAs in a second independent CRC cohort, (i.e. with an upper limit <0.9 or a lower limit >1.1 of their respective HR 95% CI; yellow marked miRNAs in Table 14 and Table 15). Due to the data of the screening set, we analyzed the expression levels of miR-92b-3p, miR-188-3p, miR-221-5p, miR-331-3p, miR-425-3p and miR-497-5p in 332 patients of the validation cohort by qRT-PCR and calculated the HR and corresponding 95% CI by univariate Cox models. Clinico-pathological characteristics of this cohort are summarized and compared to the screening cohort in Table 13. We identified significant differences in regard to the explored clinico-pathological variables including gender, age stage and location ($p<0.05$, details see Table 13). The patients in the validation cohort had a significantly worse 5-years overall survival. This observation could mainly be explained by larger number of advanced/metastatic stage IV tumors in the validation cohort (36% in cohort 2 versus 18% in cohort 1, respectively; see also Table 13) (70).

We externally validated the miRNAs with the strongest prognostic potential and definitively confirmed one, miR-188-3p, to represent an independent prognostic factor in CRC patients. Only miR-188-3p matched with the pre-specified criteria of the HR and 95% CI borders (i.e. >1.1) in univariate Cox analyses and, therefore, we focused our comprehensive prognostic and experimental analyses only on this miRNA. First, we performed an in situ hybridization and could localize miR-188-3p in epithelial cells. An increased expression of miR-188-3p in cancerous cells compared with the corresponding normal mucosa was detected.(n = 3 paired cancer and adjacent normal colon samples, fold change 1.91, $p=0.005$, paired Student t-test, Figure 27) (70).

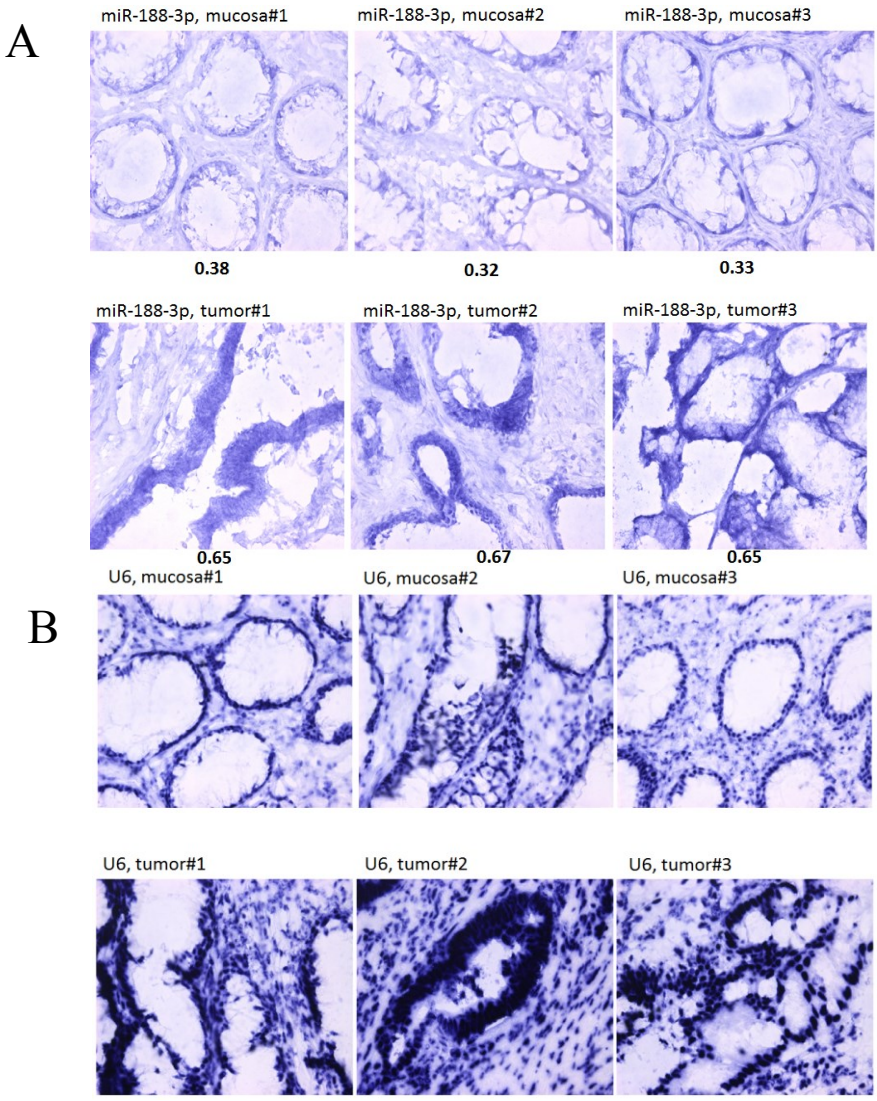

Figure 27: In situ hybridisation. (A) In situ hybridization (ISH) of miR-188-3p expression in normal mucosae (upper panel) and corresponding tumor tissue (lower panel). **(B)** In situ hybridization of U6 in normal mucosae (n = 3, upper panel) and corresponding tumor tissue (n = 3, lower panel) for normalization of miR188 expression. Figure taken from Pichler and Stiegelbauer *et al*.; Genome-wide microRNA analysis identifies miR-188-3p as novel prognostic marker and molecular factor involved in colorectal carcinogenesis; Clin. Cancer Res., 2016 September.

Consequently, we performed a qRT-PCR to measure the expression levels of miR-188-3p in 61 paired CRC samples (where RNA for both, the tumor and the adjacent normal colon mucosa were available in the validation cohort) and showed that miR-188-3p is significantly up-regulated in cancerous tissues (3.89 fold higher expression, $p<0.001$, paired Student t-test, Figure 28A). Additionally, we analyzed the association of miR-188-3p with other clinico-pathological parameters in the large validation cohort. This analysis revealed that increased miR-188-3p expression values are significantly associated with higher tumor stage ($p<0.001$, ANOVA, Figure 28B)(70).

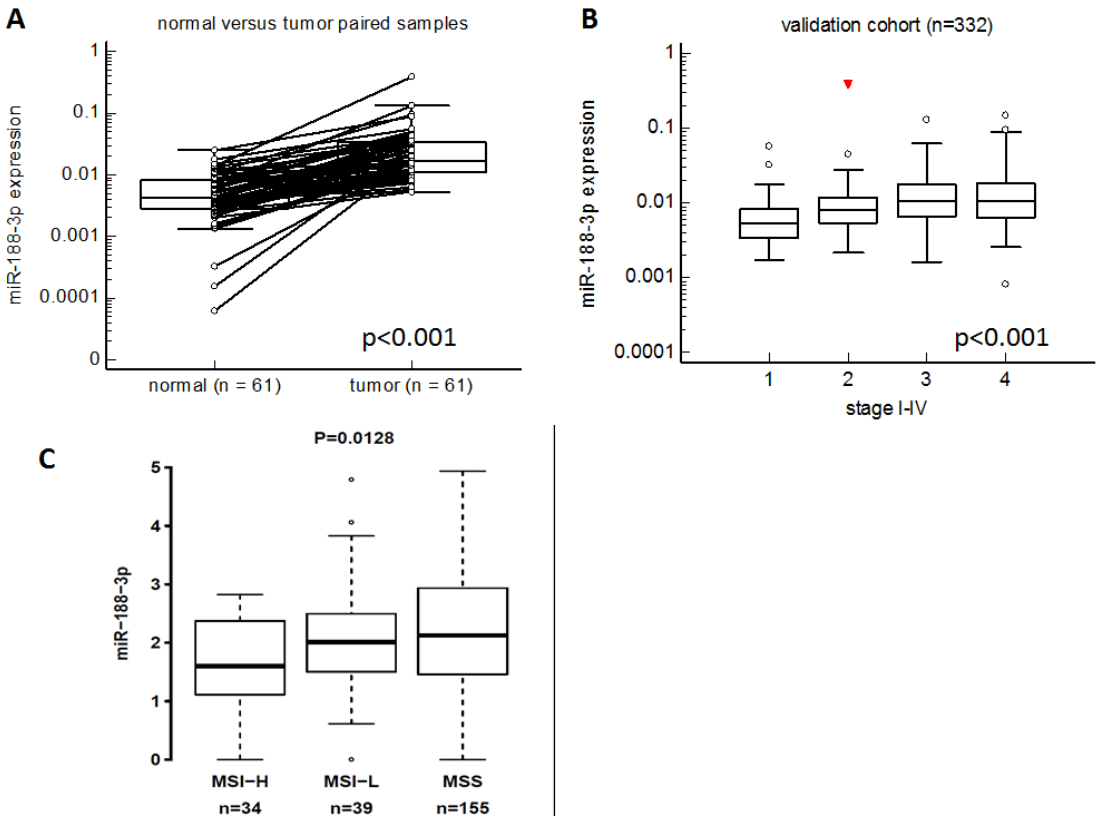

Figure 28: miR188-3p expression in CRC patients. (A) MiR-188-3p is significantly up-regulated in matched cancer tissue in comparison to the adjacent non-cancerous mucosa ($p<0.001$, paired student´s t-test). **(B)** Tumors of higher tumor stage show a significantly higher miR-188-3p expression ($p<0.001$, ANOVA). **(C)** MiR-188-3p is significantly higher expressed in tumors of microsatellite stable background. Figure taken from Pichler and Stiegelbauer *et al.*; Genome-wide microRNA analysis identifies miR-188-3p as novel prognostic marker and molecular factor involved in colorectal carcinogenesis; Clin. Cancer Res., 2016 September.

In regard to well-known mutations (KRAS, NRAS and BRAF gene) in CRC patients, we explored whether there is an association of miR-188-3p expression levels and the mutational status in one of these cancer related genes in the screening cohort. For cohort 1, 182 patients (80%) were available for mutational status: KRAS wild-type in 107 patients (58.8%); KRAS mutant in 45 (41.2%); NRAS wild-type in 164 (90.1%) and NRAS mutated in 18 (9.9%) patients and BRAF wild-type in 162 (89%) and BRAF mutated in 20 (11%) of patients. We did not observe any significant association of miR-188-3p expression levels with mutational status for KRAS and NRAS mutated patients, whereas in patients with a BRAF mutation, we found significantly lower expression levels of miR-188-3p in their tumor tissue ($p = 0.01$, Mann-Whitney U Test). Additionally, we observed significantly higher miR-188-3p expression levels in microsatellite stable tumors (Figure 28C) (70). The Kaplan-Meier curves for overall survival (OS) (Figure 29) indicate that high miR-188-3p expression is significantly associated with poor prognosis in CRC ($p =$

0.020, log-rank test). High miR-188-3p and advanced tumor stage (stage IV versus stage I-III) were identified as poor prognostic factors for survival (all p-values <0.05) by univariate analysis in the validation set. MiR-188-3p expression higher than the median levels is a significant factor for poor prognosis in CRC patients (p <0.001, log-rank test) as shown in Figure 34. In patients with stage II/III CRC we found a similar and significant poor prognostic value for miR-188-3p in both cohorts (n = 135 in cohort 1, p = 0.0495; n = 174 in cohort 2, p = 0.0005, respectively) (70).

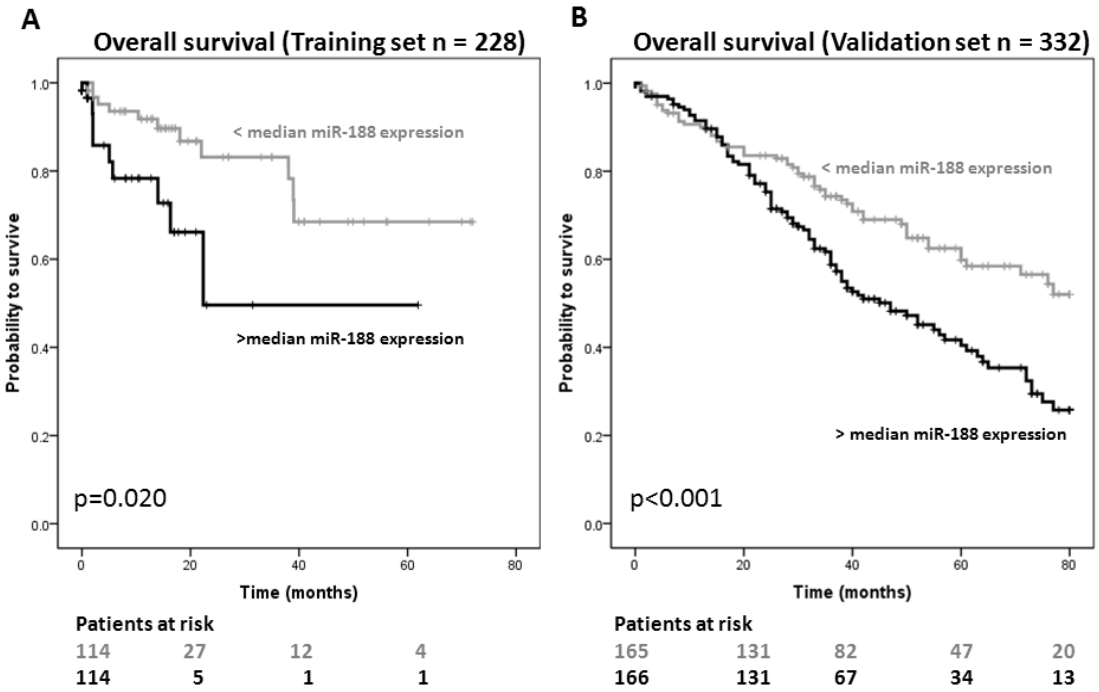

Figure 29: Kaplan-Meier curves. (A) Kaplan-Meier curve for overall survival in the screening set of 228 colorectal cancer patients. Patients were divided into two groups according to the median value of miR-188-3p expression. High miR-188-3p expression is a significant factor for poor prognosis (p = 0.020, log-rank test). **(B)** Kaplan-Meier curve for overall survival in the validation set of 332 colorectal cancer patients. Patients were dichotomized according to the median value of miR-188-3p expression. High miR-188-3p expression is a significant factor for poor prognosis (p<0.001, log-rank test). Figure taken from Pichler and Stiegelbauer *et al.*; Genome-wide microRNA analysis identifies miR-188-3p as novel prognostic marker and molecular factor involved in colorectal carcinogenesis; Clin. Cancer Res., 2016 September.

In the screening cohort, we observed that older age, high miR-188-3p and advanced tumor stage (stage IV versus stage I-III) are significantly associated with poor survival (all p-values <0.05, univariate Cox model), whereas gender and tumor location (colon versus rectum) were not significantly associated with clinical outcome (Table 16). A multivariate Cox analysis for both cohorts was performed to investigate whether the prognostic value of high miR-188-3p expression levels is independent of other well-known prognostic factors.

In cohort 1, multivariate analysis comprising age, gender, tumor location, tumor stage and miR-188-3p expression revealed that high miR-188-3p expression is an independent factor for poor survival in CRC patients (HR=4.137, 95%CI=1.568-10.917, p=0.004). In addition, we got statistically significant results for age (p=0.004) and advanced tumor stage (p<0.001), whereas all other parameters were not significantly associated with survival (Table 17). Furthermore, we analyzed the influence of miR-188-3p expression on the predictive ability of the model when added to established clinico-pathological factors in the TCGA dataset. We did a Harrel's concordance index and the predictive accuracies with and without miR-188-3p were compared. The c-index without miR-188-3p was 0.76 and improved to 0.86 when miR-188-3p was added, but was not statistically significant (p = 0.057). We could confirm a significant association of high miR-188-3p expression and poor survival in the validation cohort by performing a multivariate Cox analysis (HR=1.538, 95%CI=1.107-2.137, p=0.010, Table 17) (70).

Table 16: Univariate analysis of clinico-pathological parameters to predict overall survival in colorectal cancer patients in the screening cohort (n=228) and validation cohort (n=332)

Parameter	**Univariate analysis**			
	Screening set		**Validation set**	
	HR (95% CI)	***p*-value**	**HR (95% CI)**	***p*-value**
Age at diagnosis (years; continuous)	1.043 (1.004-1.083)	0.029	1.002 (0.987-1.016)	0.825
Gender				
Male	1 (reference)	0.746	1 (reference)	0.151
Female	0.873 (0.385-1.980)		0.788 (0.570-1.09)	
Tumor Location				
Colon	1 (reference)	0.189	1 (reference)	0.204
Rectum	0.441 (0.130-1.497)		1.297 (0.868-1.938)	
Tumor Stage				
I-III	1 (reference)	0.002	1 (reference)	<0.001
IV	3.635 (1.589-8.317)		4.93 (3.56-6.832)	
MiR-188-3p (median)				
low	1 (reference)	0.025	1 (reference)	<0.001
high	2.717 (1.135-6.507)		1.768 (1.283-2.436)	

Table 17: Multivariate analysis of clinico-pathological parameters to predict overall survival in patients with colorectal cancer in the screening set (n=228) and validation set (n=332) analyzed by multivariate analysis

Parameter	Multivariate analysis			
	Screening set		Validation set	
	HR (95% CI)	*p*-value	HR (95% CI)	*p*-value
Age at diagnosis (years; continuous)	1.067 (1.021-1.116)	0.004	1.007 (0.991-1.024)	0.387
Gender				
Male	1 (reference)	0.909	1 (reference)	0.364
Female	1.051 (0.448-2.465)		0.857 (0.615 – 1.195)	
Tumor Location				
Colon	1 (reference)	0.302	1 (reference)	0.995
Rectum	0.518 (0.148-1.808)		0.991 (0.650-1.534)	
Tumor Stage				
I-III	1 (reference)	<0.001	1 (reference)	<0.001
IV	4.739 (2.015-11.142)		4.686 (3.367-6.522)	
MiR-188-3p (median)				
low	1 (reference)	0.004	1 (reference)	0.010
high	4.137 (1.568-10.917)		1.538 (1.107-2.137)	

4.2.2 The biological role of miR-188-3p in CRC

To study the biological role of miR-188-3p and to find an explanation for the possible consequences of up-regulation of miR-188-3p in cancer tissue and the association of high tumor stage with high miR-188-3p levels as well as with poor survival, we ectopically overexpressed miR-188-3p in different CRC cell lines and anaylzed the influence on biological features. The expression levels of miR-188-3p in different CRC cell lines are shown in Figure 30 (70).

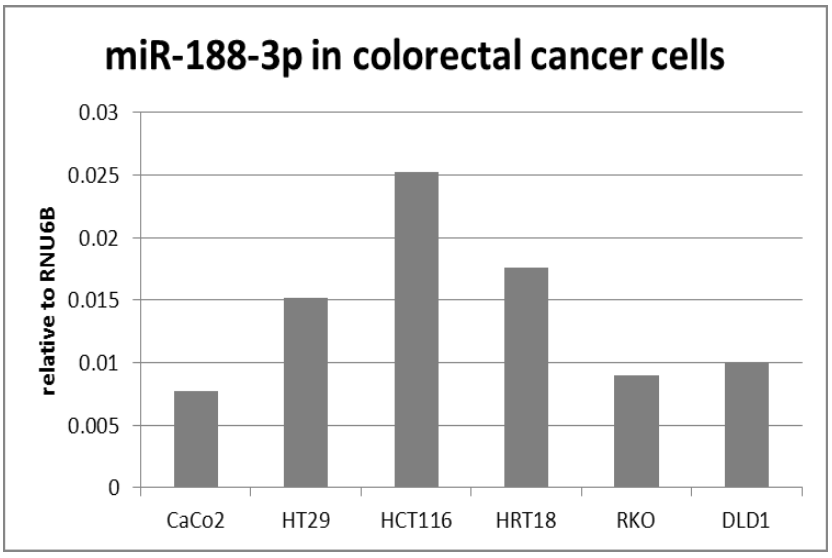

Figure 30: MiR-188-3p expression in CRC cell lines. MiR-188-3p is expressed in all tested colorectal cancer cell lines at varying levels, as measured by qRT-PCR. Figure taken from Pichler and Stiegelbauer *et al.*; Genome-wide microRNA analysis identifies miR-188-3p as novel prognostic marker and molecular factor involved in colorectal carcinogenesis; Clin. Cancer Res., 2016.

MiR-188-3p expression has no influence on cellular growth

First of all, we explored the influence of miR-188-3p expression on cellular growth, in a panel of three CRC cell lines (HCT116, HRT18 and RKO) but could not detect any significant differences or trends regarding this feature (Figures 31A,B and C).

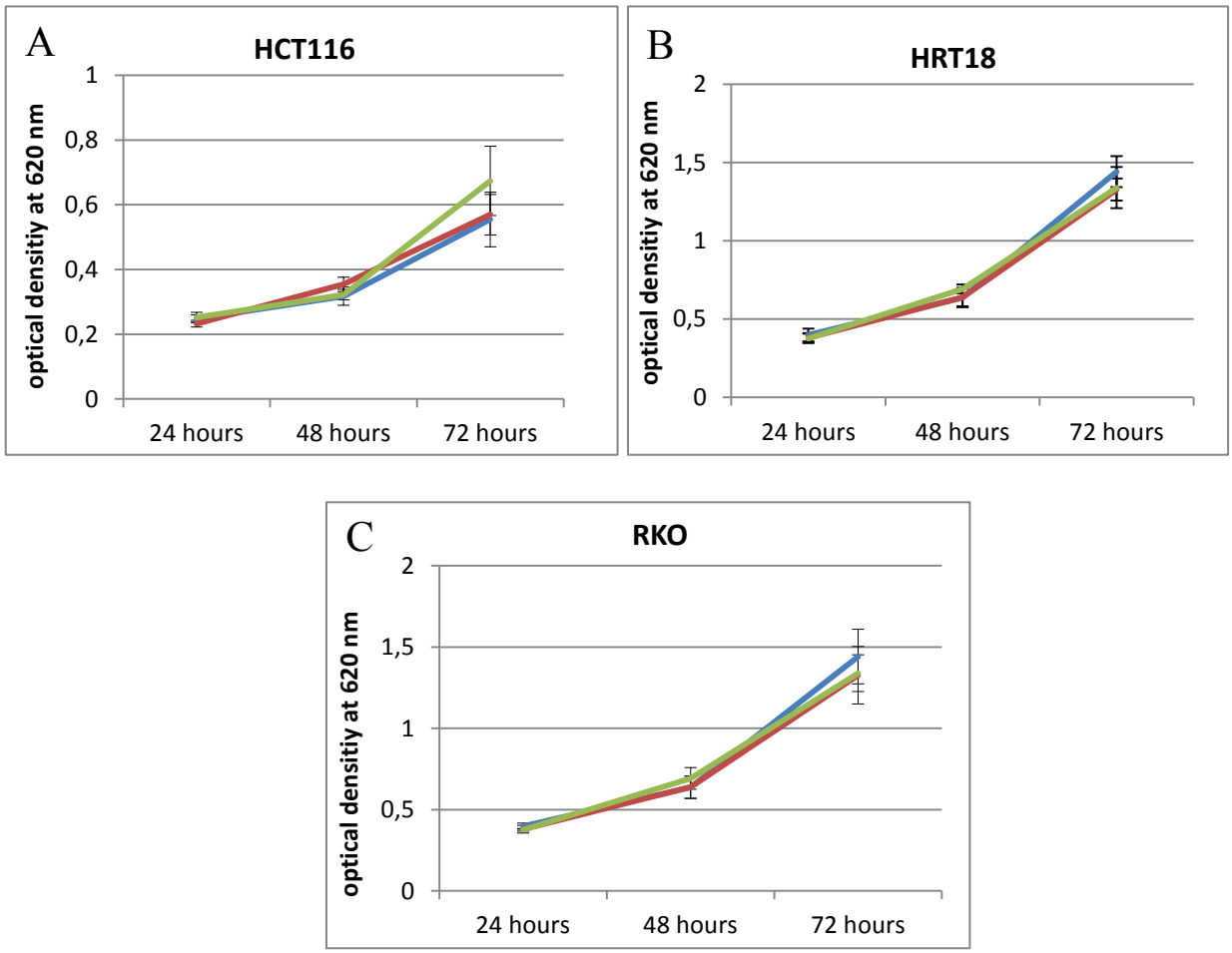

Figure 31: Cellular growth after miR-188-3p manipulation. (A-C) No significant differences or trend in three different colorectal cancer cell lines was detected by WST-1 proliferation assay after transfection with the respective control (green line), miR-188-3p mimic (blue) or inhibitor (red). Figure taken from Pichler and Stiegelbauer *et al.*; Genome-wide microRNA analysis identifies miR-188-3p as novel prognostic marker and molecular factor involved in colorectal carcinogenesis; Clin. Cancer Res., 2016 September.

MiR-188-3p expression does not have an impact on drug sensitivity

We next analyzed the influence of miR-188-3p expression levels on drug sensitivity for the three most commonly used drugs in CRC treatment (i.e. 5-Fluorouracil, Irinotecan and Oxaliplatin). As shown in figure 32-34, testing several concentrations of these drugs, we could not detect any significant differences with regard to chemotherapeutic sensitivity in

CRC cells transiently transfected with miR-188-3p mimic or inhibitor compared to control cells as measured by the WST-1 proliferation assay (70).

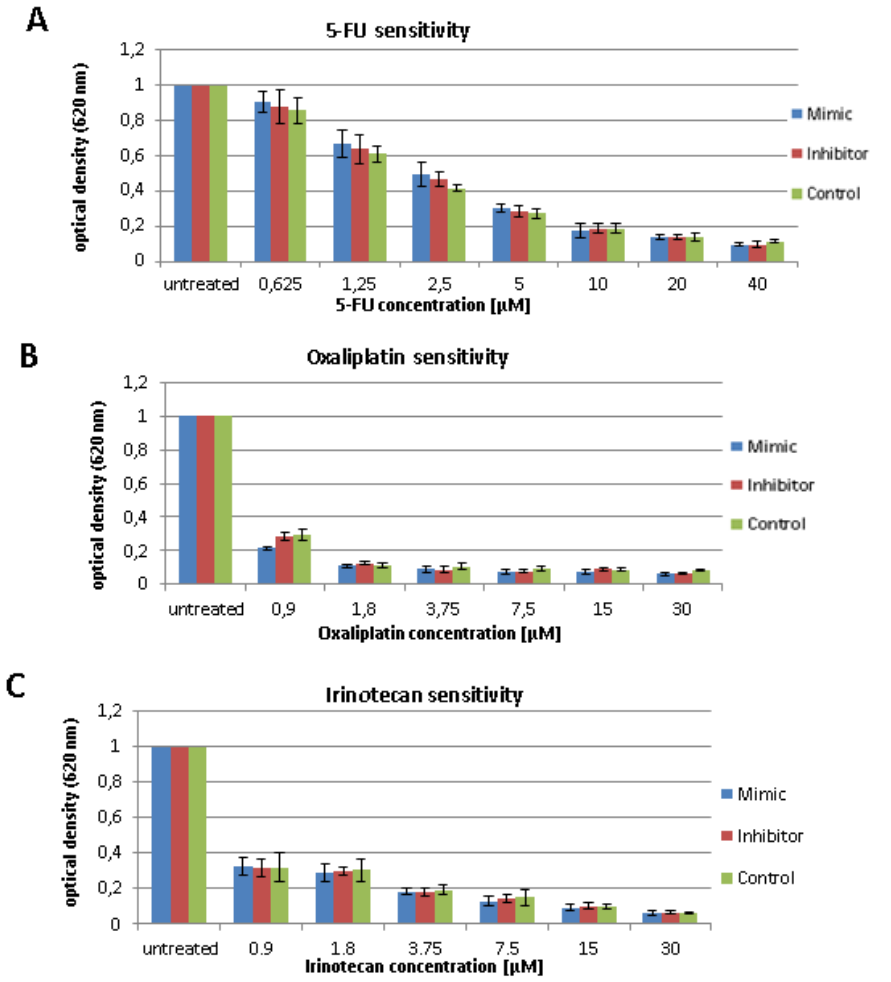

Figure 32: Sensitivity to chemotherapeutic drugs in HCT116. (A-C) No significant effects of miR-188-3p expression levels on drug sensitivity against commonly used colorectal cancer drugs were observed in HCT116 cells after transfection with miR-188-3p mimic, inhibitor or the respective control as measured by WST-1 assay. Figure taken from Pichler and Stiegelbauer *et al.*; Genome-wide microRNA analysis identifies miR-188-3p as novel prognostic marker and molecular factor involved in colorectal carcinogenesis; Clin. Cancer Res., 2016 September.

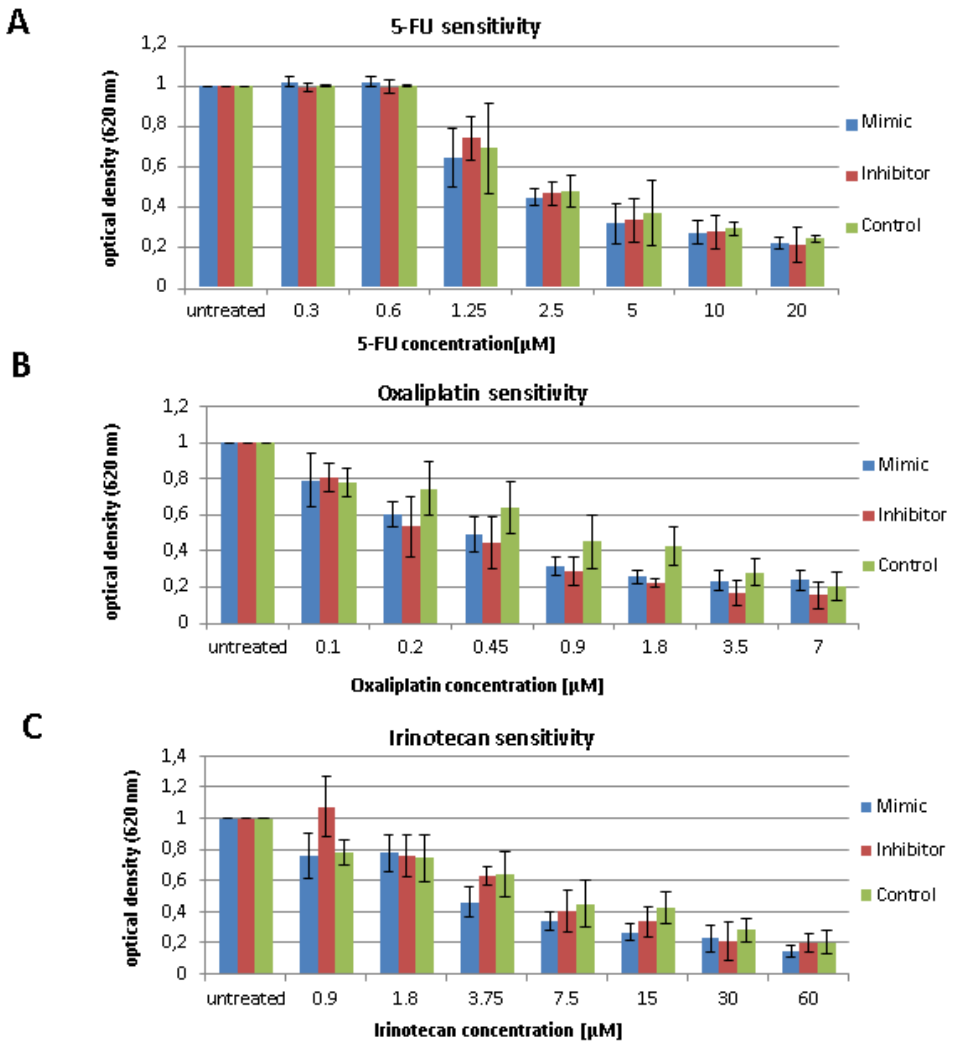

Figure 33: Sensitivity to chemotherapeutic drugs in HRT18. (A-C) No significant effects of miR-188-3p expression levels on drug sensitivity against commonly used colorectal cancer drugs were observed in HRT18 cells after transfection with miR-188-3p mimic, inhibitor or the respective control as measured by WST-1 assay. Figure taken from Pichler and Stiegelbauer *et al.*; Genome-wide microRNA analysis identifies miR-188-3p as novel prognostic marker and molecular factor involved in colorectal carcinogenesis; Clin. Cancer Res., 2016 September.

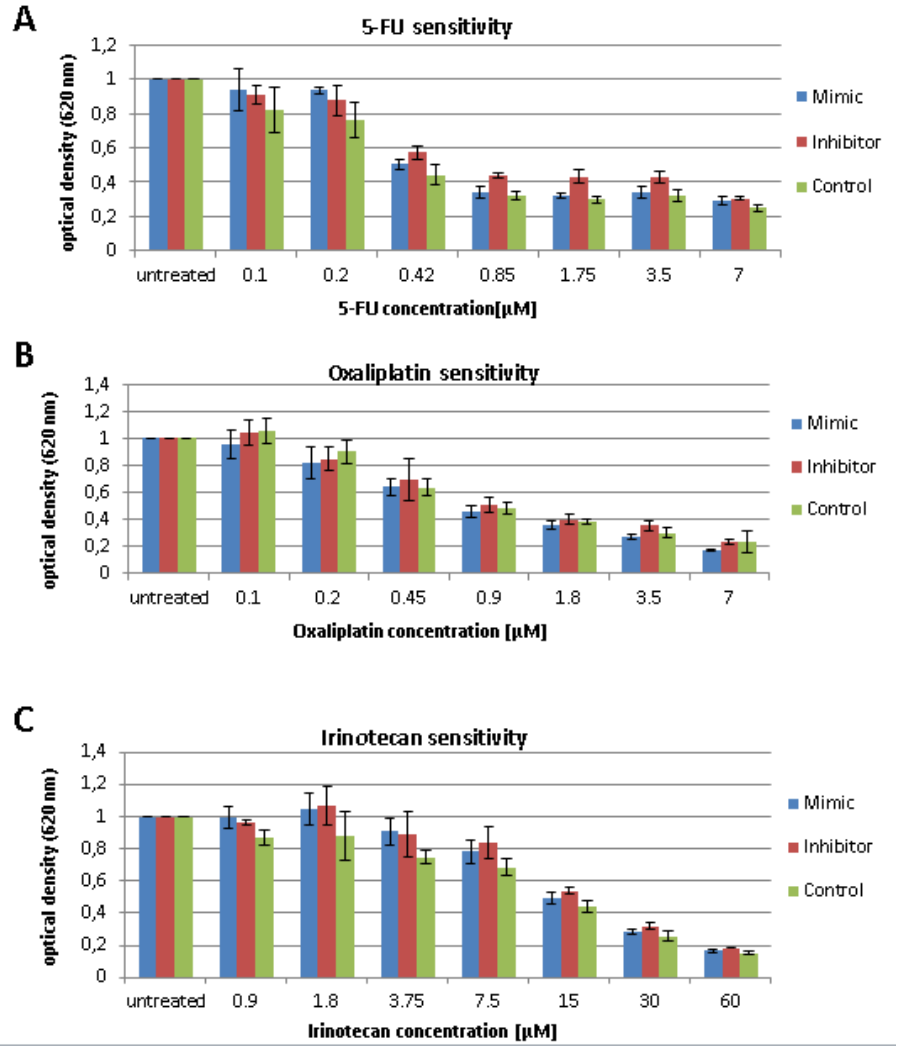

Figure 34: Sensitivity to chemotherapeutic drugs in RKO: (A-C) No significant effects of miR-188-3p expression levels on drug sensitivity against commonly used colorectal cancer drugs were detected in RKO cells after transfection with miR-188-3p mimic, inhibitor or the respective control as measured by WST-1 assay. Figure taken from Pichler and Stiegelbauer *et al.*; Genome-wide microRNA analysis identifies miR-188-3p as novel prognostic marker and molecular factor involved in colorectal carcinogenesis; Clin. Cancer Res., 2016 September.

MiR-188-3p expression influences cellular migration

After showing that miR-188-3p does not influence celluar growth of CRC cells, we further analyzed whether miR-188b-3p expression level has an effect on cellular migration. Therefore, we explored the migrational behavior after ectopic miR-188-3p expression. First, we applied the xCELLigence Real Time system. As shown in Figure 35, forced miR-188-3p expression resulted in significantly higher migration rates in HCT116, HRT18 und RKO cells in this model system.

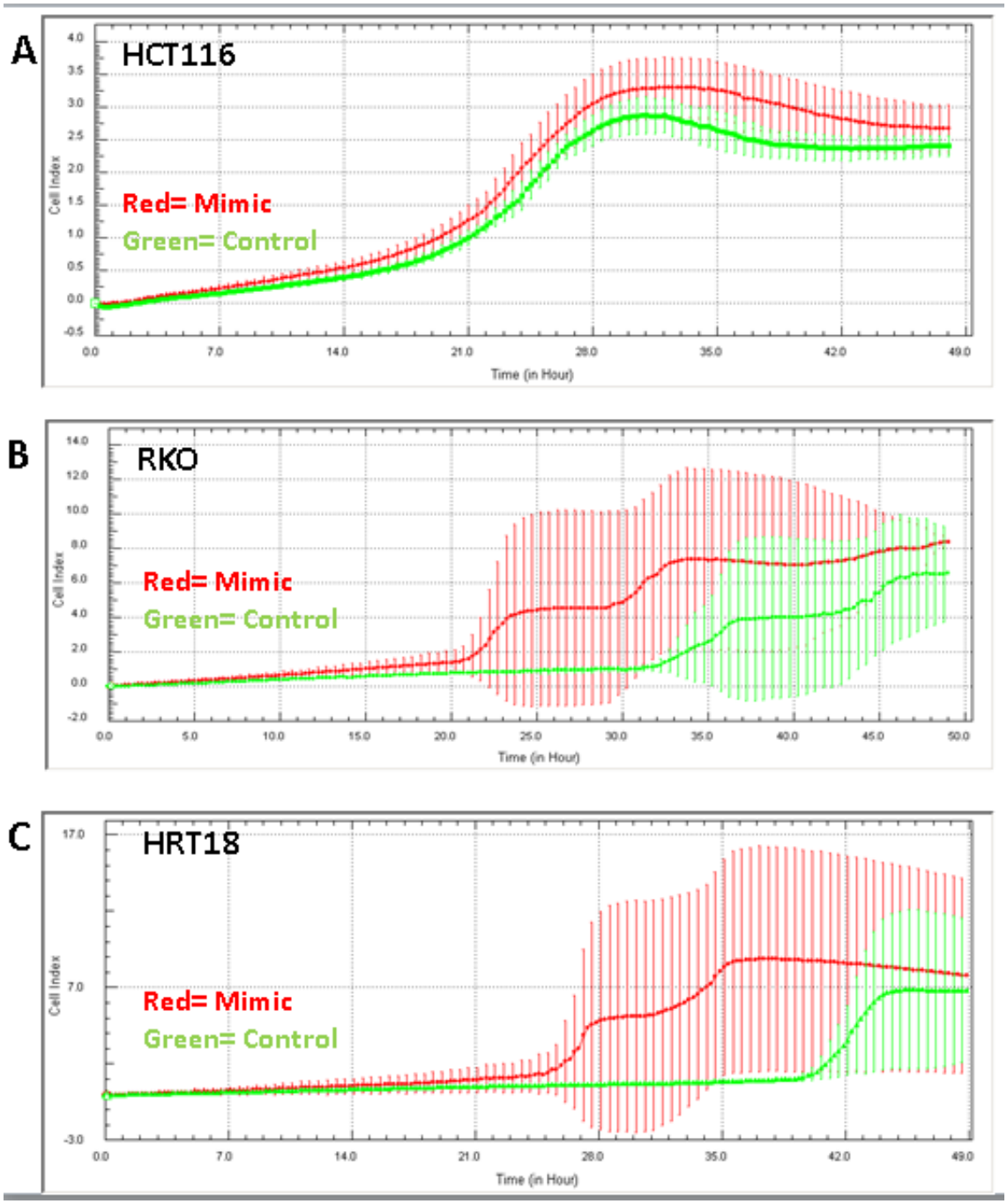

Figure 35: xCELLigence migration assay. (A) Overexpression of miR-188-3p resulted in a higher migration rate in HCT116 cells **(B)** and even significantly earlier and higher migration rate in RKO colorectal cancer cells. **(C)** In HRT18 enhanced mir188-3p expression led to increased migration rates compared to control cells ($p<0.05$, $n=3$). Figure taken from Pichler and Stiegelbauer *et al.*; Genome-wide microRNA analysis identifies miR-188-3p as novel prognostic marker and molecular factor involved in colorectal carcinogenesis; Clin. Cancer Res., 2016 September.

To confirm these findings, we used a second migration assay (scratch assay) to independently validate these results in three CRC cell lines (HCT116, RKO and HRT18).

In accordance with the data obtained from the xCELLigence assay, enhanced miR-188-3p expression led to a significantly increased scratch wound healing in all tested cell lines (Figure 36A-36F) (70).

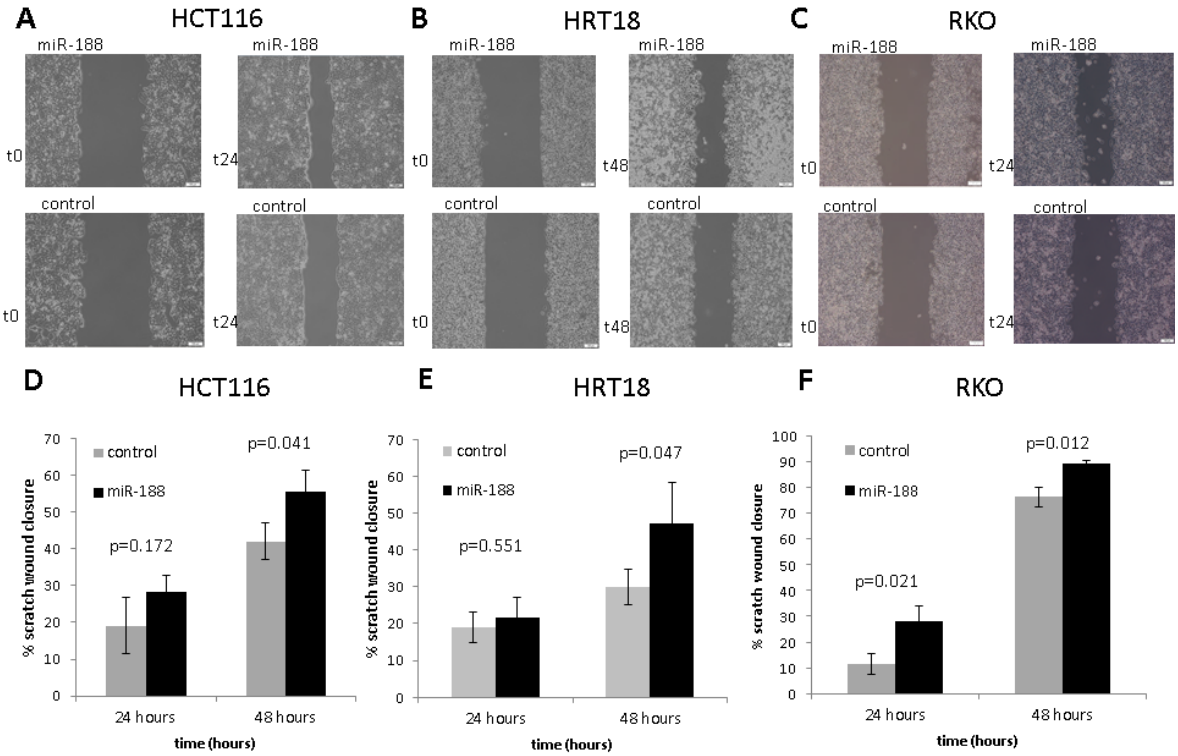

Figure 36: Scratch assays in three different colorectal cancer cell lines after miR-188-3p overexpression. (A-C) Representative pictures of scratch assays in HCT116, HRT18 and RKO cells after transfection with miR-188-3p mimic or control. t0 = scratch at beginning, t24 = scratch after 24 hours, t48 = scratch after 48 hours. **(D-F)** Bar charts graphs demonstrating the percentage of scratch closure after 24 and 48 hours for the three tested cell lines (n=4). Enhanced miR-188-3p expression led to a significantly earlier scratch closure compared to control (p-value <0.05 considered as significant, student´s t-test; error bars designate the standard deviation). Figure taken from Pichler and Stiegelbauer *et al*.; Genome-wide microRNA analysis identifies miR-188-3p as novel prognostic marker and molecular factor involved in colorectal carcinogenesis; Clin. Cancer Res., 2016 September

In contrast, when transfecting the miR-188-3p inhibitor, we could observe a decrease in cellular migration in all three (HCT116, HRT18 and RKO) cell lines (Figure 37A-F).

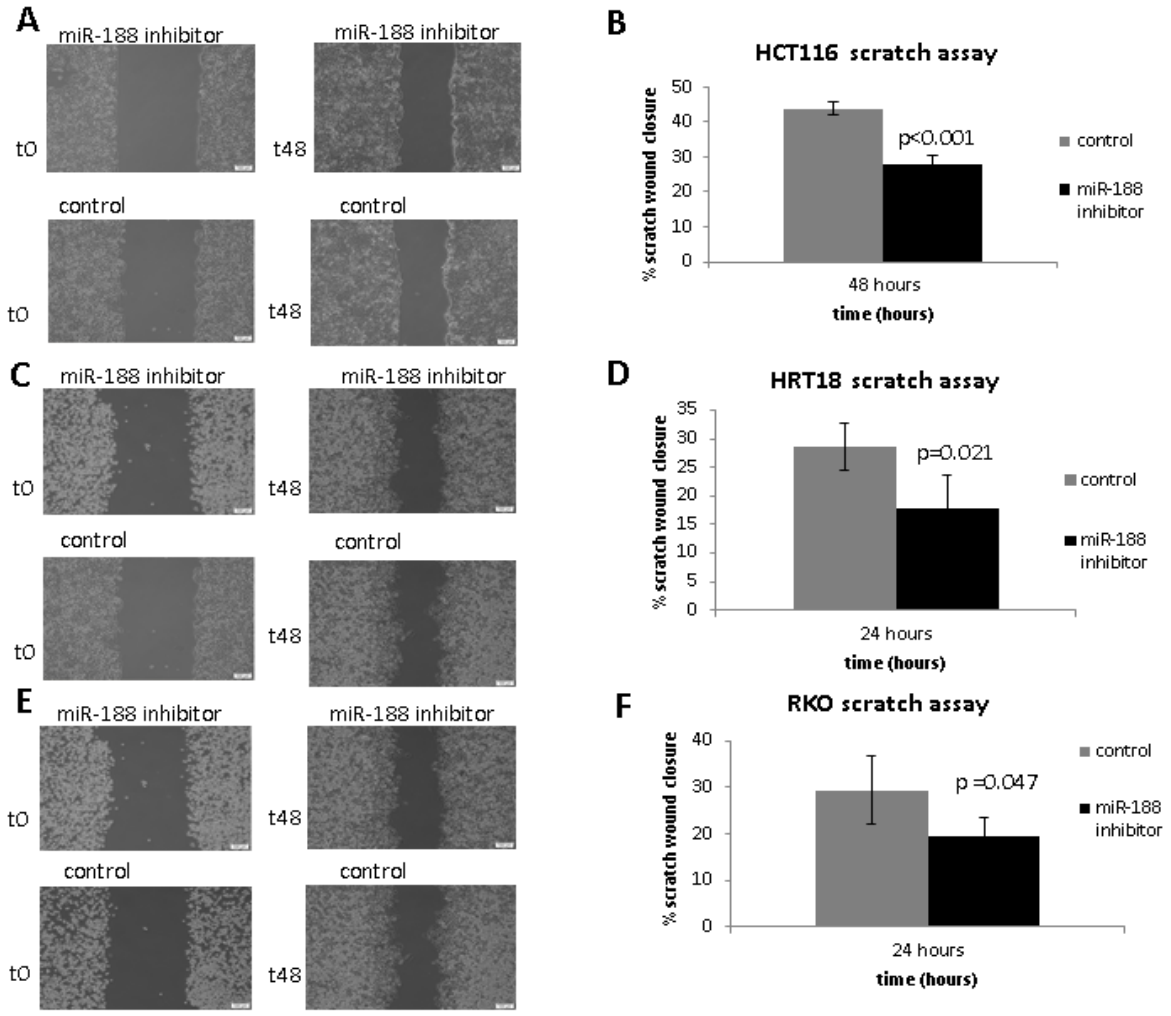

Figure 37: Scratch assay after miR-188-3p inhibition. (A-B) Inhibition of miR-188-3p resulted in decreased cellular migration in HCT116 cells, **(C-D)** in HRT18 cells and **(E-F)** in RKO cells ($p<0.05$, unpaired student´s t-test, n=4). Figure taken from Pichler and Stiegelbauer *et al*.; Genome-wide microRNA analysis identifies miR-188-3p as novel prognostic marker and molecular factor involved in colorectal carcinogenesis; Clin. Cancer Res., 2016 September

Forced miR-188-3p expression increased metastases formation in vivo

To confirm this potentially pro-metastatic phenotype of high miR-188-3p expression, we generated stable miR-188-3p overexpressing HCT116 cells. We obtained a 13 fold overexpression of miR-188-3p after stable transfection using lentiviral particles as measured by qRT-PCR (Figure 38A) (70).

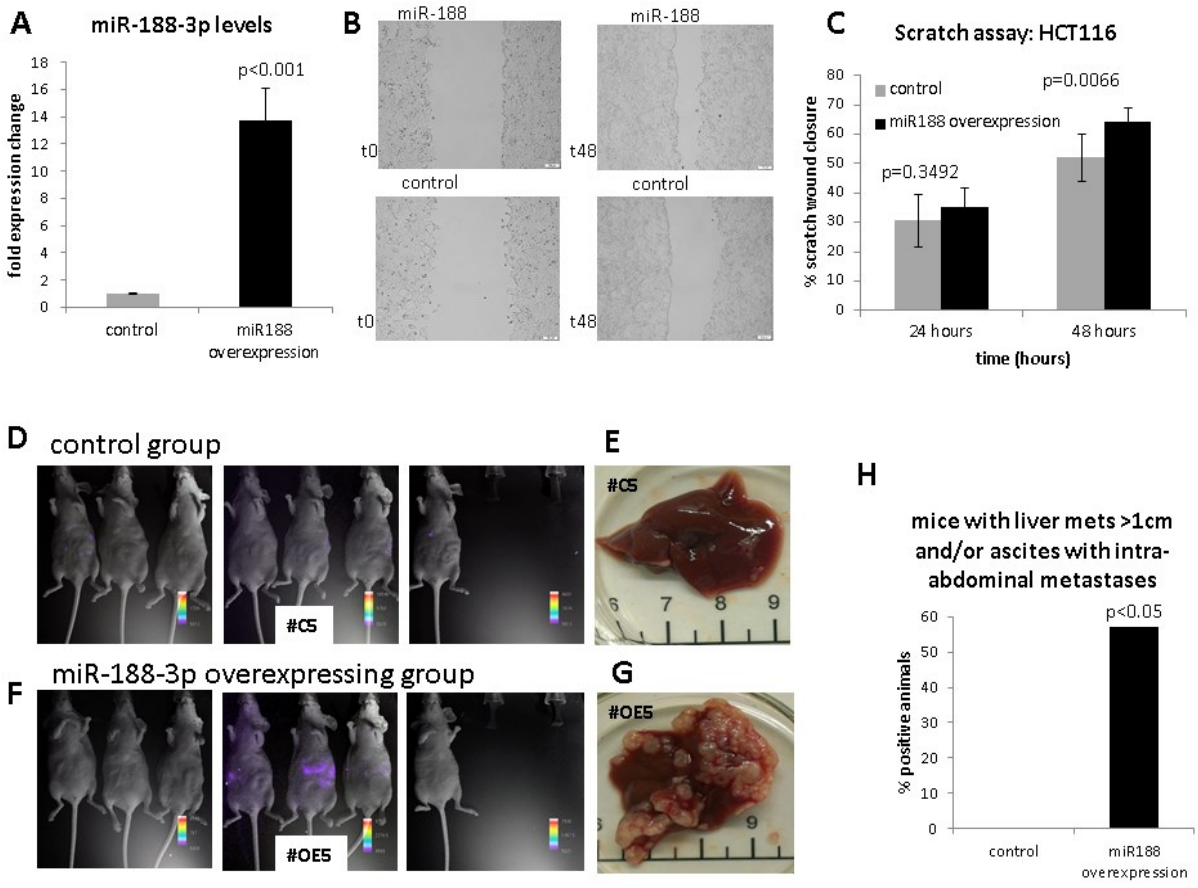

Figure 38: Forced miR-188-3p expression led to increased migration and metastasis formation. (A) A 13 fold overexpression of miR-188-3p in the stable transfected HCT116 cells was confirmed by qRT-PCR (p-value <0.05, student´s t-test). **(B)** Representative pictures of scratch assays in stable miR-188-3p overexpressing HCT116 cells; t0 = scratch at beginning, t48 = scratch after 48 hours. **(C)** Bar chart graph showing the percentage of scratch closure after 24 and 48 hours for the miR-188-3p stably overexpressing HCT116 cells. Overexpression of miR-188-3p led to significantly earlier scratch closure compared to the control (p-value <0.05 considered as significant, student´s t-test). **(D-G)** Representative pictures of in vivo imaging monitoring that revealed a high correlation between luminescence signals and pathological spread of liver metastases, e.g. for the index mouse #5 in the group of miR-188 overexpressing cells compared to control cells. **(H)** After 5 weeks of observation, we found a large extent of metastatic disease in a significantly higher number of mice in the group of miR-188-3p overexpression cells (p<0.05, Mann-Whitney U-test). Figure taken from Pichler and Stiegelbauer *et al.*; Genome-wide microRNA analysis identifies miR-188-3p as novel prognostic marker and molecular factor involved in colorectal carcinogenesis; Clin. Cancer Res., 2016 September

First, we confirmed a significantly higher migration rate for these cells *in vitro* (Figure 38B,C). Consequently, we injected HCT116 miR-188-3p stably overexpressing cells into the spleen of NMRI:nu/nu mice and compared the capacity of metastases formation to HCT116 control cells (n = 7 for each group). For vivo imaging the cells were labelled with a luciferase expressing vector before injecting the cells into the mice. The *in vivo* imaging monitoring showed the dissemination of metastases and indicated a high degree of

correlation with formation of macro-metastases (Figure 38D-G). After about 5 weeks of observation, we found metastases formation in the liver in all mice, which is consistent to findings of previous reports for this cell line (40). However, in the group of miR-188-3p overexpressing cells, a significantly higher number of animals had massive liver metastases (>1 cm in largest diameter) and/or ascites in combination with multiple intra-abdominal metastases (pancreas or peritoneum) in comparison to HCT116 control cells (57% versus 0%, $p<0.05$, Mann-Whitney U test, Figure 38H) (70).

4.2.3 Molecular mechanism of miR-188-3p

In order to find potential molecular miR-188-3p interactors related to cellular migration we performed bioinformatic analyses of putative miR-188-3p target genes. We identified several potential interaction partners and selected three of them (based on the criteria mentioned in the methods section), which have been previously involved in cancer cell migration in any type of cancer (i.e. *NLK*, *CTNNA2* and *MLLT4*). After transiently transfecting two independent CRC cell lines (HCT116 and HRT18) with a miR-188-3p mimic, we measured the expression changes of these three genes. Overexpression of miR-188-3p led to a 40-60% reduction of *MLLT4* mRNA (Figure 39A) and decreased MLLT4 proteinexpression levels (Figure 39B) in both cell lines. In contrast, miR-188-3p manipulation did not influence NLK expression levels and CNNA2 was not even detectable in these CRC cell lines (data not shown) (70).

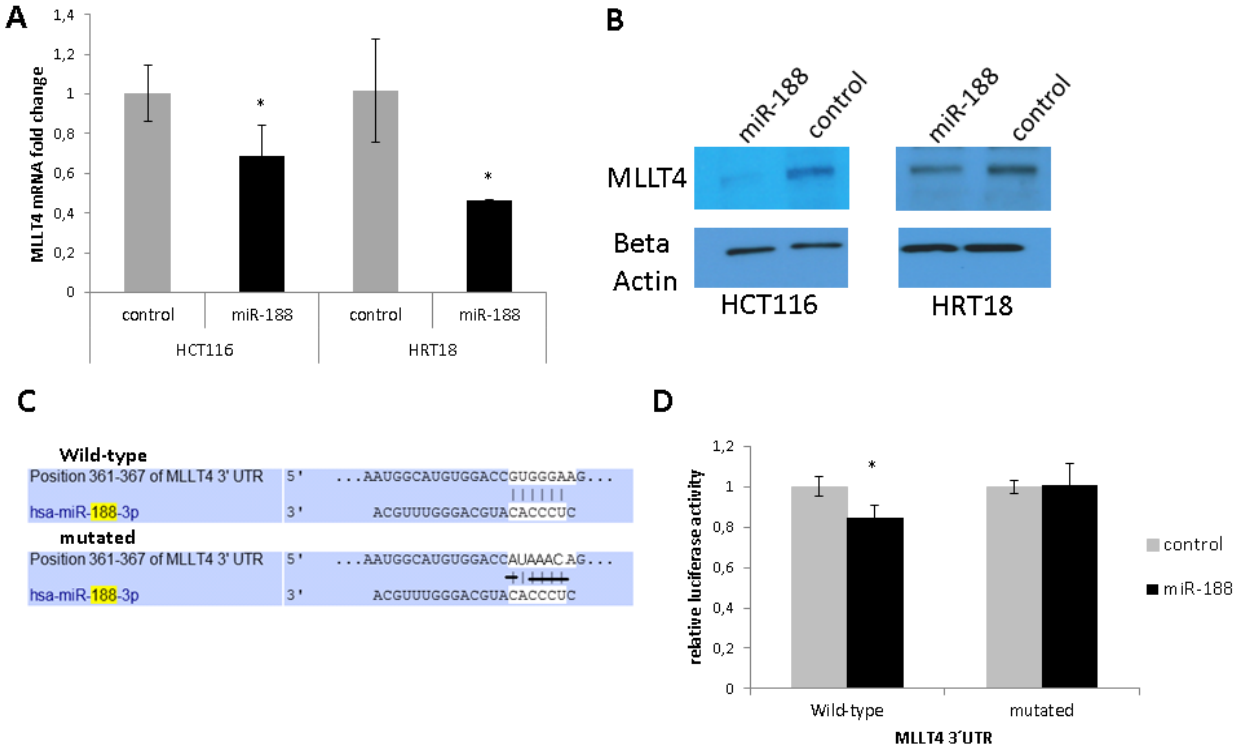

Figure 39: MLLT4 expression is regulated by miR-188-3p. MLLT4, a putative target of miR-188-3p, expression is decreased at mRNA levels **(A)** as well as protein levels **(B)** 48 hours after miR-188-3p mimic transfection in CRC cell lines. **(C)** Predicted target site of miR-188-3p within the 3´UTR (untranslated region) of MLLT4 mRNA. Two MLLT4 constructs were generated as indicated (miR-188-3p wild-type binding site and mutated binding site). **(D)** Luciferase activity was measured after co-transfection of the pMX-MLLT4 wild-type (left chart) or mutated (right chart) constructs and control/miR-188 mimetic in HEK cells. Three independent biological experiments were performed and the means and standard deviations are shown (*= significant; $p<0.05$, student´s t-test). Figure taken from Pichler and Stiegelbauer *et al.*; Genome-wide microRNA analysis identifies miR-188-3p as novel prognostic marker and molecular factor involved in colorectal carcinogenesis; Clin. Cancer Res., 2016 September.

The direct interaction of miR-188-3p with the *MLLT4* mRAN was further confimed by cloning the predicted 3´-UTR binding site in a luciferase-containing plasmid (binding site is shown in Figure 39C). After 24 hours, a reduction of luciferase activity was detected when the *MLLT4* 3´UTR wild-type sequence (Figure 39D) was co-transfected with the miR-188-3p mimic. The mutated binding site led to a restoration of normal luciferase activity (Figure 39D).

On the contrary, after miR-188-3p inhibiton, we observed a significantly increase of *MLLT4* expression of about 30% ($p<0.05$, unpaired student´s t-test, Figure 40A). Finally, to prove our hypothesis, that miR-188-3p exerts its effects on cellular migration by regulation of *MLLT4*, we performed an siRNA mediated knock-down of *MLLT4*. As

shown in Figure 40 we could confirm a significant downregulation of *MLLT4* in HCT116 and HRT18 cells on mRNA (Figure 40B-C) and protein level (Figure 40D) (70).

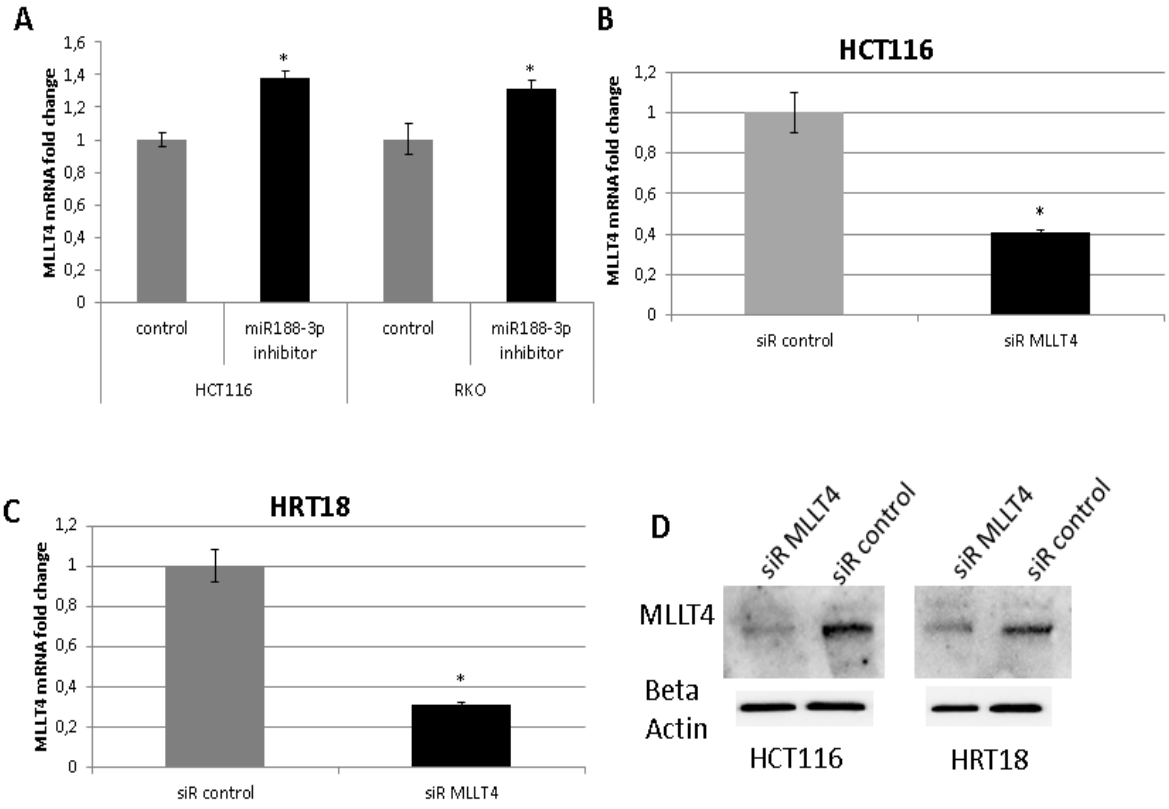

Figure 40: Knock-down of MLLT4 phenocopies the effect of miR-188-3p overexpression. **(A)** MiR-188-3p inhibition resulted in a 30% increase in MLLT4 mRNA expression after 48 hours in two independent cell lines ($p<0.05$, unpaired student´s t-test). **(B-C)** MLLT4 mRNA expression after 48 hours of *MLLT4*-directed siRNA transfection was analyzed by qRT-PCR in HCT116 and HRT18 cells. Results are presented as mean ± SD of three independent transfection experiments in HCT116 and HRT18 cells. **(D)** MLLT4 protein expression is decreased after 48 hours of siRNA transfection as detected by Western blot analysis in both cell lines. Figure taken from Pichler and Stiegelbauer *et al*.; Genome-wide microRNA analysis identifies miR-188-3p as novel prognostic marker and molecular factor involved in colorectal carcinogenesis; Clin. Cancer Res., 2016 September

Consequently, we investigated the influence of *MLLT4* on cellular migration in HRT18 and HCT116 cells. As shown in Figure 41, a reduction of *MLLT4* expression resulted in increased scratch wound closure of HCT116 and HRT18 cells. In conclusion, phenocopy and interaction experiments can partly explain the hypothesis that miR-188-3p regulates cellular migration by interacting with *MLLT4 (70)*.

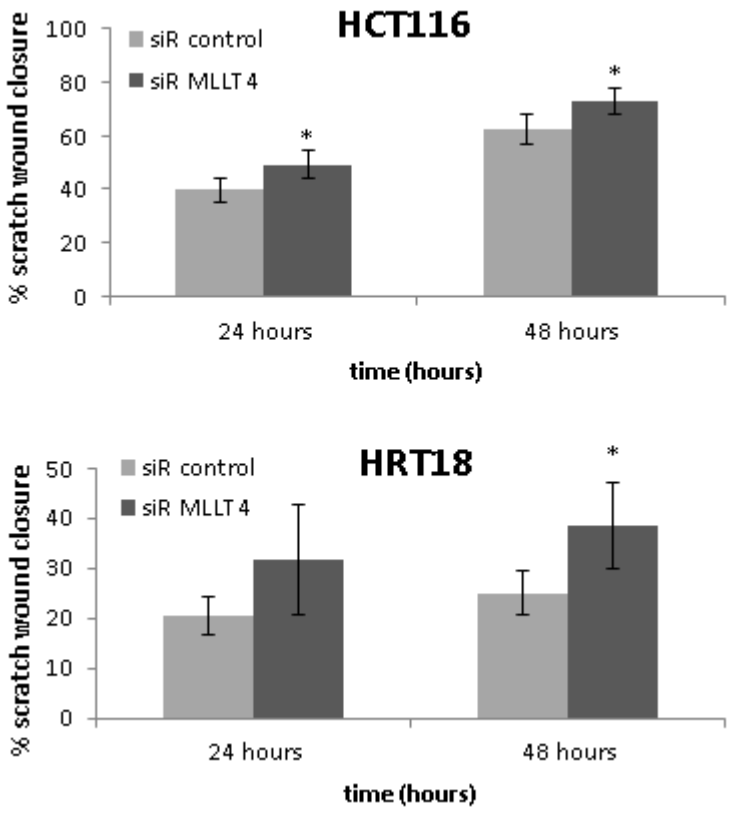

Figure 41: Scratch assay of HRT18 and HCT116 cells 24 and 48 hours after siRNA-mediated MLLT4 knock-down experiments. Reduction of MLLT4 expression resulted in an increase of migration in HCT116 (upper panel) and HRT18 (lower panel) cells (*$p<0.05$, student´s t-test). Figure taken from Pichler and Stiegelbauer *et al*.; Genome-wide microRNA analysis identifies miR-188-3p as novel prognostic marker and molecular factor involved in colorectal carcinogenesis; Clin. Cancer Res., 2016 September.

5. Discussion

Novel biomarkers are intensely investigated for clinical practice to predict prognosis and outcome of CRC patients. Such markers might be useful for risk stratification and patient surveillance and could provide a basis for decision making to avoid a potentially harmful, expensive and ineffective therapy. Since miRNAs are important regulators of carcinogenesis, cancer progression, invasion, angiogenesis and metastases in CRC, they might serve as potential prognostic factors (76). In addition, targeting miRNAs that are involved in steps of carcinogenesis may improve the therapeutic efficacy of established drugs and overcome drug resistance (77, 78). In this thesis we focused on two different miRNAs, namely miR-196b-5p and miR188-3p, and analyzed their role as prognostic marker and therapeutic target in CRC.

In the first part we investigated the association between miR-196b-5p expression and clinical outcome in CRC patients. MiR-196b-5p has been reported to be involved in several types of human malignancies including upregulation in acute lymphoblastic leukemia (79) as well as downregulation in glioblastoma (80), cervical cancer (81) and B-cell lineage lymphoma (82). These discordant observations highlight the fact that miR-196b-5p can function as either an "oncomiR" or a tumor suppressive miRNA, as previously described for many other miRNAs (37).
In regard to CRC, controversially data exist about the prognostic role and biological function of miR-196b-5p. By analyzing 292 CRC patient samples from two independent cohorts, we showed that low miR-196b-5p expression is significantly associated with poor prognosis. Our results confirm the data from Boisen *et al.*, a large three cohorts study showing that higher miR-196b-5p expression levels were associated with improved outcome regardless of bevacizumab treatment, with similar effect estimated in all three cohorts (83). The strengthen of our study and the study by Boisen *et al*. are the large number of patients and the confirmation in independent cohorts, thus establishing low levels of miR-196-5p as a poor prognostic factor in CRC patients.

In order to clarify the underlying cellular and molecular mechanisms of our observation that low levels of miR-196b-5p were significantly associated with poor patient outcome, we performed several *in vitro* experiments. We did not observe any significant differences in cancer cell growth in all three tested cell lines, suggesting this hallmark of cancer is not impacted by miR-196b-5p. Some studies reported a significant association of miR-196b-5p

and the clinical response to chemotherapy (84, 85). However, in our study there was no significant difference in drug sensitivity upon gain and loss of function experiments of miR-196b-5p for all tested CRC cell lines. Interestingly, in our clinical part we identified a significant association between low miR-196b-5p levels and the occurrence of metastatic stage IV disease in both of our cohorts. Therefore, we comprehensively studied whether cancer cell migration and invasion are influenced by miR-196b-5p levels. For this purpose, we used three independent different CRC cell lines, different models of miR-196b-5p manipulation (transient and stable), different and independent *in vitro* assays and *in vivo* metastases formation experiments. Importantly, we observed a highly consistent phenotype of increased cancer cell migration/metastases in CRC with low levels of miR-196b-5p expression. This experimental approach suggests that the observed association between low levels of miR-196b-5p and stage IV disease/poor clinical outcome is probably constituted on the capability of increased cellular migration and metastatic spread.

In order to identify a possible molecular mechanism that might explain this metastatic behaviour, we further performed a whole transcriptome analysis using a stable miR-196b-5p overexpression CRC cell line model. Based on the hypothesis that genes whose expression is regulated by miR-196b-5p and thus show decreased expression in miR-196b-5p overexpressing cells, we identified several potential candidates. We were mainly interested in direct interaction partners and, therefore, we performed *in silico* target prediction analysis of potential target genes and combined this analysis with a literature search to select candidates with possible impact on cellular migration. Finally, we identified two genes, *HOXB7* and *GalNT5* that have been previously involved in gastric and cervical cancer cell migration and/or invasion (81, 86, 87). In CRC, a study by Liao *et al.* has already demonstrated that *HOXB7* expression significantly correlates with invasive and aggressive characteristics and poor survival of patients. Liao *et al*. also showed that *HOXB7* overexpression promotes cell proliferation and tumor growth in CRC, both *in vitro* and *in vivo (88)*. This data prompted us to focus on these two genes and we demonstrated that forced miR-196b-5p expression decrease *GalNT5* and *HOXB7* expression on mRNA and protein levels. A previous study by How and colleagues (81) has already identified a direct interaction of miR-196b-5p and *HOXB7* in cervical cancer. Taken together, our findings show that miR-196b-5p acts through regulation of *HOXB7* expression across different types of cancer. Based on the already reported direct interaction of miR-196b-5p and *HOXB7*, we did not further validate the identical interaction site of the *HOXB7* 3'UTR.

However, a role of *GalNT5* in CRC has never been reported before, thus we further focused on this gene.

Generally, members of the *GalNT (*N-Acetylgalactosaminyltransferase) family are responsible for glycosylation of *O-GalNAc*s (O-glycans linked with *N*-acetylgalactosamine). A study by Zhang *and* colleagues indicates that *O*-glycosylation has an impact on the composition of the extracellular matrix and suggests a role for abundant protein modification in disease states where matrix composition and cell adhesion are changed (89). O-GalNAc glycosylation of extracellular (ECM) proteins is an important modification for their secretion and plays a role in modulating ECM composition and influencing cell adhesion, growth and embryogenesis. *O-GalNAc* glycans have been involved in several molecular mechanisms that might play key roles in tumor formation, cell invasion and cancer progression (90). A role of the *GalNT* enzyme family in cancer has already been reported in several types of human malignancies. For instance, a study by Peng *et al*. demonstrated that knockdown of *GalNT7* resulted in inhibition of cervical cancer cell proliferation, migration and invasion (91). Regarding *GalNT5* the only published study so far is from He *et al.*, who revealed that low expression of *GalNT5* is significantly associated with poor prognosis in patients with gastric cancer (87). We confirmed a direct interaction of miR-196b-5p and *GalNT5* by performing a luciferase assay with a wild-type and mutated putative binding site of this miRNA in the 3'UTR of *GalNT5*.

Finally, to test the hypothesis that *HOXB7* and *GalNT5* mediating (pheno-copying) the effects of miR-196b-5p, we performed migration assays after siRNA knock-down experiments for both genes. Notably, a reduction of *HOXB7* and *GalNT5* expression pheno-copied the effects of miR-196-5p overexpression and this anti-migratory effect was even more pronounced when a knock-down of both genes in parallel was performed. These findings underline the fact that targeting multiple mRNAs in parallel can augment the biological but also potentially therapeutic effects of miRNAs.

In the second part of this thesis we analyzed RNA seq data of numerous miRNA from more than 200 patient samples obtained from the Cancer Genome Atlas dataset. We found several six miRNAs complying the stringent inclusion criteria (miR-92b, miR-188-3p, miR-221*, miR-331, miR-425* and miR-497). Two of them, namely miR-92b (92) and miR-221* (93), have been previously suggested as prognostic factors in other CRC studies.

Additionally, miR-331 might be a circulating plasma biomarker to differentiate colon polyps from normal mucosa (94) and it has been shown that miR-497 might play a role in the regulation of the endogenous insulin-like growth factor receptor 1 expression, as well as cell survival, proliferation and invasion (95). The results from the TCGA dataset confirm their involvement in colorectal carcinogenesis. MiR-425* and miR-188-3p have not been investigated in CRC so far. Next, we wanted to validate these newly identified potential prognostic risk factors in an independent cohort to confirm their applicability as prognostic markers. Therefore, we analyzed a second large cohort and explored the correlation of these six miRNAs with patient prognosis. Applying stringent pre-specified criteria, we could only confirm that high expression levels of miR-188-3p are associated with poor prognosis in both cohorts (70).

We further characterized a possible biological role of miR-188-3p in CRC. By performing several cellular assays and a xenograft mouse model we could show that enhanced miR-188-3p expression resulted in increased cellular migration *in vitro* and metastases formation *in vivo*. These results confirm our findings that metastatic stage IV patients in the large validation cohort had higher miR-188-3p levels compared to localized stages. In order to identify possible molecular mechanisms regulated by miR-188-3p, we performed an in silico target analysis to predict putative interacting partners. We identified one candidate, namely *MLLT4*, which has been previously involved in breast and pancreatic cancer as a negative regulator of migration and metastases (96, 97). We actually showed that miR-188-3p negatively influence the expression of *MLLT4* as well as directly interacts with the predicted binding site in the 3´UTR region of the *MLLT4* mRNA We could confirm a phenocopy of the effects of miR-188-3p overexpression by siRNA knock-down experiments and identified *MLLT4* as a novel regulator of cancer cell migration in CRC (70).

It has been previously reported that miR-188-3p is involved in rectal cancer and response to neoadjuvant radio-chemotherapy (98). In contrast to our findings, miR-188 has been suggested as a tumor suppressive factor that acts through the inhibition of G1/S-phase cell cycle transition in nasopharyngeal carcinoma and growth/metastases inhibition in prostate cancer (99, 100). The prognostic value of miR188 in CRC should be further analyzed in prospective biomarker studies which might help to improve patient´s outcome, stratification in clinical trial and individual risk stratification. The use of miR-188-3p inhibitors as potential agents to decrease the risk of metastases and the spread of

metastases should be further tested in pre-clinical models. Additionally, clarifying the role of MLLT4 in CRC carcinogenesis and progression might be helpful in developing inhibitors against this pro-migratory protein (70).

Our two studies are not without limitations. All cohorts analyzed in this thesis are retrospective in their nature and like all retrospective studies prone to selection bias. The treatment schedule was heterogeneous and we cannot exclude that changes in medical treatment over the years might have an influence on our findings.

In conclusion, our findings suggest that miR-196b-5p and miR-188-3p play a role in colorectal carcinogenesis. This study establishes miR-196b-5p as a prognostic factor in CRC. MiR-196b-5p promotes CRC metastases, at least in part, through the regulation of *HOXB7* and *GalNT5*. In addition, we showed that miR-188-3p is an independent negative prognostic marker and improves the predictive ability of established prognostic risk factors in CRC patients. Prospective randomized trials are needed to further investigate the role of miR-196b-5p and miR-188-3p as a prognostic classifier in different disease settings of CRC patients (70).

6. References

1. Siegel RL, Miller KD, Jemal A. Cancer statistics, 2015. CA: a cancer journal for clinicians. 2015;65(1):5-29.
2. Winawer SJ, Fletcher RH, Miller L, Godlee F, Stolar MH, Mulrow CD, et al. Colorectal cancer screening: clinical guidelines and rationale. Gastroenterology. 1997;112(2):594-642.
3. Butterworth AS, Higgins JP, Pharoah P. Relative and absolute risk of colorectal cancer for individuals with a family history: a meta-analysis. European journal of cancer. 2006;42(2):216-27.
4. Johnson CM, Wei C, Ensor JE, Smolenski DJ, Amos CI, Levin B, et al. Meta-analyses of colorectal cancer risk factors. Cancer causes & control : CCC. 2013;24(6):1207-22.
5. Gout S, Huot J. Role of cancer microenvironment in metastasis: focus on colon cancer. Cancer microenvironment : official journal of the International Cancer Microenvironment Society. 2008;1(1):69-83.
6. Markowitz SD, Bertagnolli MM. Molecular origins of cancer: Molecular basis of colorectal cancer. The New England journal of medicine. 2009;361(25):2449-60.
7. El Zoghbi M, Cummings LC. New era of colorectal cancer screening. World journal of gastrointestinal endoscopy. 2016;8(5):252-8.
8. Hurlstone DP, Cross SS, Adam I, Shorthouse AJ, Brown S, Sanders DS, et al. A prospective clinicopathological and endoscopic evaluation of flat and depressed colorectal lesions in the United Kingdom. The American journal of gastroenterology. 2003;98(11):2543-9.
9. Kudo S, Lambert R, Allen JI, Fujii H, Fujii T, Kashida H, et al. Nonpolypoid neoplastic lesions of the colorectal mucosa. Gastrointestinal endoscopy. 2008;68(4 Suppl):S3-47.
10. Kerr D. Clinical development of gene therapy for colorectal cancer. Nature reviews Cancer. 2003;3(8):615-22.
11. Cunningham D, Atkin W, Lenz HJ, Lynch HT, Minsky B, Nordlinger B, et al. Colorectal cancer. Lancet. 2010;375(9719):1030-47.
12. Gill S, Dowden S, Colwell B, Collins LL, Berry S. Navigating later lines of treatment for advanced colorectal cancer - optimizing targeted biological therapies to improve outcomes. Cancer treatment reviews. 2014;40(10):1171-81.
13. Dallas NA, Xia L, Fan F, Gray MJ, Gaur P, van Buren G, 2nd, et al. Chemoresistant colorectal cancer cells, the cancer stem cell phenotype, and increased sensitivity to insulin-like growth factor-I receptor inhibition. Cancer research. 2009;69(5):1951-7.
14. Etienne MC, Chazal M, Laurent-Puig P, Magne N, Rosty C, Formento JL, et al. Prognostic value of tumoral thymidylate synthase and p53 in metastatic colorectal cancer patients receiving fluorouracil-based chemotherapy: phenotypic and genotypic analyses. Journal of clinical oncology : official journal of the American Society of Clinical Oncology. 2002;20(12):2832-43.
15. de la Cueva A, Ramirez de Molina A, Alvarez-Ayerza N, Ramos MA, Cebrian A, Del Pulgar TG, et al. Combined 5-FU and ChoKalpha inhibitors as a new alternative therapy of colorectal cancer: evidence in human tumor-derived cell lines and mouse xenografts. PloS one. 2013;8(6):e64961.
16. Rougier P, Bugat R, Douillard JY, Culine S, Suc E, Brunet P, et al. Phase II study of irinotecan in the treatment of advanced colorectal cancer in chemotherapy-naive patients and patients pretreated with fluorouracil-based chemotherapy. Journal of clinical oncology : official journal of the American Society of Clinical Oncology. 1997;15(1):251-60.
17. de Gramont A, Bosset JF, Milan C, Rougier P, Bouche O, Etienne PL, et al. Randomized trial comparing monthly low-dose leucovorin and fluorouracil bolus with bimonthly high-dose leucovorin and fluorouracil bolus plus continuous infusion for advanced colorectal cancer: a French intergroup study. Journal of clinical oncology : official journal of the American Society of Clinical Oncology. 1997;15(2):808-15.

18. Stiegelbauer V, Perakis S, Deutsch A, Ling H, Gerger A, Pichler M. MicroRNAs as novel predictive biomarkers and therapeutic targets in colorectal cancer. World journal of gastroenterology. 2014;20(33):11727-35.
19. Fujita K, Kubota Y, Ishida H, Sasaki Y. Irinotecan, a key chemotherapeutic drug for metastatic colorectal cancer. World journal of gastroenterology. 2015;21(43):12234-48.
20. Chang DZ, Kumar V, Ma Y, Li K, Kopetz S. Individualized therapies in colorectal cancer: KRAS as a marker for response to EGFR-targeted therapy. Journal of hematology & oncology. 2009;2:18.
21. Li S, Schmitz KR, Jeffrey PD, Wiltzius JJ, Kussie P, Ferguson KM. Structural basis for inhibition of the epidermal growth factor receptor by cetuximab. Cancer cell. 2005;7(4):301-11.
22. Voigt M, Braig F, Gothel M, Schulte A, Lamszus K, Bokemeyer C, et al. Functional dissection of the epidermal growth factor receptor epitopes targeted by panitumumab and cetuximab. Neoplasia (New York, NY). 2012;14(11):1023-31.
23. Misale S, Yaeger R, Hobor S, Scala E, Janakiraman M, Liska D, et al. Emergence of KRAS mutations and acquired resistance to anti-EGFR therapy in colorectal cancer. Nature. 2012;486(7404):532-6.
24. Jiang Z, Li C, Li F, Wang X. EGFR gene copy number as a prognostic marker in colorectal cancer patients treated with cetuximab or panitumumab: a systematic review and meta analysis. PloS one. 2013;8(2):e56205.
25. Moroni M, Veronese S, Benvenuti S, Marrapese G, Sartore-Bianchi A, Di Nicolantonio F, et al. Gene copy number for epidermal growth factor receptor (EGFR) and clinical response to antiEGFR treatment in colorectal cancer: a cohort study. The Lancet Oncology. 2005;6(5):279-86.
26. Personeni N, Fieuws S, Piessevaux H, De Hertogh G, De Schutter J, Biesmans B, et al. Clinical usefulness of EGFR gene copy number as a predictive marker in colorectal cancer patients treated with cetuximab: a fluorescent in situ hybridization study. Clinical cancer research : an official journal of the American Association for Cancer Research. 2008;14(18):5869-76.
27. Douillard JY, Oliner KS, Siena S, Tabernero J, Burkes R, Barugel M, et al. Panitumumab-FOLFOX4 treatment and RAS mutations in colorectal cancer. The New England journal of medicine. 2013;369(11):1023-34.
28. Grothey A, Allegra C. Antiangiogenesis therapy in the treatment of metastatic colorectal cancer. Therapeutic advances in medical oncology. 2012;4(6):301-19.
29. Kerbel RS. Tumor angiogenesis. The New England journal of medicine. 2008;358(19):2039-49.
30. Bottsford-Miller JN, Coleman RL, Sood AK. Resistance and escape from antiangiogenesis therapy: clinical implications and future strategies. Journal of clinical oncology : official journal of the American Society of Clinical Oncology. 2012;30(32):4026-34.
31. Ferrara N, Gerber HP, LeCouter J. The biology of VEGF and its receptors. Nature medicine. 2003;9(6):669-76.
32. Ellis LM, Hicklin DJ. VEGF-targeted therapy: mechanisms of anti-tumour activity. Nature reviews Cancer. 2008;8(8):579-91.
33. Saif MW. Anti-VEGF agents in metastatic colorectal cancer (mCRC): are they all alike? Cancer management and research. 2013;5:103-15.
34. Tejpar S, Prenen H, Mazzone M. Overcoming resistance to antiangiogenic therapies. The oncologist. 2012;17(8):1039-50.
35. Bartel DP. MicroRNAs: genomics, biogenesis, mechanism, and function. Cell. 2004;116(2):281-97.
36. Calin GA, Croce CM. MicroRNA signatures in human cancers. Nature reviews Cancer. 2006;6(11):857-66.
37. Svoronos AA, Engelman DM, Slack FJ. OncomiR or Tumor Suppressor? The Duplicity of MicroRNAs in Cancer. Cancer research. 2016;76(13):3666-70.
38. Slaby O, Svoboda M, Michalek J, Vyzula R. MicroRNAs in colorectal cancer: translation of molecular biology into clinical application. Molecular cancer. 2009;8:102.

39. Erson AE, Petty EM. MicroRNAs in development and disease. Clinical genetics. 2008;74(4):296-306.
40. Ling H, Pickard K, Ivan C, Isella C, Ikuo M, Mitter R, et al. The clinical and biological significance of MIR-224 expression in colorectal cancer metastasis. Gut. 2015.
41. Hur K, Toiyama Y, Takahashi M, Balaguer F, Nagasaka T, Koike J, et al. MicroRNA-200c modulates epithelial-to-mesenchymal transition (EMT) in human colorectal cancer metastasis. Gut. 2013;62(9):1315-26.
42. Ma L, Teruya-Feldstein J, Weinberg RA. Tumour invasion and metastasis initiated by microRNA-10b in breast cancer. Nature. 2007;449(7163):682-8.
43. Cortez MA, Bueso-Ramos C, Ferdin J, Lopez-Berestein G, Sood AK, Calin GA. MicroRNAs in body fluids--the mix of hormones and biomarkers. Nature reviews Clinical oncology. 2011;8(8):467-77.
44. Pichler M, Calin GA. MicroRNAs in cancer: from developmental genes in worms to their clinical application in patients. British journal of cancer. 2015;113(4):569-73.
45. Chen L, Yan HX, Yang W, Hu L, Yu LX, Liu Q, et al. The role of microRNA expression pattern in human intrahepatic cholangiocarcinoma. Journal of hepatology. 2009;50(2):358-69.
46. Sun W, Julie Li YS, Huang HD, Shyy JY, Chien S. microRNA: a master regulator of cellular processes for bioengineering systems. Annual review of biomedical engineering. 2010;12:1-27.
47. Valencia-Sanchez MA, Liu J, Hannon GJ, Parker R. Control of translation and mRNA degradation by miRNAs and siRNAs. Genes & development. 2006;20(5):515-24.
48. Wu L, Fan J, Belasco JG. MicroRNAs direct rapid deadenylation of mRNA. Proceedings of the National Academy of Sciences of the United States of America. 2006;103(11):4034-9.
49. Petersen CP, Bordeleau ME, Pelletier J, Sharp PA. Short RNAs repress translation after initiation in mammalian cells. Molecular cell. 2006;21(4):533-42.
50. Zeng Y, Yi R, Cullen BR. MicroRNAs and small interfering RNAs can inhibit mRNA expression by similar mechanisms. Proceedings of the National Academy of Sciences of the United States of America. 2003;100(17):9779-84.
51. Rossi S, Kopetz S, Davuluri R, Hamilton SR, Calin GA. MicroRNAs, ultraconserved genes and colorectal cancers. The international journal of biochemistry & cell biology. 2010;42(8):1291-7.
52. Pichler M, Winter E, Stotz M, Eberhard K, Samonigg H, Lax S, et al. Down-regulation of KRAS-interacting miRNA-143 predicts poor prognosis but not response to EGFR-targeted agents in colorectal cancer. British journal of cancer. 2012;106(11):1826-32.
53. Pichler M, Winter E, Ress AL, Bauernhofer T, Gerger A, Kiesslich T, et al. miR-181a is associated with poor clinical outcome in patients with colorectal cancer treated with EGFR inhibitor. Journal of clinical pathology. 2014;67(3):198-203.
54. Boni V, Bitarte N, Cristobal I, Zarate R, Rodriguez J, Maiello E, et al. miR-192/miR-215 influence 5-fluorouracil resistance through cell cycle-mediated mechanisms complementary to its post-transcriptional thymidilate synthase regulation. Molecular cancer therapeutics. 2010;9(8):2265-75.
55. Pardini B, Rosa F, Barone E, Di Gaetano C, Slyskova J, Novotny J, et al. Variation within 3'-UTRs of base excision repair genes and response to therapy in colorectal cancer patients: A potential modulation of microRNAs binding. Clinical cancer research : an official journal of the American Association for Cancer Research. 2013;19(21):6044-56.
56. Hurst DR, Edmonds MD, Welch DR. Metastamir: the field of metastasis-regulatory microRNA is spreading. Cancer research. 2009;69(19):7495-8.
57. Lujambio A, Calin GA, Villanueva A, Ropero S, Sanchez-Cespedes M, Blanco D, et al. A microRNA DNA methylation signature for human cancer metastasis. Proceedings of the National Academy of Sciences of the United States of America. 2008;105(36):13556-61.
58. Hur K. MicroRNAs: promising biomarkers for diagnosis and therapeutic targets in human colorectal cancer metastasis. BMB reports. 2015;48(4):217-22.
59. Jin D, Fang Y, Li Z, Chen Z, Xiang J. Epithelial-mesenchymal transitionassociated microRNAs in colorectal cancer and drug-targeted therapies (Review). Oncology reports. 2015;33(2):515-25.

60. Park SM, Gaur AB, Lengyel E, Peter ME. The miR-200 family determines the epithelial phenotype of cancer cells by targeting the E-cadherin repressors ZEB1 and ZEB2. Genes & development. 2008;22(7):894-907.
61. Liu M, Chen H. The role of microRNAs in colorectal cancer. Journal of genetics and genomics = Yi chuan xue bao. 2010;37(6):347-58.
62. Spaderna S, Schmalhofer O, Hlubek F, Berx G, Eger A, Merkel S, et al. A transient, EMT-linked loss of basement membranes indicates metastasis and poor survival in colorectal cancer. Gastroenterology. 2006;131(3):830-40.
63. Pichler M, Ress AL, Winter E, Stiegelbauer V, Karbiener M, Schwarzenbacher D, et al. MiR-200a regulates epithelial to mesenchymal transition-related gene expression and determines prognosis in colorectal cancer patients. British journal of cancer. 2014;110(6):1614-21.
64. Hanahan D, Weinberg RA. The hallmarks of cancer. Cell. 2000;100(1):57-70.
65. Asangani IA, Rasheed SA, Nikolova DA, Leupold JH, Colburn NH, Post S, et al. MicroRNA-21 (miR-21) post-transcriptionally downregulates tumor suppressor Pdcd4 and stimulates invasion, intravasation and metastasis in colorectal cancer. Oncogene. 2008;27(15):2128-36.
66. Volinia S, Calin GA, Liu CG, Ambs S, Cimmino A, Petrocca F, et al. A microRNA expression signature of human solid tumors defines cancer gene targets. Proceedings of the National Academy of Sciences of the United States of America. 2006;103(7):2257-61.
67. Harris TA, Yamakuchi M, Ferlito M, Mendell JT, Lowenstein CJ. MicroRNA-126 regulates endothelial expression of vascular cell adhesion molecule 1. Proceedings of the National Academy of Sciences of the United States of America. 2008;105(5):1516-21.
68. Lu LF, Liston A. MicroRNA in the immune system, microRNA as an immune system. Immunology. 2009;127(3):291-8.
69. Bu P, Chen KY, Chen JH, Wang L, Walters J, Shin YJ, et al. A microRNA miR-34a-regulated bimodal switch targets Notch in colon cancer stem cells. Cell stem cell. 2013;12(5):602-15.
70. Pichler M, Stiegelbauer V, Vychytilova-Faltejskova P, Ivan C, Ling H, Winter E, et al. Genome-wide microRNA analysis identifies miR-188-3p as novel prognostic marker and molecular factor involved in colorectal carcinogenesis. Clinical cancer research : an official journal of the American Association for Cancer Research. 2016.
71. Schmittgen TD, Livak KJ. Analyzing real-time PCR data by the comparative C(T) method. Nature protocols. 2008;3(6):1101-8.
72. Van Cutsem E, Cervantes A, Nordlinger B, Arnold D. Metastatic colorectal cancer: ESMO Clinical Practice Guidelines for diagnosis, treatment and follow-up. Annals of oncology : official journal of the European Society for Medical Oncology / ESMO. 2014;25 Suppl 3:iii1-9.
73. Dweep H, Gretz N. miRWalk2.0: a comprehensive atlas of microRNA-target interactions. Nature methods. 2015;12(8):697.
74. Bartel DP. MicroRNAs: target recognition and regulatory functions. Cell. 2009;136(2):215-33.
75. Margulis V, Lotan Y, Karakiewicz PI, Fradet Y, Ashfaq R, Capitanio U, et al. Multi-institutional validation of the predictive value of Ki-67 labeling index in patients with urinary bladder cancer. Journal of the National Cancer Institute. 2009;101(2):114-9.
76. Pichler M, Calin GA. MicroRNAs in cancer: from developmental genes in worms to their clinical application in patients. British Journal of Cancer. 2015;113(4):569-73.
77. Adams BD, Parsons C, Slack FJ. The tumor-suppressive and potential therapeutic functions of miR-34a in epithelial carcinomas. Expert opinion on therapeutic targets. 2016;20(6):737-53.
78. Cortez MA, Ivan C, Valdecanas D, Wang X, Peltier HJ, Ye Y, et al. PDL1 Regulation by p53 via miR-34. Journal of the National Cancer Institute. 2016;108(1).
79. Schotte D, Chau JC, Sylvester G, Liu G, Chen C, van der Velden VH, et al. Identification of new microRNA genes and aberrant microRNA profiles in childhood acute lymphoblastic leukemia. Leukemia. 2009;23(2):313-22.
80. Lakomy R, Sana J, Hankeova S, Fadrus P, Kren L, Lzicarova E, et al. MiR-195, miR-196b, miR-181c, miR-21 expression levels and O-6-methylguanine-DNA methyltransferase methylation

status are associated with clinical outcome in glioblastoma patients. Cancer science. 2011;102(12):2186-90.
81. How C, Hui AB, Alajez NM, Shi W, Boutros PC, Clarke BA, et al. MicroRNA-196b regulates the homeobox B7-vascular endothelial growth factor axis in cervical cancer. PloS one. 2013;8(7):e67846.
82. Bhatia S, Kaul D, Varma N. Potential tumor suppressive function of miR-196b in B-cell lineage acute lymphoblastic leukemia. Molecular and cellular biochemistry. 2010;340(1-2):97-106.
83. Boisen MK, Dehlendorff C, Linnemann D, Nielsen BS, Larsen JS, Osterlind K, et al. Tissue microRNAs as predictors of outcome in patients with metastatic colorectal cancer treated with first line Capecitabine and Oxaliplatin with or without Bevacizumab. PloS one. 2014;9(10):e109430.
84. Svoboda M, Sana J, Fabian P, Kocakova I, Gombosova J, Nekvindova J, et al. MicroRNA expression profile associated with response to neoadjuvant chemoradiotherapy in locally advanced rectal cancer patients. Radiation Oncology. 2012;7.
85. Hu JS, Xu Y, Cai SJ. Specific microRNAs as novel biomarkers for combination chemotherapy resistance detection of colon adenocarcinoma. European Journal of Medical Research. 2015;20.
86. Joo MK, Park JJ, Yoo HS, Lee BJ, Chun HJ, Lee SW, et al. The roles of HOXB7 in promoting migration, invasion and anti-apoptosis in gastric cancer. Journal of gastroenterology and hepatology. 2016.
87. He H, Shen Z, Zhang H, Wang X, Tang Z, Xu J, et al. Clinical significance of polypeptide N-acetylgalactosaminyl transferase-5 (GalNAc-T5) expression in patients with gastric cancer. British journal of cancer. 2014;110(8):2021-9.
88. Liao WT, Jiang D, Yuan J, Cui YM, Shi XW, Chen CM, et al. HOXB7 as a prognostic factor and mediator of colorectal cancer progression. Clinical cancer research : an official journal of the American Association for Cancer Research. 2011;17(11):3569-78.
89. Zheng PS, Wen J, Ang LC, Sheng W, Viloria-Petit A, Wang Y, et al. Versican/PG-M G3 domain promotes tumor growth and angiogenesis. FASEB journal : official publication of the Federation of American Societies for Experimental Biology. 2004;18(6):754-6.
90. Chia J, Goh G, Bard F. Short O-GalNAc glycans: regulation and role in tumor development and clinical perspectives. Biochimica et biophysica acta. 2016;1860(8):1623-39.
91. Peng RQ, Wan HY, Li HF, Liu M, Li X, Tang H. MicroRNA-214 suppresses growth and invasiveness of cervical cancer cells by targeting UDP-N-acetyl-alpha-D-galactosamine:polypeptide N-acetylgalactosaminyltransferase 7. The Journal of biological chemistry. 2012;287(17):14301-9.
92. Ng EK, Chong WW, Jin H, Lam EK, Shin VY, Yu J, et al. Differential expression of microRNAs in plasma of patients with colorectal cancer: a potential marker for colorectal cancer screening. Gut. 2009;58(10):1375-81.
93. Yuan K, Xie K, Fox J, Zeng H, Gao H, Huang C, et al. Decreased levels of miR-224 and the passenger strand of miR-221 increase MBD2, suppressing maspin and promoting colorectal tumor growth and metastasis in mice. Gastroenterology. 2013;145(4):853-64 e9.
94. Kanaan Z, Roberts H, Eichenberger MR, Billeter A, Ocheretner G, Pan J, et al. A plasma microRNA panel for detection of colorectal adenomas: a step toward more precise screening for colorectal cancer. Annals of surgery. 2013;258(3):400-8.
95. Guo ST, Jiang CC, Wang GP, Li YP, Wang CY, Guo XY, et al. MicroRNA-497 targets insulin-like growth factor 1 receptor and has a tumour suppressive role in human colorectal cancer. Oncogene. 2013;32(15):1910-20.
96. Fournier G, Cabaud O, Josselin E, Chaix A, Adelaide J, Isnardon D, et al. Loss of AF6/afadin, a marker of poor outcome in breast cancer, induces cell migration, invasiveness and tumor growth. Oncogene. 2011;30(36):3862-74.
97. Xu Y, Chang R, Peng Z, Wang Y, Ji W, Guo J, et al. Loss of polarity protein AF6 promotes pancreatic cancer metastasis by inducing Snail expression. Nature communications. 2015;6:7184.
98. Della Vittoria Scarpati G, Falcetta F, Carlomagno C, Ubezio P, Marchini S, De Stefano A, et al. A specific miRNA signature correlates with complete pathological response to neoadjuvant

chemoradiotherapy in locally advanced rectal cancer. International journal of radiation oncology, biology, physics. 2012;83(4):1113-9.
99. Zhang H, Qi S, Zhang T, Wang A, Liu R, Guo J, et al. miR-188-5p inhibits tumour growth and metastasis in prostate cancer by repressing LAPTM4B expression. Oncotarget. 2015;6(8):6092-104.
100. Wu J, Lv Q, He J, Zhang H, Mei X, Cui K, et al. MicroRNA-188 suppresses G1/S transition by targeting multiple cyclin/CDK complexes. Cell communication and signaling : CCS. 2014;12:66.

7. Supplementary data

Table 18: Up- and downregulated transcripts obtained from a microarray whole transcriptome profiling analysis in three independent biological replicates comparing the HCT116 miR-196b-5p stably overexpressing cells against control cells

Gene Symbol	Gene Assignment	Fold-Change(miR-196b-5p OE vs. OE Control)
PRF1	NM_001083116	2,24563
MBNL3	NM_001170704	1,9677
RNU7-55P	ENST00000459426	1,95474
HIF1A-AS2	ENST00000554254	1,86226
SAT1	NM_002970	1,79687
METTL7A	NM_014033	1,70887
CALCRL	ENST00000409998	1,68066
LEMD1	NM_001001552	1,67825
LOC151760	XR_171398	1,66902
PELI2	NM_021255	1,66612
NR2F1	NM_005654	1,66005
B3GALT1	NM_020981	1,64909
GRIN2B	NM_000834	1,64811
MAPK8IP1	NM_005456	1,64206
ZNF221	NM_013359	1,62754
IL23A	ENST00000390418	1,6275
KLRK1	ENST00000396451	1,62234
TM4SF18	NM_001184723	1,61283
FAT4	NM_001291285	1,60888
OR2A42	NM_001001802	1,607
NFIB	NM_001190737	1,59117
TANK	NM_001199135	1,59064
ACTR3C	ENST00000478393	1,58428
CNTNAP3B	OTTHUMT00000129769	1,58131
SESN3	NM_001271594	1,58118
RNA5SP221	ENST00000411271	1,57367
CLCNKB	NM_001165945	1,56909
LOC100506127	ENST00000530460	1,5645
TNFSF18	NM_005092	1,56157

SESTD1	NM_178123	1,56049
MIR548I2	NR_031688	1,55382
OR2A1	NM_001005287	1,54072
GRAMD1C	NM_001172105	1,53522
PBX1	NM_001204961	1,51931
RNU7-57P	ENST00000459540	1,51705
TNRC6C-AS1	NR_040071	1,51501
MIR548I2	NR_031688	1,50798
TAS2R10	ENST00000240619	1,50222
MIR548L	NR_031630	-1,50385
MIR4486	NR_039706	-1,50391
CGN	AF263462	-1,50964
GSTTP1	NR_003081	-1,51934
ZBED2	ENST00000317012	-1,52435
RNA5SP361	ENST00000362686	-1,53585
RNA5SP409	ENST00000516815	-1,53643
RNU4-63P	ENST00000411313	-1,5407
ZNF804A	NM_194250	-1,54416
LOC101060542	NR_110764	-1,54904
HOXB7	NM_004502	-1,55316
IPW	ENST00000547292	-1,55897
RNA5SP207	ENST00000390874	-1,56357
TRGV5	ENST00000390344	-1,57482
MIR130B	NR_029845	-1,58401
CCDC106	NM_013301	-1,5897
TXLNGY	ENST00000445715	-1,59438
MIR544B	NR_036088	-1,6022
TXLNGY	NR_045128	-1,60561
LOC101927171	XR_242040	-1,61848
LOC100130172	ENST00000500267	-1,64255
GAS6-AS2	NR_044993	-1,66338
MIR149	NR_029702	-1,68
RNU6ATAC18P	ENST00000408413	-1,70476
ARL14EPL	NM_001195581	-1,71038
DKK1	NM_012242	-1,77465
MUC13	NM_033049	-1,80149

KIR2DS1	NM_014512	-1,82954
RNU6-736P	ENST00000516436	-1,83458
TTTY15	NR_001545	-1,89931
ANXA10	NM_007193	-1,90447
LOC101928687	NR_120641	-2,05617
LOC101928102	XR_248922	-2,09693
RNA5SP295	ENST00000362655	-2,11431
GALNT5	NM_014568	-2,13099
RNU6-893P	ENST00000458841	-2,30349
KRTAP2-3	NM_001165252	-2,4029
KRTAP3-1	NM_031958	-2,44953
CPA4	NM_001163446	-2,60247
DDX3Y	NM_004660	-2,66755
HIST1H2BB	NM_021062	-3,05063